



## Supporting Information

### **Nutzung des Perfluornaphthalin-Radikalkations als selektiver Deelektronierer zur Erzeugung einer Vielzahl stark oxidierender reaktiver Kationen**

*M. Sellin, J. Willrett, D. Röhner, T. Heizmann, J. Fischer, M. Seiler, C. Holzmann,  
T. A. Engesser, V. Radtke, I. Krossing\**

# Supporting Information

to

## Utilizing the Perfluoronaphthalene Radical Cation as a Selective Deelectronator to Access a Variety of Strongly Oxidizing Reactive Cations

by

Malte Sellin, Julie Willrett, David Röhner, Tim Heizmann, Julia Fischer, Matthis Seiler, Celia Holzmann,  
Tobias A. Engesser, Valentin Radtke, Ingo Krossing\*

<sup>a)</sup> MSc. M. Sellin, MSc. J. Willrett, MSc. D. Röhner, MSc. T. Heizmann, BSc. J. Fischer, BSc. M. Seiler, BSc. C. Holzmann, Dr. V. Radtke, Prof. Dr. I. Krossing\*; Institut für Anorganische und Analytische Chemie und Freiburger Materialforschungszentrum (FMF); Albert-Ludwigs-Universität Freiburg; Albertstr. 21, 79104 Freiburg (Germany). \* E-mail: [krossing@uni-freiburg.de](mailto:krossing@uni-freiburg.de)

<sup>b)</sup> Dr. T. A. Engesser; Institut für Anorganische Chemie; Christian-Albrechts-Universität zu Kiel; Max-Eyth-Straße 2, 24118 Kiel (Germany).

## Content

1.	General Procedures .....	2
2.	Experimental Procedures .....	5
2.1	[Naphthalene <sup>F</sup> ] <sup>+</sup> [F{Al(OR <sup>F</sup> ) <sub>3</sub> } <sub>2</sub> ] <sup>-</sup> .....	5
2.2	Bis(scorpionato)iron(II-IV) .....	15
2.3	Ferrocene .....	24
2.4	Anthracene .....	30
2.5	Tetracene.....	34
2.6	Pentacene.....	37
2.7	Naphthalene <sup>Cl</sup> .....	42
2.8	Copper .....	47
2.9	White Phosphorous .....	49
3.	scXRD Data Tables .....	51
4.	DFT Calculations .....	59
4.1	Born-Fajans-Haber Cycles of Deelectronation Reactions in Solution .....	59
4.2	Born-Fajans-Haber Cycles of Deelectronation Reactions in Solid-State .....	60
4.3	Solvation Energies of the Dications.....	63
4.4	Coordinates of the DFT-Optimized Structures .....	64
5.	References .....	73

## 1. General Procedures

All manipulations were carried out by using standard Schlenk technique or a nitrogen filled glovebox ( $O_2/H_2O < 0.1$  ppm). All the reactions were performed in Schlenk tubes with grease free PTFE-valves. The solvent 1,2,3,4-tetrafluorobenzene (4FB,  $C_6F_4H_2$ , from Fluorochem) was stirred a few days over calcium hydride ( $CaH_2$ ) and distilled. The distillate was stirred over  $Ag^+[Al(OR^F)_4]^-$  and condensed to remove traces of less fluorinated benzenes. This leads to a minor contamination of  $R^FOH$  ( $<1\%$ ), which does not affect the reactions. The solvents 1,2,3-trifluorobenzene (3FB), pentafluorobenzene (5FB) and hexafluorobenzene were stirred a few days over calcium hydride ( $CaH_2$ ) and distilled. *N*-pentane was dried using a Grubbs apparatus. 3FB, 4FB, 5FB, 6FB and *n*-pentane were stored over 3 Å molar sieves. Octafluoronaphthalene (ABCR), Octachloronaphthalene (ABCR), 9,10-Dichlorooctafluoroanthracene (Sigma Aldrich), Anthracene (TCI), Tetracene (TCI) and Pentacene (BLD Pharm) were bought from commercial sources. Bis(scorpionato)iron(II),<sup>[1]</sup> [tetracene]<sup>+</sup> $[F\{Al(OR^F)_3\}_2]^-$ ,<sup>[2]</sup> [pentacene]<sup>+</sup> $[F\{Al(OR^F)_3\}_2]^-$ ,<sup>[2]</sup>  $[NO]^+[F\{Al(OR^F)_3\}_2]^-$ <sup>[3]</sup> and  $Ag^+[F\{Al(OR^F)_3\}_2]^-$ <sup>[3]</sup> were prepared according to literature procedures. Copper powder was activated under a stream of Argon/Hydrogen (90:10) at 400 °C for 4 h.

Important note: The [naphthalene]<sup>F</sup> cation and most of the herein prepared cations react with alkanes as *n*-pentane. Therefore, the crystallisation and purification of the targeted salts is done using other methods. The single-crystals are typically obtained by slow evaporation of the reaction solution in a glovebox. Purification of 1:1 salts from naphthalene<sup>F</sup> is done by thorough washing with 6FB, while the purification of 1:2 salts is done with cautious washing with 5FB, to remove 1:1 salts. Neutral compounds, e.g. ion-pairs, can be purified by removing the naphthalene<sup>F</sup> in high-vacuum.

### Vibrational Spectroscopy

FTIR spectra were recorded inside a glovebox with a Bruker ALPHA equipped with QuickSnap Eco ATR module and ZnSe or Diamond crystal. The spectra were measured at RT in the range of 4000–550  $cm^{-1}$  (ZnSe) or 4000–400  $cm^{-1}$  (Diamond) with 32 scans and a resolution of 2  $cm^{-1}$ . The data were processed with the Bruker OPUS 7.5 software package. FT Raman spectra were recorded with a VERTEX 70 with Bruker RAM II Modul (1064 nm exciting line of a Nd-YAG laser) and liquid nitrogen cooled Ge detector. The samples were flame-sealed in soda-lime glass Pasteur pipettes and were measured at RT in the range of 4000–30  $cm^{-1}$  with up to 10,000 scans and a resolution of 4  $cm^{-1}$  with a laser power of 10–50 mW. The Raman spectra contain two sharp artefacts at 2900  $cm^{-1}$  and 2700  $cm^{-1}$  and a broad one at 1900  $cm^{-1}$ . The intensities are reported as follows:  $\geq 0.8$  = very strong (vs),  $\geq 0.6$  = strong (s),  $\geq 0.4$  = medium (m),  $\geq 0.2$  = weak (w),  $< 0.2$  = very weak (vw). The data were processed with the Bruker OPUS 7.5 software package. The graphical representations were created with ORIGINPRO 2021.

### NMR Spectroscopy

NMR spectra were recorded at RT either on a Bruker Avance II Widebore 400 MHz, Bruker Avance III HD 300 MHz or Bruker Avance DPX 200 MHz. The samples were dissolved in 4FB (0.6 ml) in a 5 mm thick-walled NMR tube with J. Young PTFE valve. The spectra were calibrated by using the  $^1H$  signal of the solvent 4FB ( $\delta = 6.97$  ppm, rel. to tetramethylsilane). The field corrections of other nuclei were adjusted accordingly. Typically, small impurities of  $HOC(CF_3)_3$  were detected in the  $^{19}F$  NMR at  $-76.0$  ppm. The MestReNova software package was used for measuring, processing and creation of the graphical representations of the spectra.  $^1H$  and  $^{13}C$  NMR spectra are referenced against TMS and  $^{19}F$  NMR spectra against  $CFCl_3$ .

### Single Crystal X-ray Diffraction

The data were collected on a Bruker D8 VENTURE dual wavelength Mo/Cu three-circle diffractometer

with a microfocus sealed X-ray tube using mirror optics as monochromator and a Bruker PHOTON III detector. Single crystals were selected at RT in PFPE oil JC 1800 (Sunoit Performance Material Science), mounted on CryoLoops with a diameter of 0.1 to 0.2 mm and shock-cooled using an Oxford Cryostream 800 low temperature device. The data were gathered at 100(2) K using Mo K $\alpha$  radiation ( $\lambda = 0.71073 \text{ \AA}$ ). All data were integrated with SAINT (version 8.38A) and a multi-scan absorption correction using SADABS or TWINABS was applied. The structures were solved by direct methods using SHELXT<sup>[4]</sup> and refined by full-matrix least-squares methods against  $F^2$  by SHELXL-2018/3<sup>[5]</sup> using the GUI software ShelXle.<sup>[6]</sup> Disordered moieties were refined using bond lengths restraints and displacement parameter restraints and were modelled with the program DSR.<sup>[7]</sup> The gathered data were finalized with the tool FinalCif.<sup>[8]</sup> The graphical representations of the crystal structures were generated with Mercury (version 4.0).<sup>[9]</sup> Crystallographic data for the structures reported in this paper have been deposited with the Cambridge Crystallographic Data Centre.<sup>[10]</sup> Copies of the data can be obtained free of charge from the Cambridge Crystallographic Data Centre via [www.ccdc.cam.ac.uk/structures](http://www.ccdc.cam.ac.uk/structures).

### Powder X-ray Diffraction

Powder diffractograms were recorded on a STOE STADI P powder diffractometer with Mo K $\alpha_1$  radiation ( $\lambda = 0.709300 \text{ \AA}$ ), Ge-(111) monochromator and Mythen 1K detector at 100(10) K. The samples were sealed in a 0.5 mm thick capillary (Hilgenberg GmbH, wall thickness 0.01 mm) with silicon grease. Data acquisition, processing, and the calculation of powder diffractograms from single-crystal data was performed using the STOE WinXPOW<sup>®</sup> package.

### Cyclic Voltammetry

The cyclic voltammograms were recorded in an argon filled glovebox ( $\text{O}_2/\text{H}_2\text{O} < 0.1 \text{ ppm}$ ). A three-electrode arrangement was used with a 1 mm diameter platinum disc working electrode, a platinum mesh as counter electrode and a platinum wire in a compartment as a reference. The reference electrode is placed in a glass compartment with a frit to allow a direct measurement against a Pt|Fc<sup>+0</sup> reference electrode. The solution in the compartment electrode has a mixture of 100 mM [NBu<sub>4</sub>]<sup>+</sup>[Al(OR<sup>F</sup>)<sub>4</sub>]<sup>-</sup>, 10 mM Fc and 10 mM [Fc]<sup>+</sup>[Al(OR<sup>F</sup>)<sub>4</sub>]<sup>-</sup> in 4FB. The analyte solution is composed from 100 mM [NBu<sub>4</sub>]<sup>+</sup>[Al(OR<sup>F</sup>)<sub>4</sub>]<sup>-</sup> and 10 mM analyte in 4FB. A VMP3 potentiostat (BIO-LOGICSCIENCE INSTRUMENTS) was used for the measurements, controlled *via* PC using the software EC-LAB (V11.21). The graphical representations were created with ORIGINPRO 2021.

### Mössbauer Spectroscopy

Mössbauer measurements were recorded with an in-house built spectrometer using standard transmission geometry. The Mössbauer Drive System MR260A and the Mössbauer Velocity Transducer MVT-1000 from the Wissenschaftliche Elektronik (WissEl) GmbH were used. As source of radiation, <sup>57</sup>Co within a rhodium matrix and a starting activity of 25 mCi was used. For the temperature control an ITC502 temperature controller with a continuous flow cryostat CF506 from Oxford Instruments was used. All shifts are indicated relative to iron. The spectra were fitted and the line width, isomer shifts and quadrupole splittings were determined with the software "FitSuite 2.0.0".<sup>[11]</sup>

### Computational Details

Geometry optimizations were performed with the TURBOMOLE software<sup>[12]</sup> (v7.2 or v7.5) using the DFT functionals B3LYP<sup>[13]</sup> with the def2-TZVPP<sup>[14]</sup> basis set, the resolution-of-identity (RI) approximation,<sup>[15]</sup> dispersion correction (D3BJ),<sup>[16]</sup> a fine integration grid (m4 or 5 for NMR chemical shift calculations) and the default SCF convergence criteria ( $10^{-6} \text{ a.u.}$ ). All structures were checked for proper spin occupancies and imaginary frequencies with the integrated *EIGER* and *AOFORCE*<sup>[17]</sup>

modules. IR and Raman spectra were simulated at B3LYP(D3BJ)/def2-TZVPP level with a scaling factor of 0.9657,<sup>[18]</sup> for transition metal carbonyls, the specialized scaling factor of 0.968 was used.<sup>[19]</sup> Gibbs free energies of solvation were calculated with the COSMO-RS model<sup>[20]</sup> at the BP86(D3)/def2-TZVPD//BP86(D3)/def-TZVP level of theory using the fine cavity construction algorithm (\$cosmo\_isorad) and the CosmoThermX software.

The Mössbauer calculations were performed with ORCA v. 4.2.1.<sup>[21]</sup> The simulation was performed according to the method of F. Neese et al.<sup>[22]</sup> The geometric parameters were taken from the XRD solid-state structures. Single points on the XRD structures were calculated by using the TpSSH functional,<sup>[23]</sup> in combination with the core basis set CP(PPP)<sup>[24]</sup> for iron or def2-TZVPP<sup>[14]</sup> with the relativistic Douglas-Kroll-Hess method<sup>[25]</sup> for all other atoms. Simulated isomeric shifts were then obtained by taking the DFT electronic densities at the iron center ( $\rho_0$ ) and by using a linear fit with equation  $\delta = \alpha (\rho - C) + \beta$  and the values for calibration from Bjornsson and DeBeer et al. "Römel test set":  $\alpha = -0.172806013$ ;  $\beta = 0.323223706$ ;  $C = 23600$ .<sup>[26]</sup>

## 2. Experimental Procedures

### 2.1 [Naphthalene]<sup>F</sup>+ [F{Al(OR<sup>F</sup>)<sub>3</sub>]<sub>2</sub>]<sup>-</sup>

#### 2.1.1 Cyclic Voltammetry of Naphthalene<sup>F</sup>

Table S1: Key data of the electrochemical transition [naphthalene]<sup>F</sup> → [naphthalene]<sup>F</sup>+ at different scan rates (20–1000 mV s<sup>-1</sup>) with of naphthalene<sup>F</sup> (20 mM) in 1,2,3,4-tetrafluorobenzene using [NBu<sub>4</sub>]<sup>+</sup>[Al(OR<sup>F</sup>)<sub>4</sub>]<sup>-</sup> (100 mM) as supporting electrolyte.

Scan rate in mV s <sup>-1</sup>	Electronation potential in V	Deelectronation potential in V	Half-wave potential in V	Fc corrected half-wave potential in V	Peak difference in V	Current at anodic peak potential in μA
20	1.945	2.079	2.012	2.001	0.134	27.60
50	1.935	2.091	2.013	2.002	0.156	38.97
100	1.919	2.113	2.016	2.005	0.194	50.69
200	1.899	2.125	2.012	2.001	0.226	62.19
500	1.872	2.160	2.016	2.005	0.288	89.27
1000	1.851	2.194	2.023	2.011	0.343	118.4

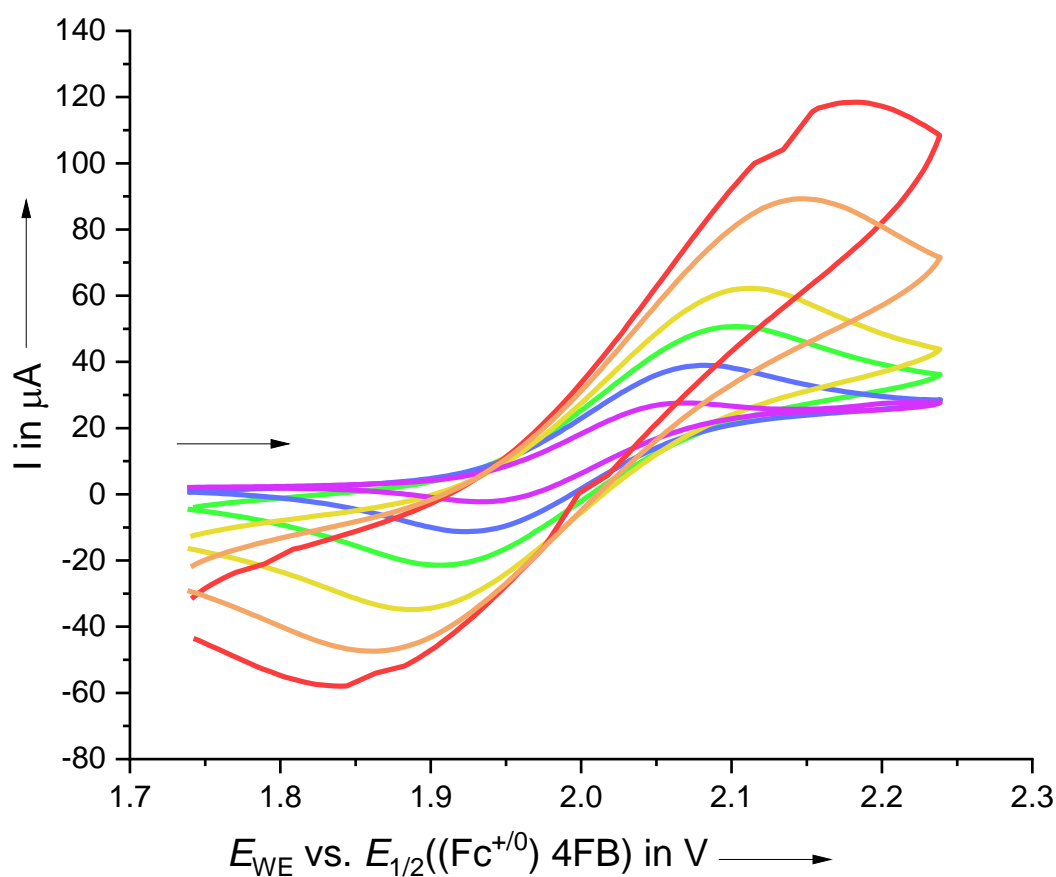


Figure S1: Cyclic voltammograms (2<sup>nd</sup> cycle) at different scan rates (purple (20 mV s<sup>-1</sup>) → green (100 mV s<sup>-1</sup>) → red (1000 mV s<sup>-1</sup>)) of naphthalene<sup>F</sup> (20 mM) in 1,2,3,4-tetrafluorobenzene using [NBu<sub>4</sub>]<sup>+</sup>[Al(OR<sup>F</sup>)<sub>4</sub>]<sup>-</sup> (100 mM) as supporting electrolyte.

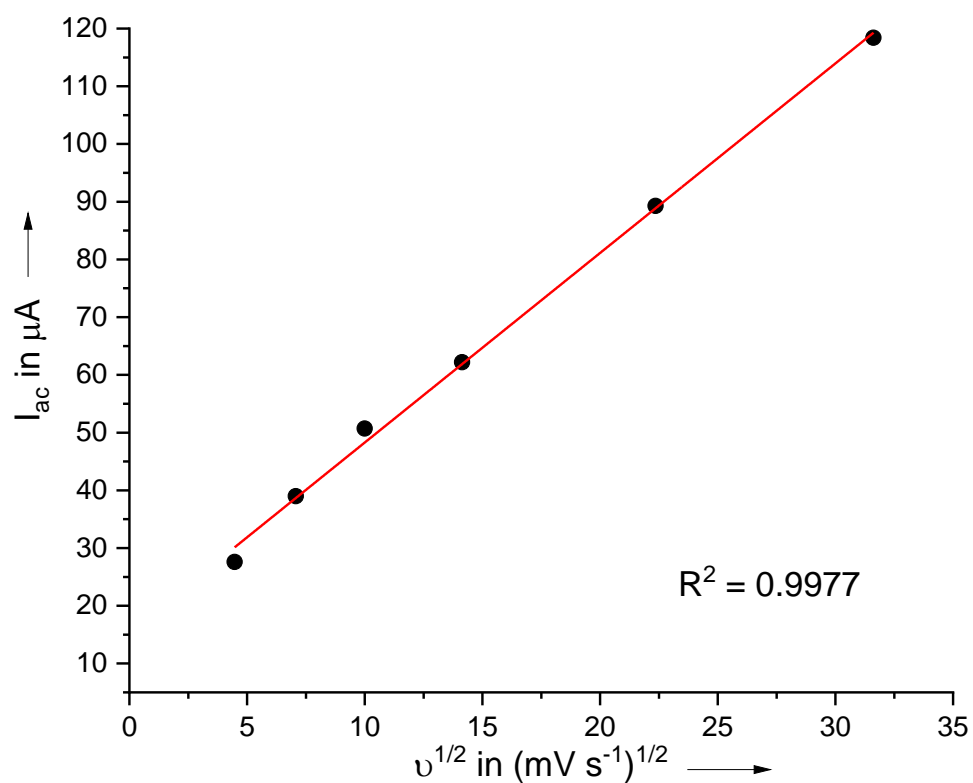


Figure S2: Linear fit of the anodic peak current  $I_{ac}$  against the square root of the scan rate  $v^{1/2}$  of naphthalene<sup>F</sup>.

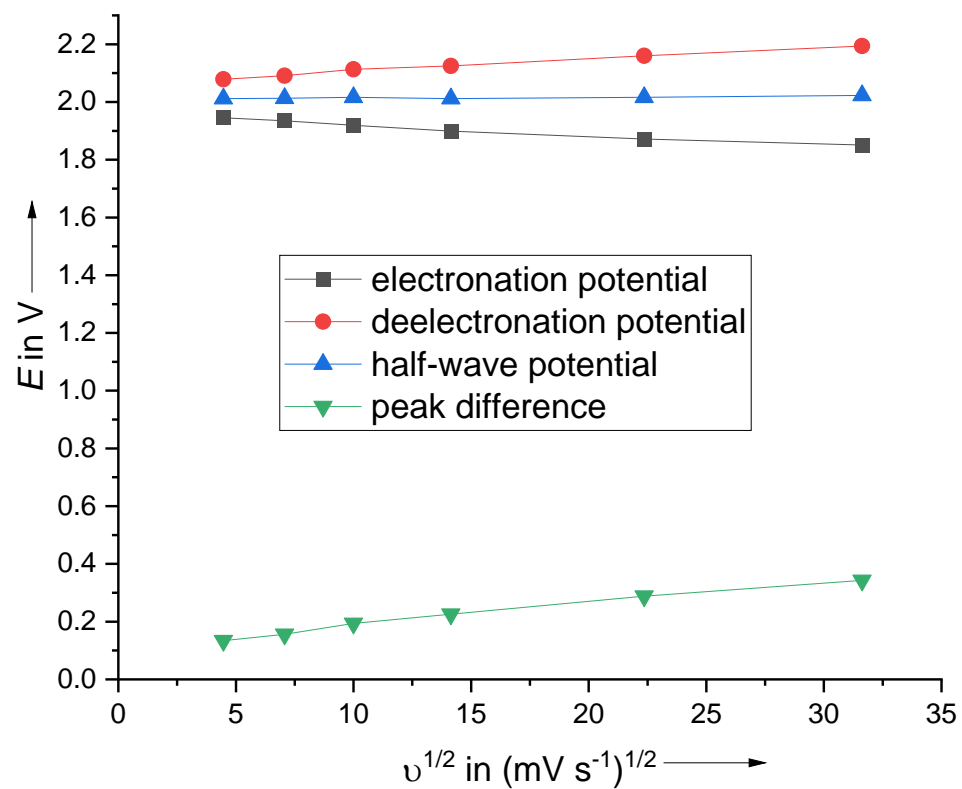


Figure S3: Electronation-, deelectronation- and half-wave potential & peak difference against the square root of the scan rate  $v^{1/2}$  of naphthalene<sup>F</sup>.

## 2.1.2 Synthesis and Characterization of [Naphthalene<sup>F</sup>]<sup>+</sup>[F{Al(OR<sup>F</sup>)<sub>3</sub>]<sub>2</sub>]<sup>-</sup>

### Method 1a: Deelectronation using [Ag]<sup>+</sup>[F{Al(OR<sup>F</sup>)<sub>3</sub>]<sub>2</sub>]<sup>-</sup> / 0.5 I<sub>2</sub> in 4FB

Ag<sup>+</sup>[F{Al(OR<sup>F</sup>)<sub>3</sub>]<sub>2</sub>]<sup>-</sup> (160 mg, 100 μmol, 1.0 eq.) and diiodine (13 mg, 50 μmol, 0.5 eq.) were dissolved in 1,2,3,4-tetrafluorobenzene (1-2 mL) and naphthalene<sup>F</sup> (30 mg, 0.11 μmol, 1.1 eq.) was added to the purple solution. In the course of the next minutes, the color of the solution changes to a dark green. After a few hours, the yellow-white silver iodide precipitate is removed by filtration through a G4 frit. The solvent is removed under vacuum and the product is obtained as a dark green (almost black) powder (144 mg, 82 %, 82 μmol).

### Method 1b: Deelectronation using [Ag]<sup>+</sup>[F{Al(OR<sup>F</sup>)<sub>3</sub>]<sub>2</sub>]<sup>-</sup> / 0.5 Br<sub>2</sub> in SO<sub>2</sub>

Naphthalene<sup>F</sup> (220 mg, 810 μmol, 1.3 eq.) and Ag<sup>+</sup>[F{Al(OR<sup>F</sup>)<sub>3</sub>]<sub>2</sub>]<sup>-</sup> (1.0 g, 630 μmol, 1.0 eq.) were weighed into a double Schlenk flask and a mixture of SO<sub>2</sub> and Br<sub>2</sub> (5 mL) were condensed onto the substances at -78 °C. Upon warming to room-temperature, the color of the solution turned from brown to green. To ensure, that bromine was used in excess, the volatiles were condensed on the other side of the double Schlenk flask, yielding again to a light brown solution. The solvent was condensed back, the solution was filtered through the frit and all the volatiles were removed under vacuum. [Naphthalene<sup>F</sup>]<sup>+</sup>[F{Al(OR<sup>F</sup>)<sub>3</sub>]<sub>2</sub>]<sup>-</sup> was obtained in 94 % yield as a dark green (almost black) powder (1.04 g, 590 μmol).

### Method 2: Deelectronation using [NO]<sup>+</sup>[F{Al(OR<sup>F</sup>)<sub>3</sub>]<sub>2</sub>]<sup>-</sup>

[NO]<sup>+</sup>[F{Al(OR<sup>F</sup>)<sub>3</sub>]<sub>2</sub>]<sup>-</sup> (0.76 g, 1.0 eq., 0.50 mmol) and naphthalene<sup>F</sup> (0.14 g, 1.0 eq, 0.50 mmol) were suspended in hexafluorobenzene (3 mL). The solvent was evaporated slowly at atmospheric pressure in a glovebox overnight. The procedure was repeated two times, yielding dark green crystals suitable for scXRD. Unreacted starting material was removed by filtration by suspending the product in hexafluorobenzene (2x4 mL) and decanting the solution. Afterwards the remaining dark green (almost black) solid product was dried in vacuum (590 mg, 68 %, 0.34 mmol).

### scXRD

directly from the reaction (Method 2):

[naphthalene<sup>F</sup>]<sup>+</sup>[F{Al(OR<sup>F</sup>)<sub>3</sub>]<sub>2</sub>]<sup>-</sup>·(6FB):  $P\bar{1}$ ,  $a = 10.3239(17) \text{ \AA}$ ,  $b = 11.885(2) \text{ \AA}$ ,  $c = 13.278(3) \text{ \AA}$ ,  $\alpha = 107.402(6)^\circ$ ,  $\beta = 108.225(5)^\circ$ ,  $\gamma = 100.577(6)^\circ$ ,  $V = 1405.6(5) \text{ \AA}^3$ ,  $Z = 1$ .

[naphthalene<sup>F</sup>]<sup>+</sup>[F{Al(OR<sup>F</sup>)<sub>3</sub>]<sub>2</sub>]<sup>-</sup>·(naphthalene<sup>F</sup>):  $P\bar{1}$ ,  $a = 13.197(5) \text{ \AA}$ ,  $b = 13.902(4) \text{ \AA}$ ,  $c = 36.579(13) \text{ \AA}$ ,  $\alpha = 84.884(7)^\circ$ ,  $\beta = 84.184(9)^\circ$ ,  $\gamma = 63.547(11)^\circ$ ,  $V = 5970(4) \text{ \AA}^3$ ,  $Z = 4$ .

Recrystallization from 5FB:

[naphthalene<sup>F</sup>]<sup>+</sup>[F{Al(OR<sup>F</sup>)<sub>3</sub>]<sub>2</sub>]<sup>-</sup>·(5FB):  $P\bar{1}$ ,  $a = 10.359(3) \text{ \AA}$ ,  $b = 11.891(3) \text{ \AA}$ ,  $c = 13.295(3) \text{ \AA}$ ,  $\alpha = 107.296(12)^\circ$ ,  $\beta = 108.150(8)^\circ$ ,  $\gamma = 100.836(12)^\circ$ ,  $V = 1413.0(6) \text{ \AA}^3$ ,  $Z = 1$ .

### Vibrational Spectroscopy

Raman  $\tilde{\nu} / \text{cm}^{-1} = 1623 \text{ (m)}$ ,  $1460 \text{ (s)}$ ,  $1408 \text{ (vs)}$ ,  $1294 \text{ (m)}$ ,  $1102 \text{ (m)}$ ,  $1087 \text{ (m)}$ ,  $815 \text{ (m)}$ ,  $753 \text{ (s)}$ ,  $512 \text{ (s)}$ ,  $391 \text{ (s)}$ ,  $327 \text{ (s)}$ ,  $294 \text{ (s)}$ .

ATR IR  $\tilde{\nu} / \text{cm}^{-1} = 1664 \text{ (vw)}$ ,  $1580 \text{ (vw)}$ ,  $1543 \text{ (vw)}$ ,  $1477 \text{ (w)}$ ,  $1468 \text{ (vw)}$ ,  $1441 \text{ (vw)}$ ,  $1406 \text{ (w)}$ ,  $1385 \text{ (vw)}$ ,  $1354 \text{ (vw)}$ ,  $1301 \text{ (w)}$ ,  $1265 \text{ (s)}$ ,  $1243 \text{ (vs)}$ ,  $1214 \text{ (vs)}$ ,  $1177 \text{ (s)}$ ,  $1120 \text{ (w)}$ ,  $971 \text{ (vs)}$ ,  $948 \text{ (m)}$ ,  $864 \text{ (w)}$ ,  $791 \text{ (vw)}$ ,  $786 \text{ (vw)}$ ,  $760 \text{ (vw)}$ ,  $726 \text{ (vs)}$ ,  $702 \text{ (w)}$ ,  $639 \text{ (w)}$ ,  $569 \text{ (w)}$ .



## NMR

$^1\text{H}$  NMR (400 MHz, 4FB, 298 K): only solvent signal (6.97 ppm) and minor contaminations of  $R^F\text{OH}$  (3.68 ppm) coming from the solvent

$^{19}\text{F}$  NMR (376 MHz, 4FB, 298 K):  $\delta/\text{ppm} = -76.0$  (s, 54F,  $[\text{F}\{\text{Al}(\text{OC}(\text{CF}_3)_3)_2\}]^-$ ),  $-165.0$  (s, 6F,  $\text{C}_6\text{F}_6$ ),  $-184.8$  (s, 54F,  $[\text{F}\{\text{Al}(\text{OC}(\text{CF}_3)_3)_2\}]^-$ ). The neutral naphthalene $^F$  co-crystallized in the product is not observable due to rapid electron transfer with the paramagnetic  $[\text{naphthalene}^F]^{+\bullet}$ .

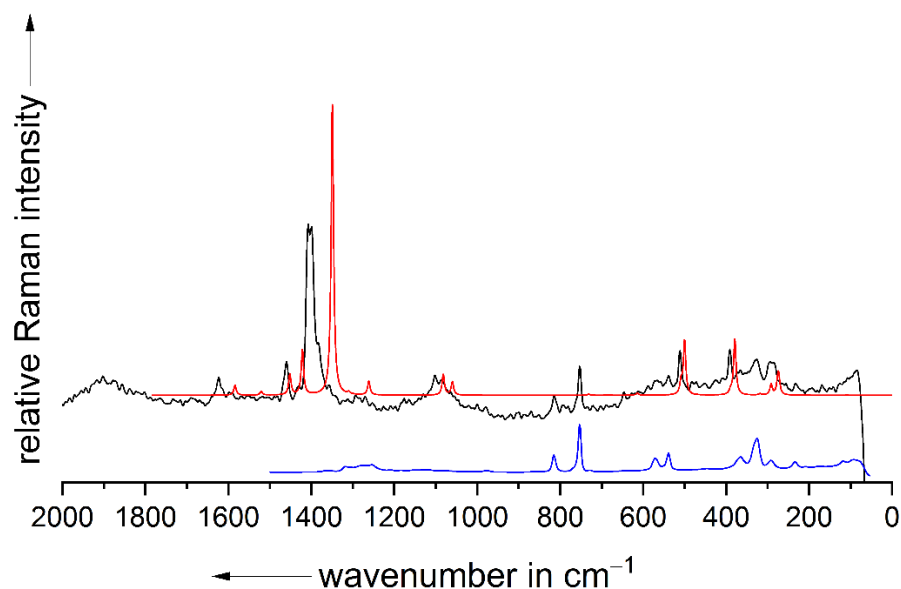


Figure S4: Comparison of the Raman spectrum of crystalline  $[\text{naphthalene}^F]^+[\text{F}\{\text{Al}(\text{OR}^F)_3\}_2]^-$  (1000 scans, 20 mW, black line) with the B3LYP(D3BJ)/def2-TZVPP calculated Raman spectrum of  $[\text{naphthalene}^F]^{+\bullet}$  (red line) scaled by 0.9657 and the Raman spectrum of  $[\text{NO}]^+[\text{F}\{\text{Al}(\text{OR}^F)_3\}_2]^-$  (blue line; to show the expectation spectrum of the anion bands).

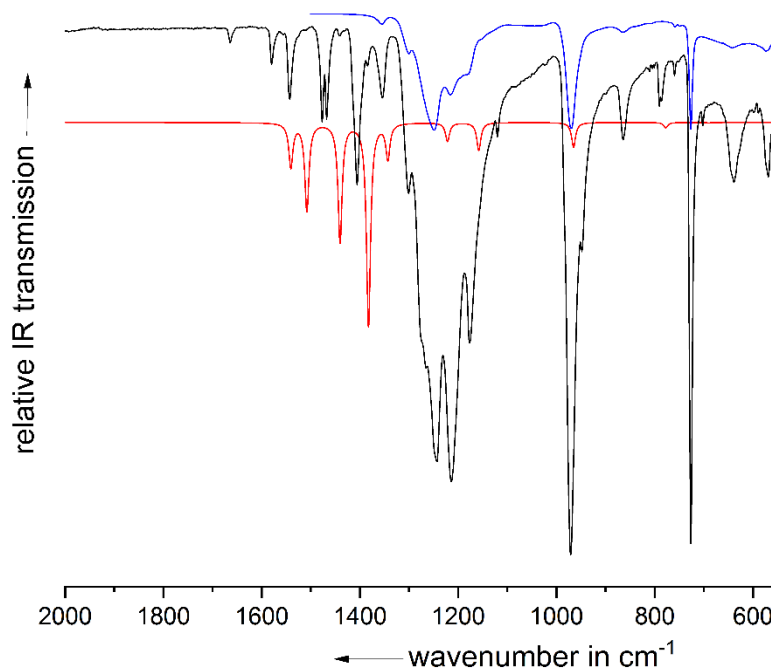


Figure S5: Comparison of the ATR-IR spectrum (ZnSe) of crystalline  $[\text{naphthalene}^F]^+[\text{F}\{\text{Al}(\text{OR}^F)_3\}_2]^-$  (32 scans, black line) with the B3LYP(D3BJ)/def2-TZVPP calculated IR spectrum of  $[\text{naphthalene}^F]^{+\bullet}$  (red line) scaled by 0.9657 and the IR spectrum of  $[\text{NO}]^+[\text{F}\{\text{Al}(\text{OR}^F)_3\}_2]^-$  (blue line; to show the expectation spectrum of the anion bands).

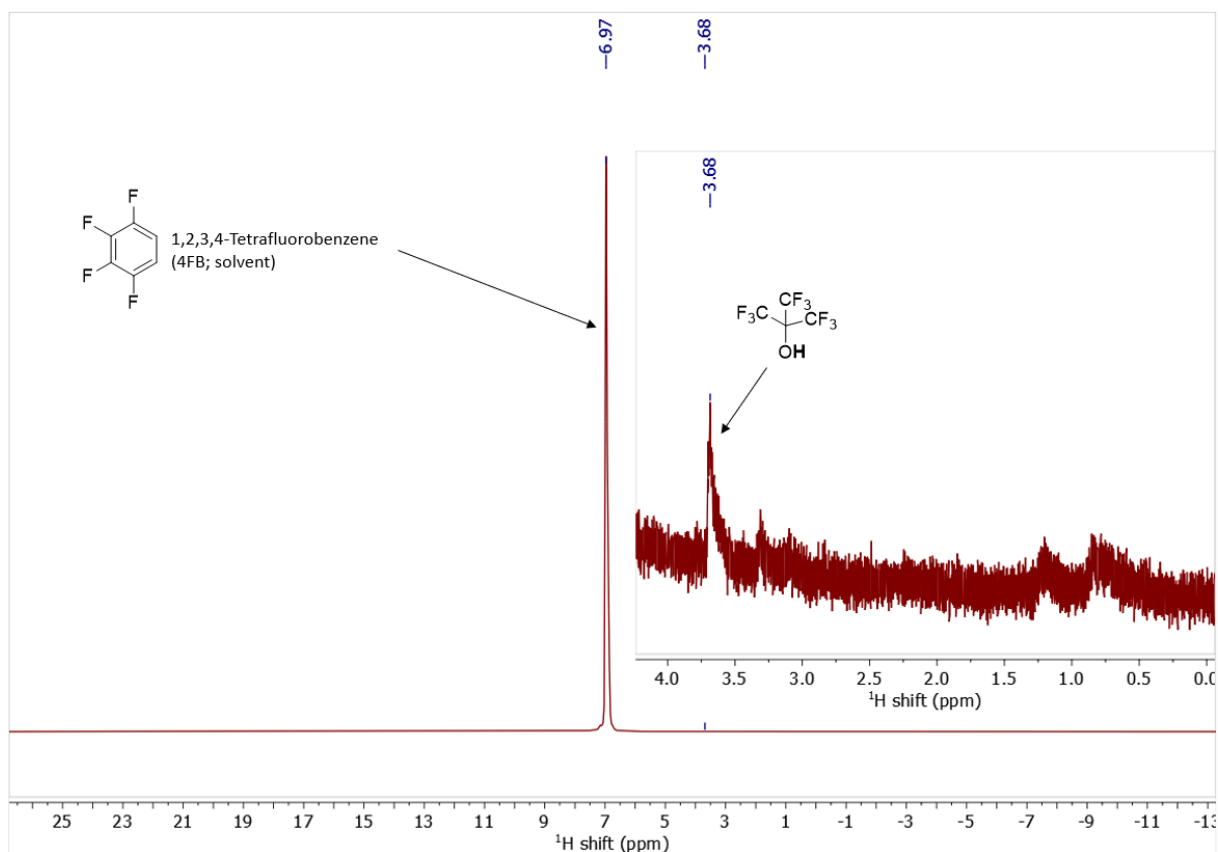


Figure S6:  $^1\text{H}$  NMR spectrum of  $[\text{naphthalene}^{\text{F}}]^+[\text{F}\{\text{Al}(\text{OR}^{\text{F}})_3\}_2]^-$  in 1,2,3,4-tetrafluorobenzene (4FB) at room temperature.

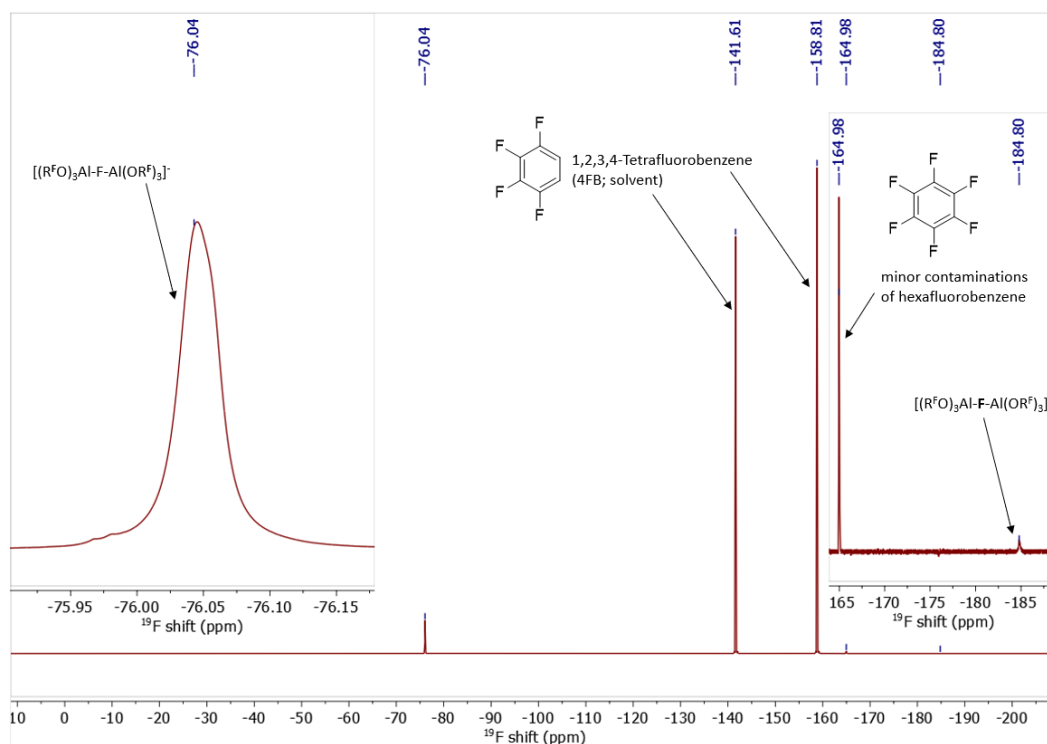


Figure S7:  $^{19}\text{F}$  NMR spectrum of  $[\text{naphthalene}^{\text{F}}]^+[\text{F}\{\text{Al}(\text{OR}^{\text{F}})_3\}_2]^-$  in 1,2,3,4-tetrafluorobenzene (4FB) at room temperature.  $\text{C}_6\text{F}_6$  results from the solid-state structure which includes co-crystallized  $\text{C}_6\text{F}_6$  from the preparation.

### 2.1.3 Phase purity of $[\text{Naphthalene}^{\text{F}}]^+[\text{F}\{\text{Al}(\text{OR}^{\text{F}})_3\}_2]^-$ & Synthesis of $[\text{W}(\text{CO})_6]^+$

Using the described method 2 *via* the nitrosonium salt, the reactions happens in the transition between the solution and the solid-state. Due to its lower potential in solution and other potential reactivity, the full removal of remaining  $[\text{NO}]^+$  has to be ensured. Additionally, we observed both the presence of 6FB and naphthalene<sup>F</sup> solvates *via* scXRD and in part also NMR. Therefore, the ratio between the crystalline content of  $[\text{naphthalene}^{\text{F}}]^+[\text{F}\{\text{Al}(\text{OR}^{\text{F}})_3\}_2]^- \cdot (6\text{FB})$  and  $[\text{naphthalene}^{\text{F}}]^+[\text{F}\{\text{Al}(\text{OR}^{\text{F}})_3\}_2]^- \cdot \text{naphthalene}^{\text{F}}$  has to be determined for accurate stoichiometries in the follow-up reactions.

First, we examined the product from method 2 *via* powder X-ray diffraction (pXRD) and compared the resulting diffractogram with the three possible phases  $[\text{naphthalene}^{\text{F}}]^+[\text{F}\{\text{Al}(\text{OR}^{\text{F}})_3\}_2]^- \cdot (6\text{FB})$  (PH1),  $[\text{naphthalene}^{\text{F}}]^+[\text{F}\{\text{Al}(\text{OR}^{\text{F}})_3\}_2]^- \cdot \text{naphthalene}^{\text{F}}$  (PH2) and  $[\text{NO}]^+[\text{F}\{\text{Al}(\text{OR}^{\text{F}})_3\}_2]^-$  (PH3). The experimental diffractogram features a large amorphous portion (Figure S8), therefore the background corrected diffractogram is compared to PH1-PH3 for clarity (Figure S9, Figure S10 & Figure S11).

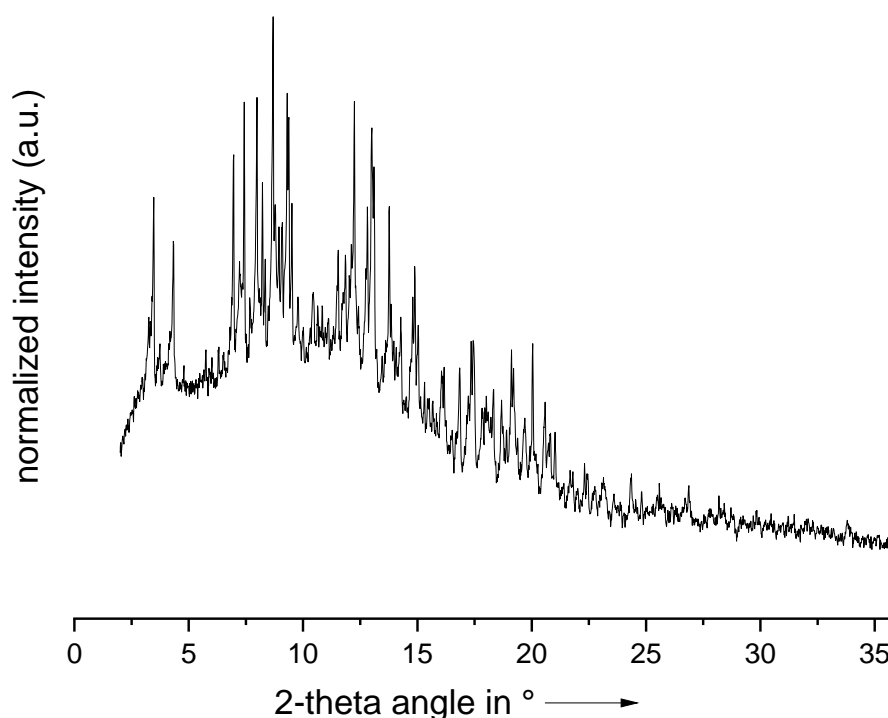


Figure S8: Powder diffractogram of  $[\text{naphthalene}^{\text{F}}]^+[\text{F}\{\text{Al}(\text{OR}^{\text{F}})_3\}_2]^- \cdot x$  prepared by method 2.

First, the existence of PH3 has to be ruled out, therefore, the simulated powder pattern from the scXRD data of  $[\text{NO}]^+[\text{F}\{\text{Al}(\text{OR}^{\text{F}})_3\}_2]^-$  was compared with the diffractogram of the product. The reflections at  $2\theta \approx 5^\circ$  are expected in PH3 (circled in blue in Figure S9), but non-existent in the experimental diffractogram, which gives a good hint for the absence of the nitrosonium salt in the product.

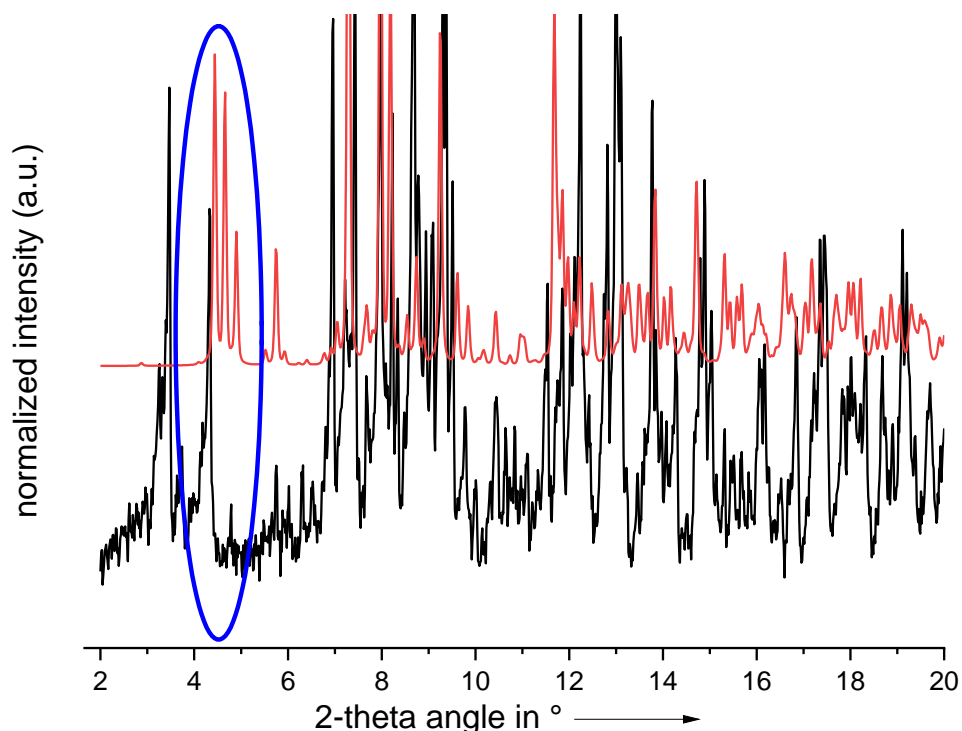


Figure S9: Comparison of the background corrected pXRD diffractogram of the probe (black line) with the simulated pXRD obtained from scXRD data of PH3  $[\text{NO}]^+[\text{F}\{\text{Al}(\text{OR}^{\text{F}})_3\}_2]^-$  (red line).

The main features of the experimental powder diffractogram can be clearly assigned to the 6FB solvate (PH1). However, other reflections are matching with the naphthalene<sup>F</sup> solvate (PH2). To obtain the exact fraction between the 6FB and the naphthalene<sup>F</sup> solvate, a Rietveld refinement would be required. However due to the large unit cells, resulting in a large number of reflections, and the data quality, we chose to determine the fraction *via* NMR spectroscopy.

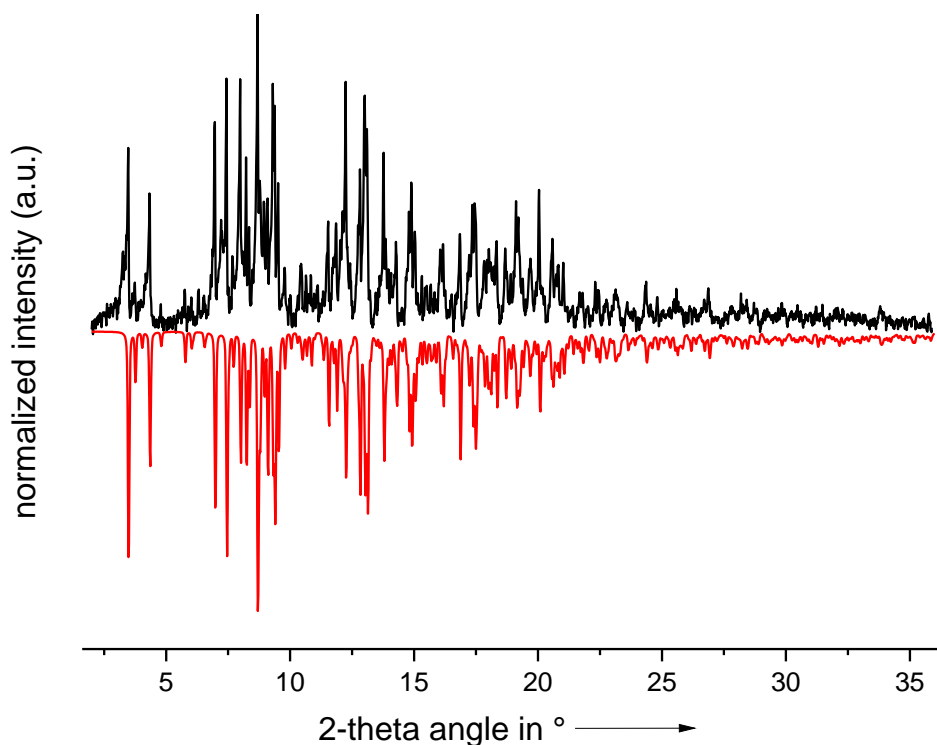


Figure S10: Comparison of the background corrected pXRD diffractogram of the probe (black line) with the simulated pXRD obtained from scXRD data of a 80:20 mixture of PH1  $[\text{naphthalene}^{\text{F}}]^+[\text{F}\{\text{Al}(\text{OR}^{\text{F}})_3\}_2]^- \cdot (6\text{FB})$  and  $[\text{naphthalene}^{\text{F}}]^+[\text{F}\{\text{Al}(\text{OR}^{\text{F}})_3\}_2]^- \cdot (\text{naphthalene}^{\text{F}})$  (red line).

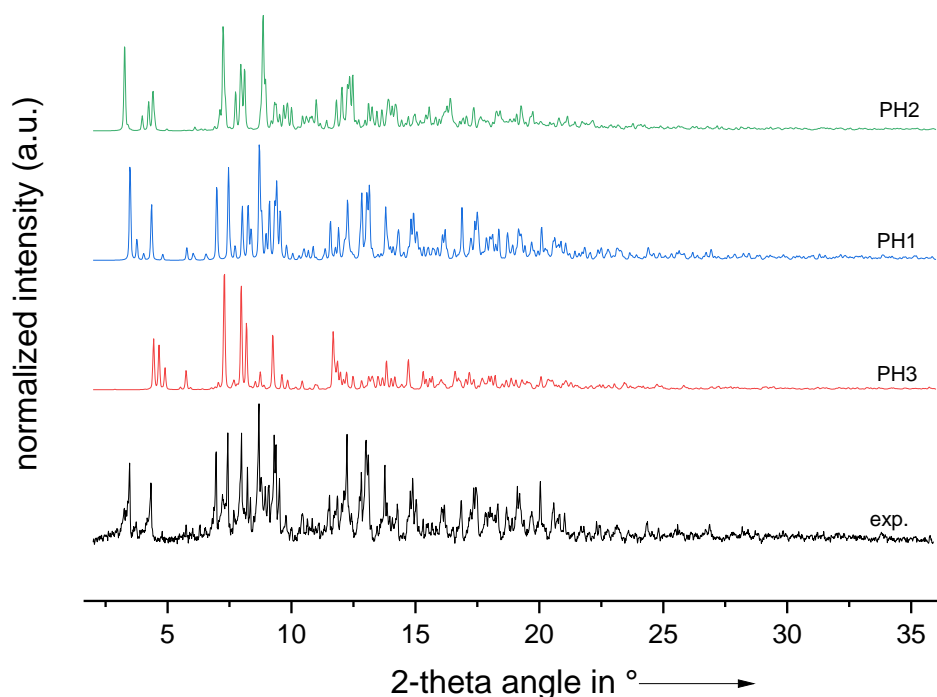


Figure S11: Comparison of the background corrected pXRD diffractogram of the probe (black line) with the simulated pXRD obtained from scXRD data of PH1 [naphthalene<sup>F</sup>]<sup>+</sup>[F{Al(OR<sup>F</sup>)<sub>3</sub>}<sub>2</sub>]<sup>-</sup>·6FB (blue line), PH2 [naphthalene<sup>F</sup>]<sup>+</sup>[F{Al(OR<sup>F</sup>)<sub>3</sub>}<sub>2</sub>]<sup>-</sup>·naphthalene<sup>F</sup> (green line) and PH3 [NO]<sup>+</sup>[F{Al(OR<sup>F</sup>)<sub>3</sub>}<sub>2</sub>]<sup>-</sup> (red line).

An easier test to rule out residual [NO]<sup>+</sup> content in [naphthalene<sup>F</sup>]<sup>+</sup>[F{Al(OR<sup>F</sup>)<sub>3</sub>}<sub>2</sub>]<sup>-</sup> is IR spectroscopy. While free [NO]<sup>+</sup> has only a weakly IR active  $\nu_{\text{NO}}$  vibration, nitrosonium ligands are typically strongly IR active. Tungsten hexacarbonyl W(CO)<sub>6</sub> reacts nearly quantitatively with [NO]<sup>+</sup> under ligand substitution towards the heteroleptic 18 VE complex [W(CO)<sub>5</sub>(NO)]<sup>+</sup>.<sup>[27]</sup> The [naphthalene<sup>F</sup>]<sup>+</sup> deelectronator, on the other hand, should react as a deelectronator forming the 17 VE complex [W(CO)<sub>6</sub>]<sup>+</sup>. Indeed, when the crude product [naphthalene<sup>F</sup>]<sup>+</sup>[F{Al(OR<sup>F</sup>)<sub>3</sub>}<sub>2</sub>]<sup>-</sup> (not washed with 6FB) was reacted with W(CO)<sub>6</sub>, a mixture of [W(CO)<sub>5</sub>(NO)]<sup>+</sup> and [W(CO)<sub>6</sub>]<sup>+</sup> formed (Figure S12). However, when the purified [naphthalene<sup>F</sup>]<sup>+</sup>[F{Al(OR<sup>F</sup>)<sub>3</sub>}<sub>2</sub>]<sup>-</sup> is used, the reaction yields very pure [W(CO)<sub>6</sub>]<sup>+</sup>[F{Al(OR<sup>F</sup>)<sub>3</sub>}<sub>2</sub>]<sup>-</sup> with only a very limited tiny contamination of [W(CO)<sub>5</sub>(NO)]<sup>+</sup> (Figure S13).

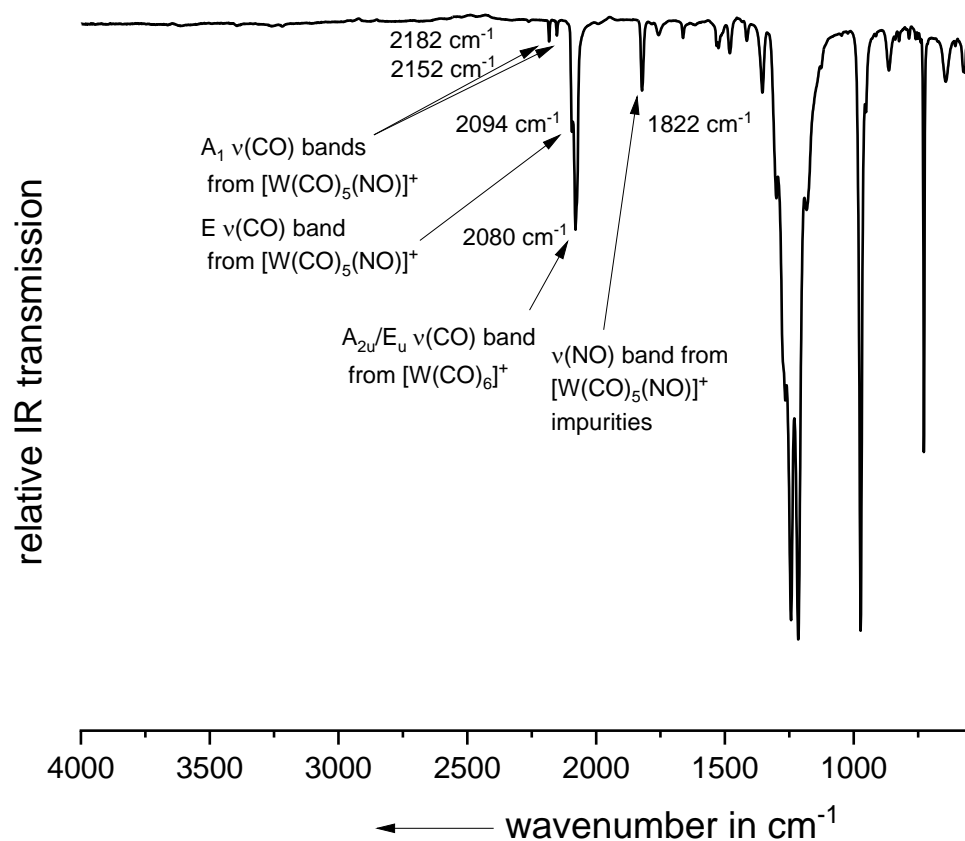


Figure S12: ATR-IR spectrum (ZnSe) of the reaction of unpurified  $[\text{naphthalene}^{\text{F}}]^+[\text{F}\{\text{Al}(\text{OR}^{\text{F}})_3\}_2]^-$  contaminated with  $[\text{NO}]^+[\text{F}\{\text{Al}(\text{OR}^{\text{F}})_3\}_2]^-$  with  $\text{W}(\text{CO})_6$ , yielding to a mixture of  $[\text{W}(\text{CO})_6]^+[\text{F}\{\text{Al}(\text{OR}^{\text{F}})_3\}_2]^-$  and  $[\text{W}(\text{CO})_5(\text{NO})]^+[\text{F}\{\text{Al}(\text{OR}^{\text{F}})_3\}_2]^-$ .

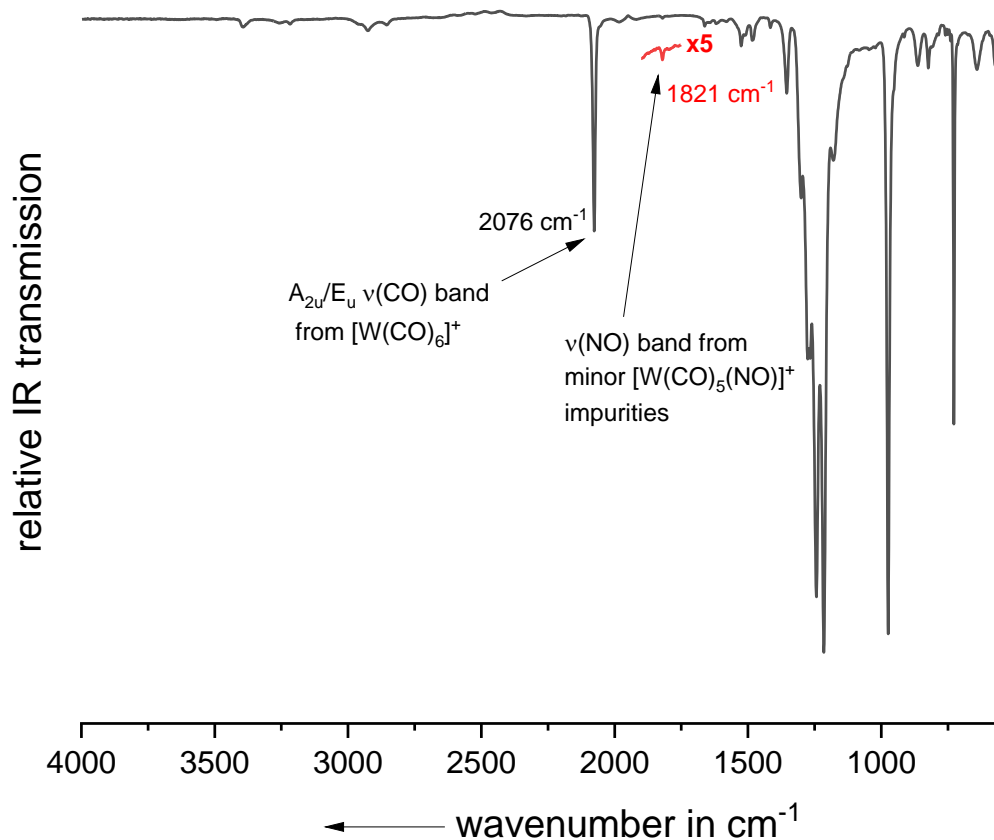


Figure S13: ATR-IR spectrum (ZnSe) of the reaction of purified  $[\text{naphthalene}^{\text{F}}]^+[\text{F}\{\text{Al}(\text{OR}^{\text{F}})_3\}_2]^-$  with  $\text{W}(\text{CO})_6$ , yielding nearly quantitatively  $[\text{W}(\text{CO})_6]^+[\text{F}\{\text{Al}(\text{OR}^{\text{F}})_3\}_2]^-$ .

While the paramagnetic  $[\text{naphthalene}^{\text{F}}]^+$  radical cation was not observed in the  $^{19}\text{F}$  NMR, after the reaction with an excess of ferrocene, its neutral state  $\text{naphthalene}^{\text{F}}$  gave rise to sharp peaks in the typical fluoroaromatic range (Figure S14). The integrals of these peaks can be compared to the integral of 6FB. The relation between these peaks gives the fraction of PH1 and PH2, which is estimated to be around 85:15  $[\text{naphthalene}^{\text{F}}]^+[\text{F}\{\text{Al}(\text{OR}^{\text{F}})_3\}_2]^- \cdot 6\text{FB} : [\text{naphthalene}^{\text{F}}]^+[\text{F}\{\text{Al}(\text{OR}^{\text{F}})_3\}_2]^- \cdot \text{naphthalene}^{\text{F}}$ .

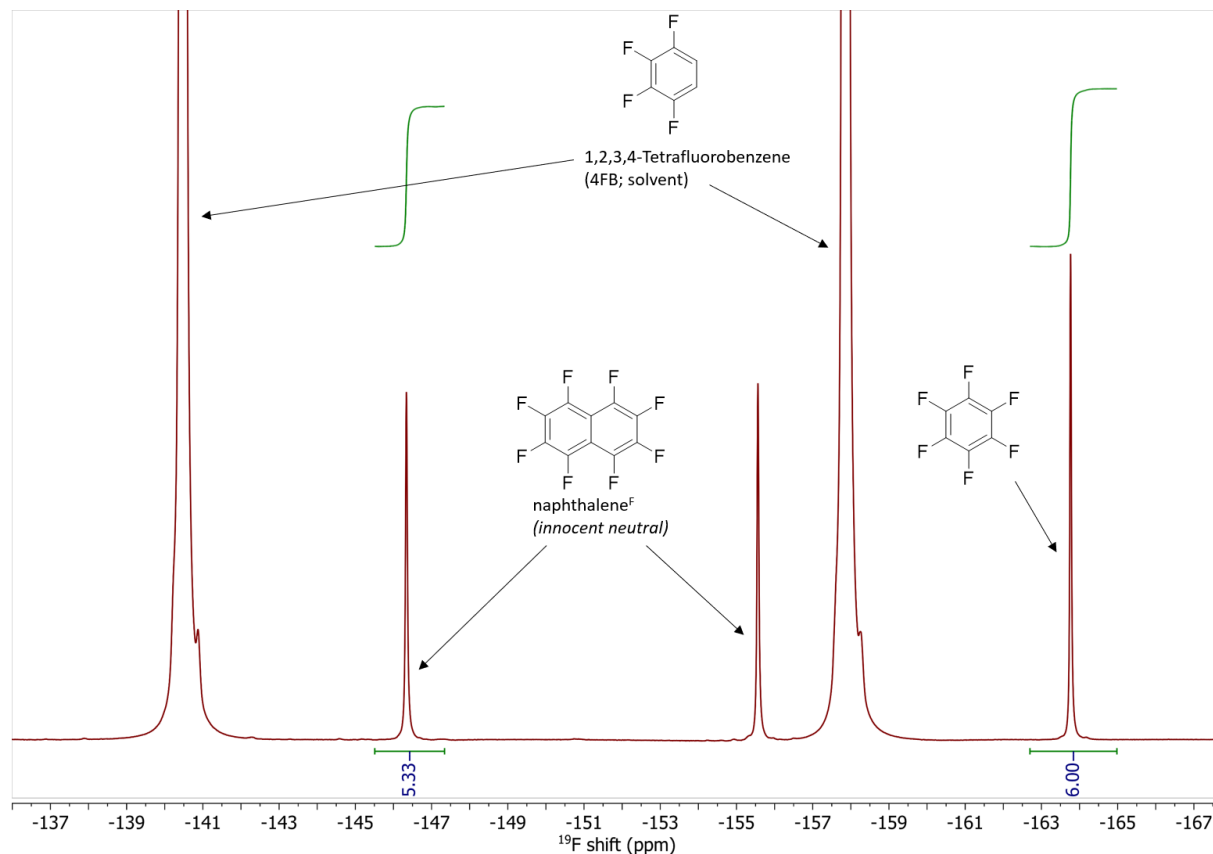


Figure S14:  $^{19}\text{F}$  NMR spectrum of  $[\text{naphthalene}^{\text{F}}]^+[\text{F}\{\text{Al}(\text{OR}^{\text{F}})_3\}_2]^-$  after the reaction with an excess of ferrocene.

## 2.2 Bis(scorpionato)iron(II-IV)

### 2.2.1 Cyclic Voltammetry of $\text{Fe}(\text{sc})_2$

Table S2: Key data of the electrochemical transition  $[\text{Fe}(\text{sc})_2]^0 \rightarrow [\text{Fe}(\text{sc})_2]^+$  at different scan rates (20–1000  $\text{mV s}^{-1}$ ) with of  $\text{Fe}(\text{sc})_2$  (10 mM) in 1,2,3,4-tetrafluorobenzene using  $[\text{NBu}_4]^+[\text{Al}(\text{OR}^F)_4]^-$  (100 mM) as supporting electrolyte.

Scan rate in $\text{mV s}^{-1}$	Electronation potential in V	Deelectronation potential in V	Half-wave potential in V	Fc corrected half-wave potential in V	Peak difference in V	Current at anodic peak potential in $\mu\text{A}$
20	-0.363	-0.285	-0.324	-0.332	0.078	8.34
50	-0.364	-0.276	-0.320	-0.327	0.088	12.14
100	-0.372	-0.276	-0.324	-0.331	0.096	16.27
200	-0.371	-0.267	-0.319	-0.327	0.104	22.23
500	-0.385	-0.258	-0.321	-0.329	0.127	33.67
1000	-0.393	-0.255	-0.324	-0.332	0.139	45.68

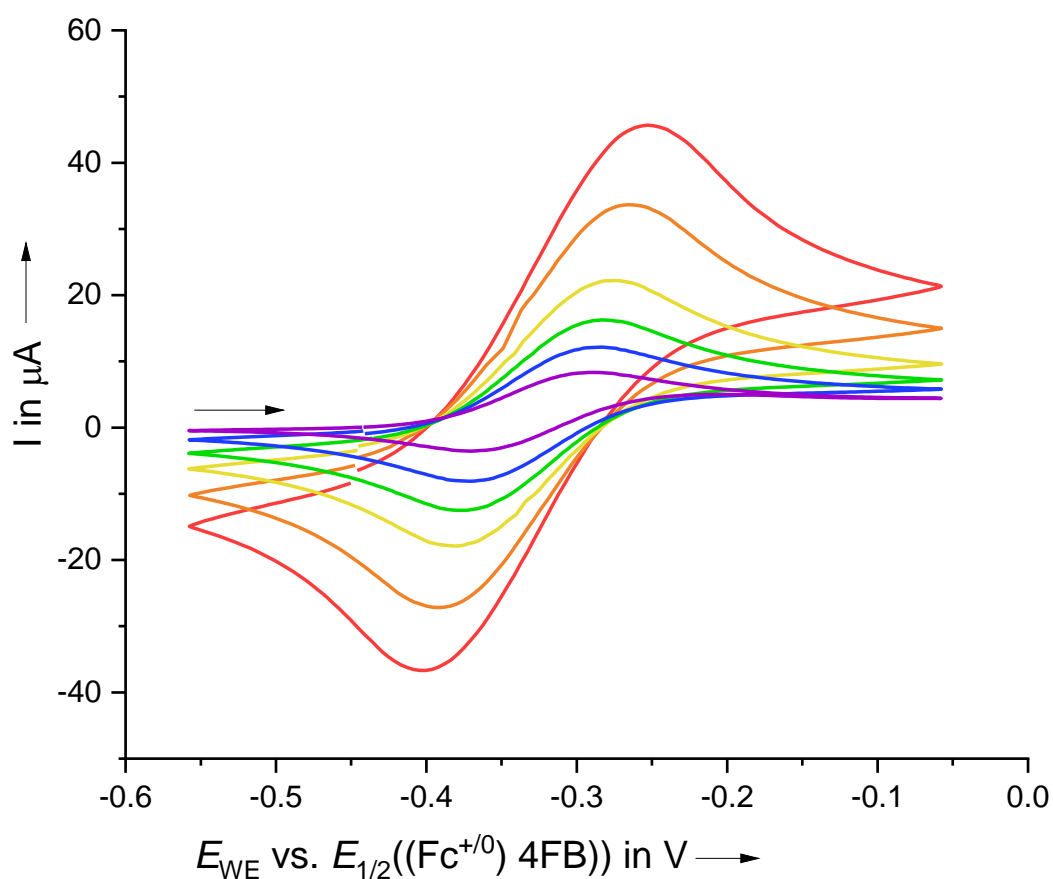


Figure S15: Cyclic voltammograms (2<sup>nd</sup> cycle) at different scan rates (purple (20  $\text{mV s}^{-1}$ )  $\rightarrow$  green (100  $\text{mV s}^{-1}$ )  $\rightarrow$  red (1000  $\text{mV s}^{-1}$ )) of  $\text{Fe}(\text{sc})_2$  (10 mM) in 1,2,3,4-tetrafluorobenzene using  $[\text{NBu}_4]^+[\text{Al}(\text{OR}^F)_4]^-$  (100 mM) as supporting electrolyte.



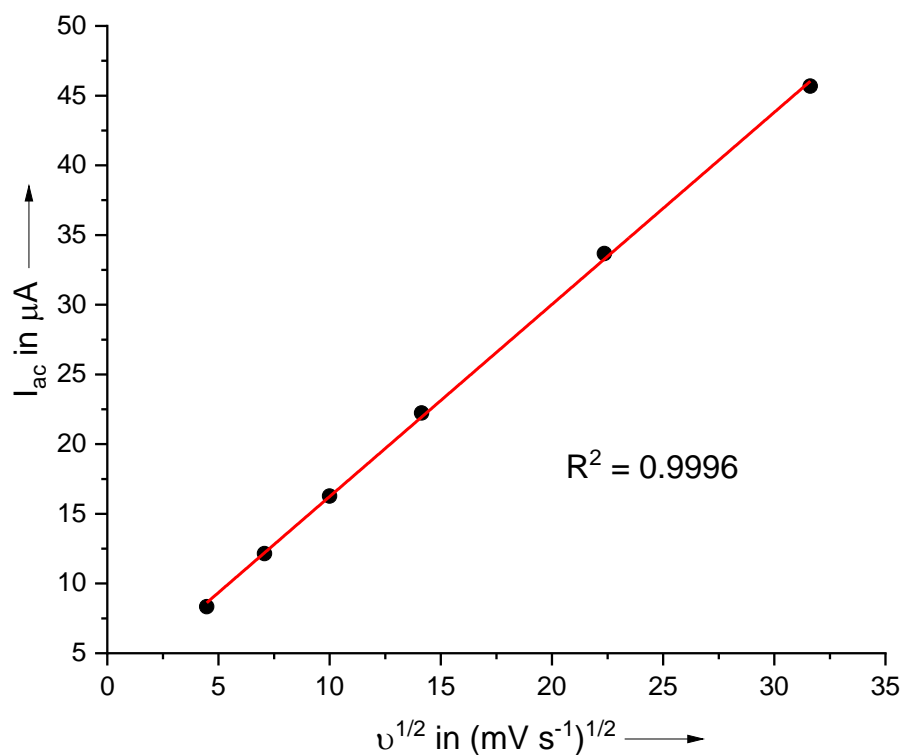


Figure S16: Linear fit of the anodic peak current  $I_{ac}$  against the square root of the scan rate  $v^{1/2}$  of  $[Fe(sc)_2]^{+/-0}$ .

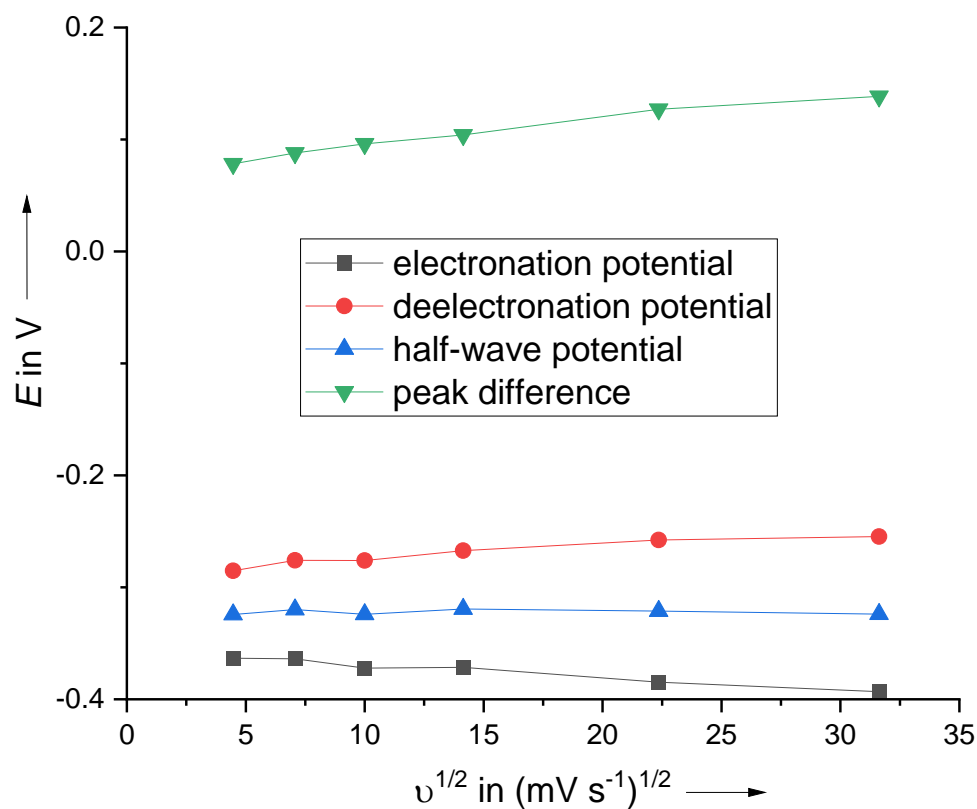


Figure S17: Electronation-, deelectronation- and half-wave potential & peak difference against the square root of the scan rate  $v^{1/2}$  of  $Fe(sc)_2]^{+/-0}$ .

Table S3: Key data of the electrochemical transition  $[\text{Fe}(\text{sc})_2]^+ \rightarrow [\text{Fe}(\text{sc})_2]^{2+}$  at different scan rates (20-1000  $\text{mV s}^{-1}$ ) with of  $\text{Fe}(\text{sc})_2$  (10 mM) in 1,2,3,4-tetrafluorobenzene using  $[\text{NBu}_4]^+[\text{Al}(\text{OR}^{\text{F}})_4]^-$  (100 mM) as supporting electrolyte.

Scan rate in $\text{mV s}^{-1}$	Electronation potential in V	Deelectronation potential in V	Half-wave potential in V	Fc corrected half-wave potential in V	Peak difference in V	Current at anodic peak potential in $\mu\text{A}$
20	--- no maximum peak current observed ---					
50	1.783	1.979	1.881	1.874	0.196	16.18
100	1.753	2.001	1.877	1.870	0.248	19.35
200	1.724	2.058	1.891	1.884	0.334	21.43
500	1.635	2.073	1.854	1.847	0.438	27.51
1000	1.626	2.112	1.869	1.862	0.486	37.71

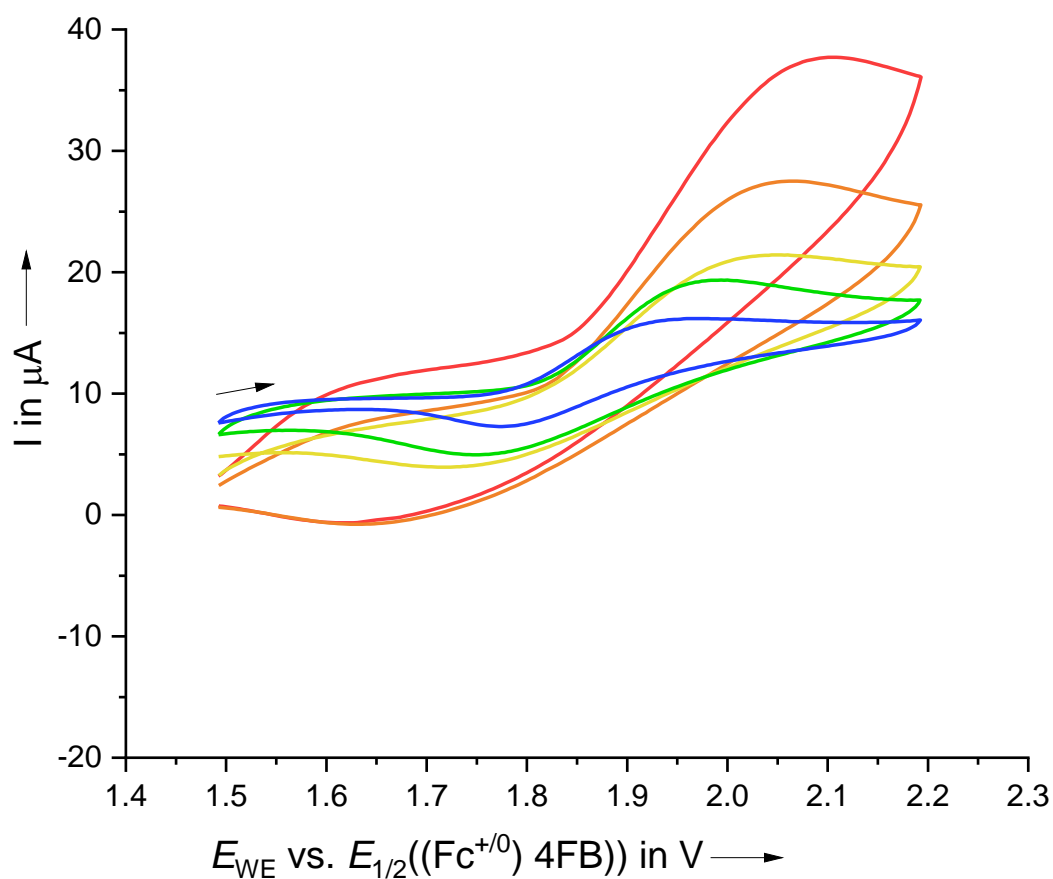


Figure S18: Cyclic voltammograms (2<sup>nd</sup> cycle) at different scan rates (blue (50  $\text{mV s}^{-1}$ )  $\rightarrow$  green (100  $\text{mV s}^{-1}$ )  $\rightarrow$  red (1000  $\text{mV s}^{-1}$ )) of  $\text{Fe}(\text{sc})_2$  (10 mM) in 1,2,3,4-tetrafluorobenzene using  $[\text{NBu}_4]^+[\text{Al}(\text{OR}^{\text{F}})_4]^-$  (100 mM) as supporting electrolyte.

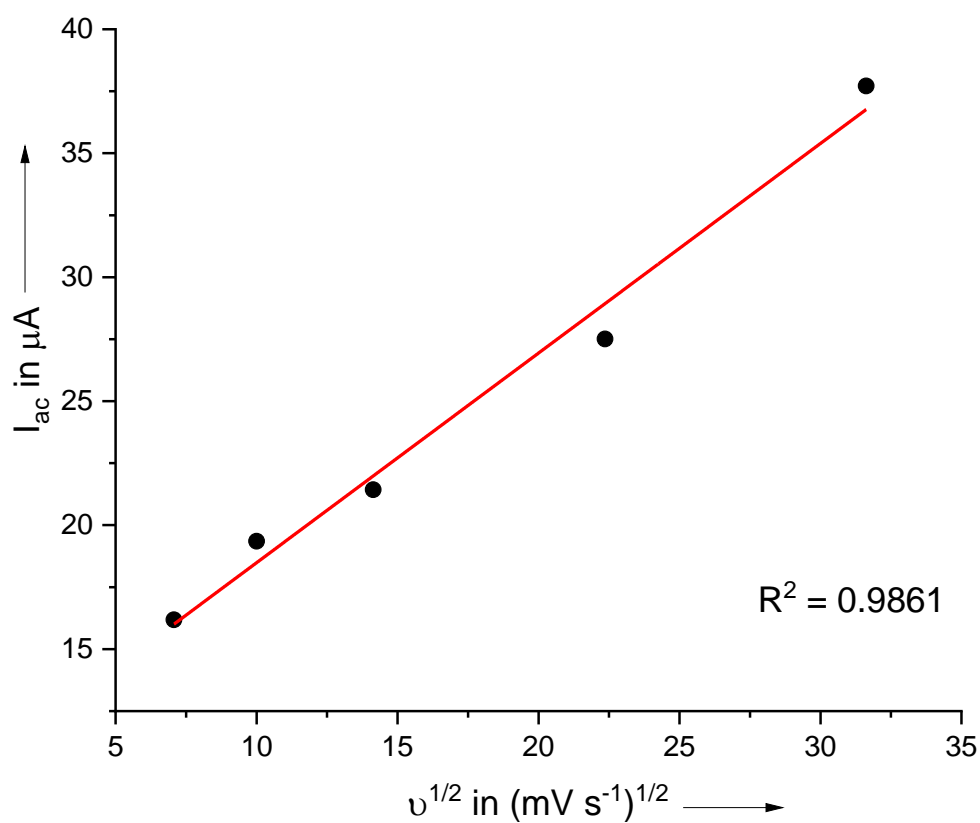


Figure S19: Linear fit of the anodic peak current  $I_{ac}$  against the square root of the scan rate  $v^{1/2}$  of  $[Fe(sc)_2]^{++/+}$ .

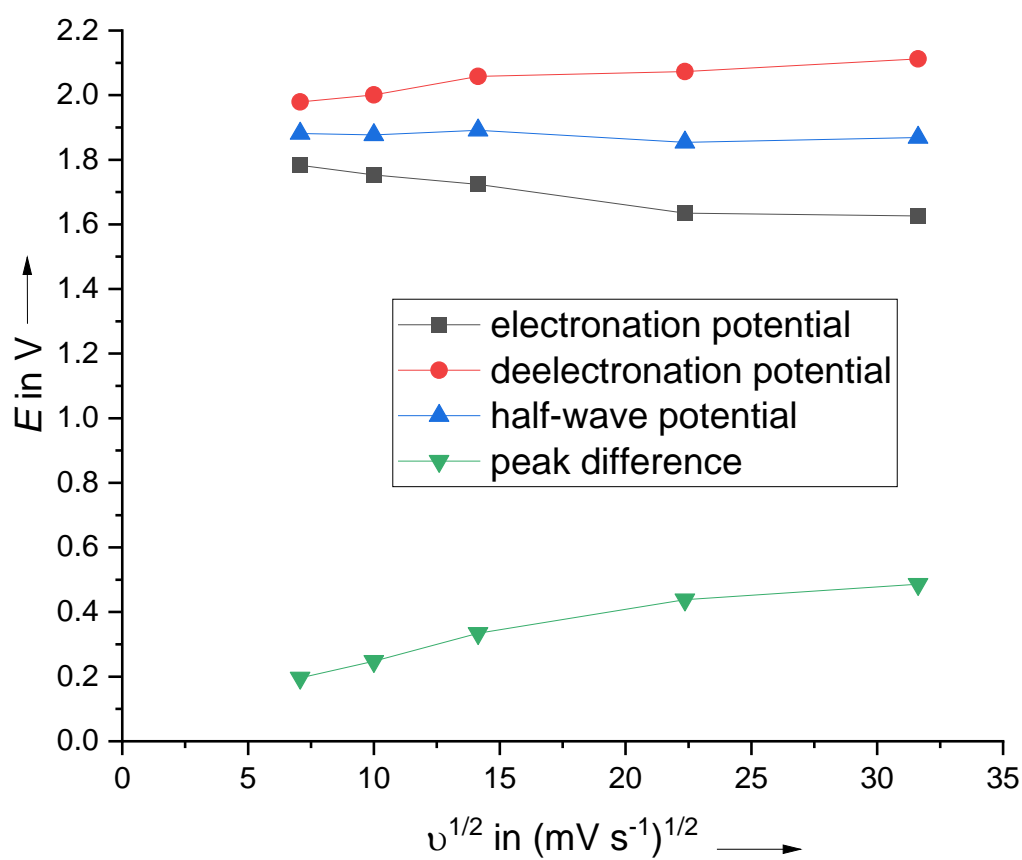


Figure S20: Electronation-, deelectronation- and half-wave potential & peak difference against the square root of the scan rate  $v^{1/2}$  of  $Fe(sc)_2]^{++/+}$ .

### 2.2.2 Synthesis and Characterization of Fe(sc)<sub>2</sub>

Iron sulfate heptahydrate (0.28 g, 1.0 eq., 1.0 mmol) and potassium scorpionate ( $K^+[HB(C_3N_2H_3)_3]^-$ ) (0.50 g, 2.0 eq., 2.0 mmol) were dissolved in water (50 mL). After 30 minutes of stirring, the mixture was filtrated and the purple residue was washed with water and dried afterwards at the high vacuum for two hours. The product, bis(scorpionato)iron(II) was obtained as a light purple powder (0.46 g, 95 %, 0.95 mmol).

#### Vibrational Spectroscopy

ATR IR (Diamond, powder)  $\tilde{\nu} / \text{cm}^{-1} = 3133 \text{ (vw)}, 3112 \text{ (vw)}, 2493 \text{ (vw)}, 1707 \text{ (vw)}, 1679 \text{ (vw)}, 1604 \text{ (vw)}, 1580 \text{ (vw)}, 1495 \text{ (vw)}, 1427 \text{ (vw)}, 1408 \text{ (w)}, 1401 \text{ (w)}, 1310 \text{ (w)}, 1211 \text{ (m)}, 1109 \text{ (s)}, 1071 \text{ (w)}, 1041 \text{ (s)}, 984 \text{ (vw)}, 929 \text{ (vw)}, 923 \text{ (vw)}, 885 \text{ (vw)}, 866 \text{ (vw)}, 842 \text{ (vw)}, 824 \text{ (vw)}, 798 \text{ (w)}, 759 \text{ (m)}, 748 \text{ (m)}, 740 \text{ (s)}, 728 \text{ (w)}, 716 \text{ (vs)}, 676 \text{ (w)}, 670 \text{ (m)}, 619 \text{ (w)}.$

Raman  $\tilde{\nu} / \text{cm}^{-1} = 3142 \text{ (w)}, 3112 \text{ (w)}, 2494 \text{ (w)}, 1685 \text{ (w)}, 1635 \text{ (w)}, 1553 \text{ (w)}, 1499 \text{ (w)}, 1403 \text{ (s)}, 1312 \text{ (vs)}, 1219 \text{ (vs)}, 1163 \text{ (w)}, 1138 \text{ (w)}, 1111 \text{ (w)}, 1092 \text{ (m)}, 1071 \text{ (w)}, 1041 \text{ (w)}, 1000 \text{ (vw)}, 986 \text{ (w)}, 929 \text{ (w)}, 800 \text{ (w)}, 485 \text{ (vw)}, 442 \text{ (w)}, 413 \text{ (w)}, 391 \text{ (vw)}, 350 \text{ (vw)}, 319 \text{ (vw)}, 278 \text{ (vw)}, 278 \text{ (vw)}, 256 \text{ (vw)}, 247 \text{ (vw)}, 199 \text{ (m)}, 184 \text{ (w)}, 150 \text{ (w)}, 107 \text{ (vs)}.$

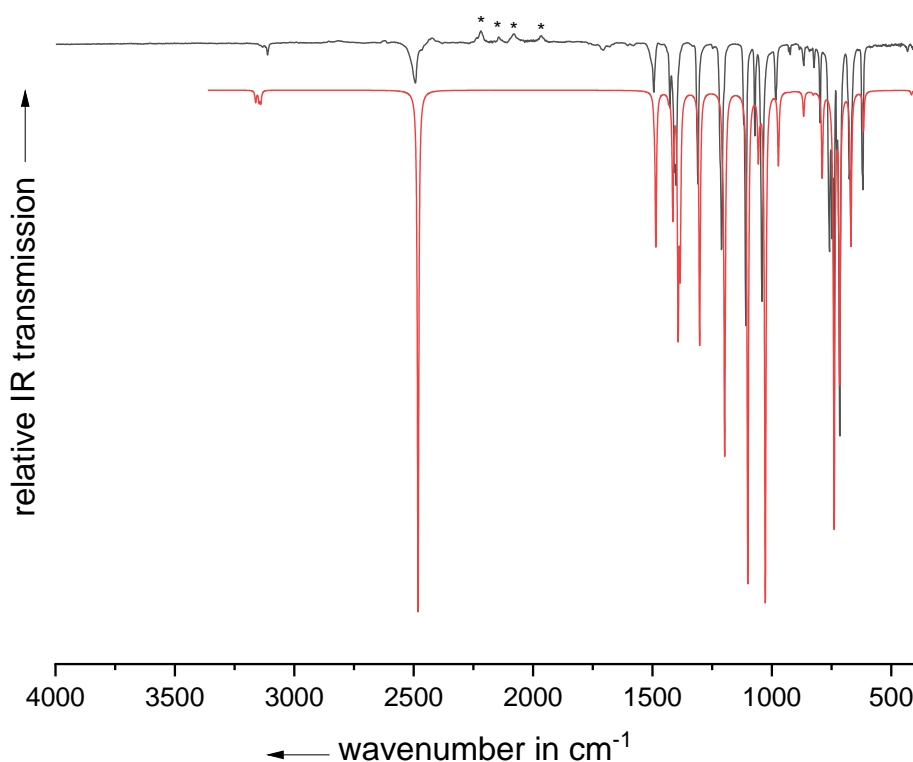


Figure S21: Comparison of the ATR-IR spectrum (Diamond) of Fe(sc)<sub>2</sub> powder (32 scans, black line) with the B3LYP(D3BJ)/def2-TZVPP calculated IR spectrum of Fe(sc)<sub>2</sub> (red line) scaled by 0.9657. Bands marked with “\*” are artefacts of the diamond window.

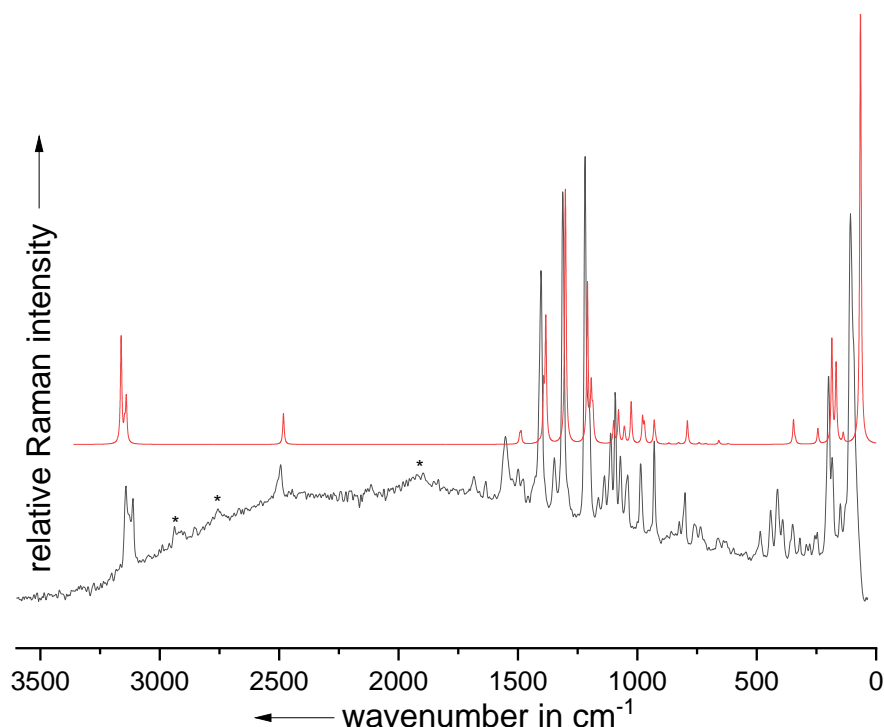


Figure S22: Comparison of the Raman spectrum of  $\text{Fe}(\text{sc})_2$  (1000 scans, 50 mW, black line) with the B3LYP(D3BJ)/def2-TZVPP calculated Raman spectrum of  $\text{Fe}(\text{sc})_2$  (red line) scaled by 0.9657. Bands marked with “\*” are artefacts of the spectrometer.

### 2.2.3 Synthesis and Characterization of $[\text{Fe}(\text{sc})_2]^+[\text{F}\{\text{Al}(\text{OR}^{\text{F}})_3\}_2]^-$

$[\text{NO}]^+[\text{F}\{\text{Al}(\text{OR}^{\text{F}})_3\}_2]^-$  (0.10 g, 66  $\mu\text{mol}$ , 1.1 eq.) and bis(scorpionato)iron(II) (29 mg, 60  $\mu\text{mol}$ , 1.0 eq.) were dissolved in 1,2-difluorobenzene (1 mL). The intense orange solution was stirred for a few minutes and was layered with *n*-pentane (10 mL) afterwards. A few days later, the solvent was removed and the crystalline product was washed with *n*-pentane (10 mL). The product was obtained as crystalline bright orange/red blocks (71 mg, 60 %, 36  $\mu\text{mol}$ ).

#### scXRD

$P\bar{1}$ ,  $a = 12.616(3) \text{ \AA}$ ,  $b = 14.712(2) \text{ \AA}$ ,  $c = 19.020(5) \text{ \AA}$ ,  $\alpha = 77.082(11)^\circ$ ,  $\beta = 71.115(15)^\circ$ ,  $\gamma = 89.325(10)^\circ$ ,  $V = 3248.5(13) \text{ \AA}^3$ ,  $Z = 2$ .

#### Vibrational Spectroscopy

ATR IR (Diamond, crystals)  $\tilde{\nu} / \text{cm}^{-1} = 3170 (\text{vw})$ , 2503 (vw), 1751 (vw), 1504 (vw), 1421 (vw), 1409 (vw), 1394 (vw), 1353 (vw), 1323 (vw), 1300 (w), 1277 (m), 1241 (vs), 1214 (vs), 1193 (s), 1170 (m), 1122 (w), 1106 (vw), 1074 (w), 1052 (m), 996 (vw), 973 (vs), 896 (vw), 861 (vw), 825 (vw), 798 (w), 767 (s), 727 (vs), 710 (m), 663 (w), 634 (w), 615 (w), 568 (w), 537 (m), 460 (m), 449 (m).

Raman  $\tilde{\nu} / \text{cm}^{-1} = 3168 (\text{vw})$ , 3159 (vw), 3136 (vw), 2520 (vw), 1450 (vw), 1439 (vw), 1410 (w), 1389 (m), 1325 (m), 1229 (m), 1217 (w), 1192 (w), 1112 (w), 1080 (w), 1050 (vw), 995 (w), 929 (w), 866 (w), 815 (w), 753 (s), 734 (m), 675 (s), 644 (s), 570 (s), 543 (s), 375 (w), 325 (w), 302 (m), 268 (w), 200 (s), 166 (s), 96 (vs).

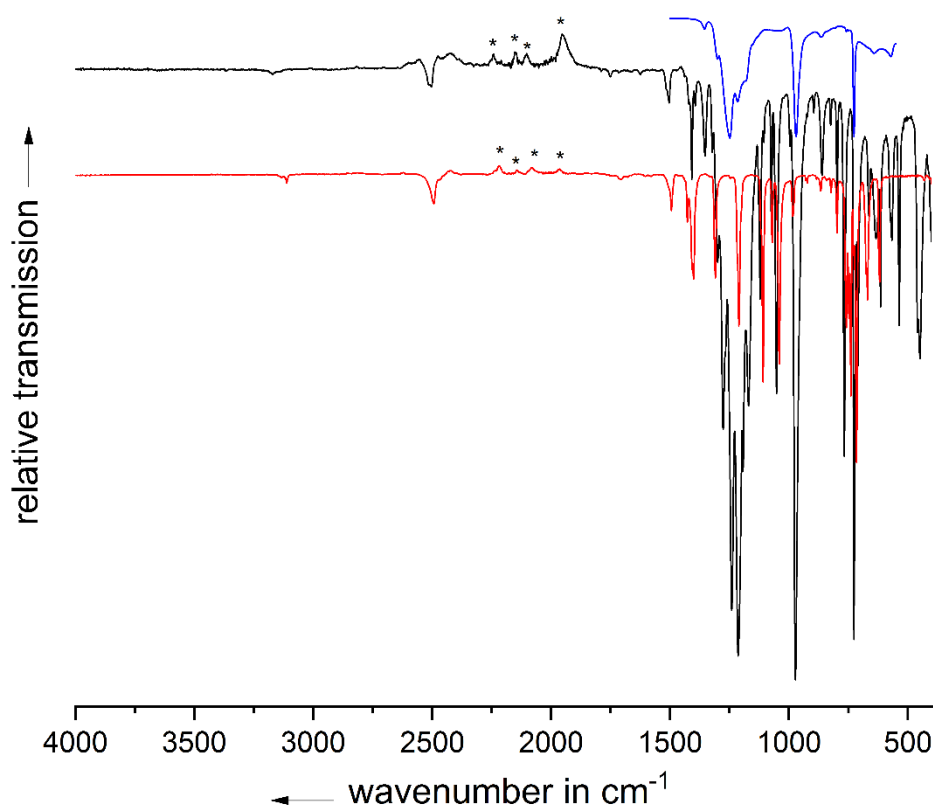


Figure S23: Comparison of ATR-IR spectrum (Diamond) spectrum of crystalline  $[\text{Fe}(\text{sc})_2]^+[\text{F}\{\text{Al}(\text{OR}^{\text{F}})_3\}_2]^-$  (32 scans, black line) with the IR spectrum of neutral  $\text{Fe}(\text{sc})_2$  (red line) and  $[\text{NO}]^+[\text{F}\{\text{Al}(\text{OR}^{\text{F}})_3\}_2]^-$  (blue line; to show the expectation spectrum of the anion bands). Bands marked with "\*" are artefacts of the diamond window.

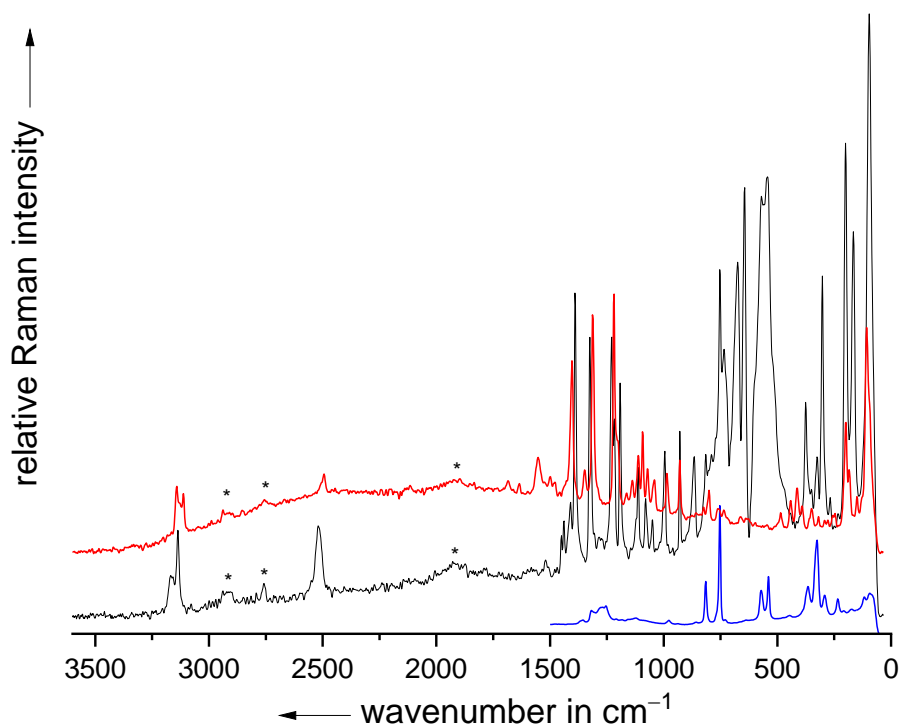


Figure S24: Comparison of the Raman spectrum of  $[\text{Fe}(\text{sc})_2]^+[\text{F}\{\text{Al}(\text{OR}^{\text{F}})_3\}_2]^-$  (1000 scans, 50 mW, black line) with the Raman spectrum of neutral  $\text{Fe}(\text{sc})_2$  (red line) and  $[\text{NO}]^+[\text{F}\{\text{Al}(\text{OR}^{\text{F}})_3\}_2]^-$  (blue line; to show the expectation spectrum of the anion bands). Bands marked with "\*" are artefacts of the spectrometer.

#### 2.2.4 Synthesis and Characterization of $[\text{Fe}(\text{sc})_2]^{2+}([\text{F}\{\text{Al}(\text{OR}^{\text{F}})_3\}_2]^-)_2$

$[\text{Fe}(\text{sc})_2]^+[\text{F}\{\text{Al}(\text{OR}^{\text{F}})_3\}_2]^-$  (25 mg, 18  $\mu\text{mol}$ , 1.0 eq.) and  $[\text{naphthalene}^{\text{F}}]^+[\text{F}\{\text{Al}(\text{OR}^{\text{F}})_3\}_2]^-$  (38 mg, 21  $\mu\text{mol}$ , 1.2 eq.) were filled into a Schlenk tube and 1,2,3,4-tetrafluorobenzene (1 mL) was added. The solution was evaporated in a glove box, which gave brown single-crystals of  $[\text{Fe}(\text{sc})_2]^{2+}([\text{F}\{\text{Al}(\text{OR}^{\text{F}})_3\}_2]^-)_2 \cdot (4\text{FB})_3$  suitable for scXRD. The product was washed with 6FB to remove naphthalene<sup>F</sup> (45 mg, 72 %, 13  $\mu\text{mol}$ ).

The Mössbauer spectrum just shows an iron-based purity of ca. 80 %, with 10 %  $[\text{Fe}(\text{sc})_2]^+$  and 10 %  $\text{Fe}(\text{sc})_2$  impurities, which could be either a result of an incomplete reaction or partial decomposition during the sample preparation (in Freiburg) and transportation (to Kiel, over several days at r.t.).

#### scXRD

$P\bar{1}$ ,  $a = 12.344(2)$  Å,  $b = 14.699(3)$  Å,  $c = 18.545(4)$  Å,  $\alpha = 77.130(16)^\circ$ ,  $\beta = 72.296(15)^\circ$ ,  $\gamma = 88.16(2)^\circ$ ,  $V = 3122.6(11)$  Å<sup>3</sup>,  $Z = 1$ .

#### IR spectroscopy

ATR-IR (ZnSe, crystals)  $\tilde{\nu} / \text{cm}^{-1} = 3168$  (vw), 2513 (vw), 2502 (vw), 1929 (vw), 1663 (vw), 1545 (vw), 1504 (vw), 1481 (vw), 1416 (vw), 1409 (vw), 1354 (vw), 1300 (w), 1276 (m), 1266 (m), 1243 (vs), 1215 (vs), 1179 (w), 1161 (w), 1123 (w), 1075 (vw), 1053 (vw), 974 (vs), 952 (w), 863 (vw), 798 (vw), 786 (vw), 768 (w), 727 (s), 710 (vw), 663 (vw), 634 (vw), 616 (vw), 568 (vw).

Raman spectra could not be obtained due to fluorescence of the probe

#### Mössbauer

$\delta_{\text{is}} / \text{mm s}^{-1}$ : -0.25;  $\Delta E_{\text{Q}} / \text{mm s}^{-1}$ : 2.41.

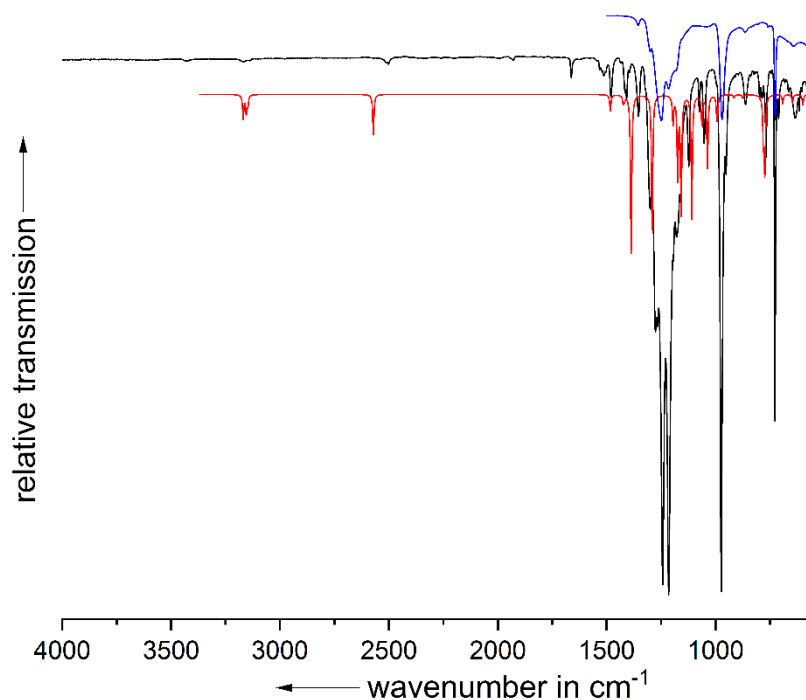


Figure S25: Comparison of the ATR-IR spectrum (ZnSe) spectrum of crystalline  $[\text{Fe}(\text{sc})_2]^{2+}([\text{F}\{\text{Al}(\text{OR}^{\text{F}})_3\}_2]^-)_2$  (32 scans, black line) with the B3LYP(D3BJ)/def2-TZVPP calculated IR spectrum of  $[\text{Fe}(\text{sc})_2]^{2+}$  (red line) scaled by 0.9657 and the IR spectrum of  $[\text{NO}]^+[\text{F}\{\text{Al}(\text{OR}^{\text{F}})_3\}_2]^-$  (blue line; to show the expectation spectrum of the anion bands).

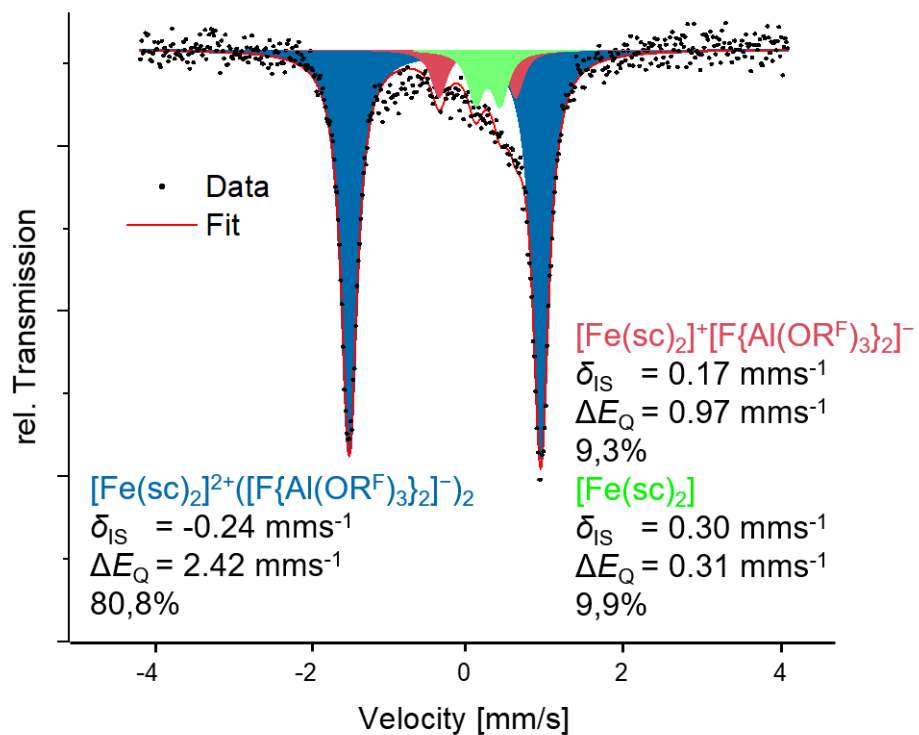


Figure S26: Zero-field  $^{57}\text{Fe}$  Mössbauer spectra of  $[\text{Fe}(\text{sc})_2]^{2+}([\text{F}\{\text{Al}(\text{OR}^{\text{F}})_3\}_2]^-)_2$ , recorded under zero applied magnetic field and at 80 K (relative transmission versus velocity, in mm/s).



## 2.3 Ferrocene

### 2.3.1 Cyclic Voltammetry of Ferrocene

To observe a possible second deelectronation of ferrocene, the potential was scanned up to the solvent decomposition. With exception to the first deelectronation of ferrocene, the cyclic voltammogram is identical to the solvent window. The second deelectronation is expected at +2.40 V vs.  $\text{Fc}^{+/0}$  in 4FB (see main text), a deelectronation at this potential would be too close to the solvent decomposition at +2.43 V vs.  $\text{Fc}^{+/0}$  to observe.

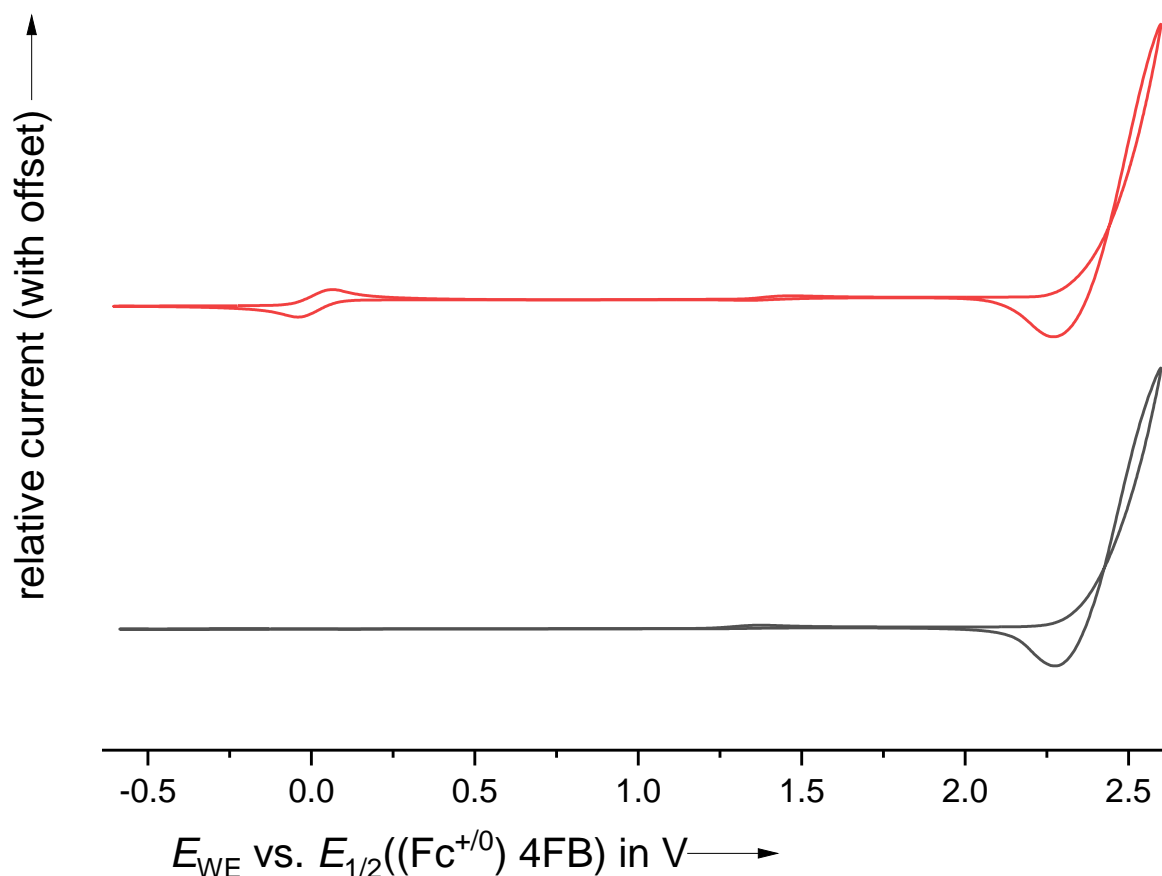


Figure S27: Cyclic voltammogram (1<sup>st</sup> cycle) at 100 mV s<sup>-1</sup> of ferrocene (10 mM) in 1,2,3,4-tetrafluorobenzene using  $[\text{NBu}_4]^+[\text{Al}(\text{OR}^{\text{F}})_4]^-$  (100 mM) as supporting electrolyte (red line) in comparison with the solvent window  $[\text{NBu}_4]^+[\text{Al}(\text{OR}^{\text{F}})_4]^-$  (100 mM) in 1,2,3,4-tetrafluorobenzene (black line).

### 2.3.2 Synthesis and Characterization of $[\text{Fc}]^+[\text{F}\{\text{Al}(\text{OR}^{\text{F}})_3\}_2]^-$

$[\text{NO}]^+[\text{F}\{\text{Al}(\text{OR}^{\text{F}})_3\}_2]^-$  (0.10 g, 66  $\mu\text{mol}$ , 1.1 eq.) and ferrocene (11 mg, 60  $\mu\text{mol}$ , 1.0 eq.) were dissolved in 1,2-Difluorobenzene (1.0 mL). The intense blue solution was stirred for a few minutes and was layered with *n*-pentane (10 mL) afterwards. A few days later, the solvent was removed by filtration and the crystalline product was washed with *n*-pentane (10 mL). The product was obtained as large crystalline blue blocks (68 mg, 68 %, 41  $\mu\text{mol}$ ).

#### scXRD

$P2_1/c$ ,  $a = 10.513(3)$  Å,  $b = 18.004(3)$  Å,  $c = 13.813(4)$  Å,  $\alpha = 90^\circ$ ,  $\beta = 103.709(18)^\circ$ ,  $\gamma = 90^\circ$ ,  $V = 2540.0(11)$  Å<sup>3</sup>,  $Z = 2$ .

### Vibrational Spectroscopy

ATR-IR (Diamond, crystals)  $\tilde{\nu} / \text{cm}^{-1} = 3137 \text{ (vw)}, 1510 \text{ (vw)}, 1425 \text{ (vw)}, 1354 \text{ (vw)}, 1300 \text{ (w)}, 1266 \text{ (m)}, 1240 \text{ (s)}, 1209 \text{ (vs)}, 1174 \text{ (m)}, 1016 \text{ (vw)}, 970 \text{ (vs)}, 854 \text{ (w)}, 760 \text{ (vw)}, 726 \text{ (vs)}, 634 \text{ (w)}, 568 \text{ (w)}, 537 \text{ (m)}, 450 \text{ (m)}$ .

Raman  $\tilde{\nu} / \text{cm}^{-1} = 3139 \text{ (vw)}, 3123 \text{ (vw)}, 1426 \text{ (vw)}, 1363 \text{ (vw)}, 1307 \text{ (vw)}, 1272 \text{ (vw)}, 1257 \text{ (vw)}, 1115 \text{ (m)}, 1066 \text{ (vw)}, 850 \text{ (vw)}, 816 \text{ (vw)}, 753 \text{ (w)}, 569 \text{ (vw)}, 539 \text{ (vw)}, 364 \text{ (vw)}, 325 \text{ (w)}, 300 \text{ (vs)}, 233 \text{ (vw)}, 117 \text{ (vw)}, 78 \text{ (vw)}$ .

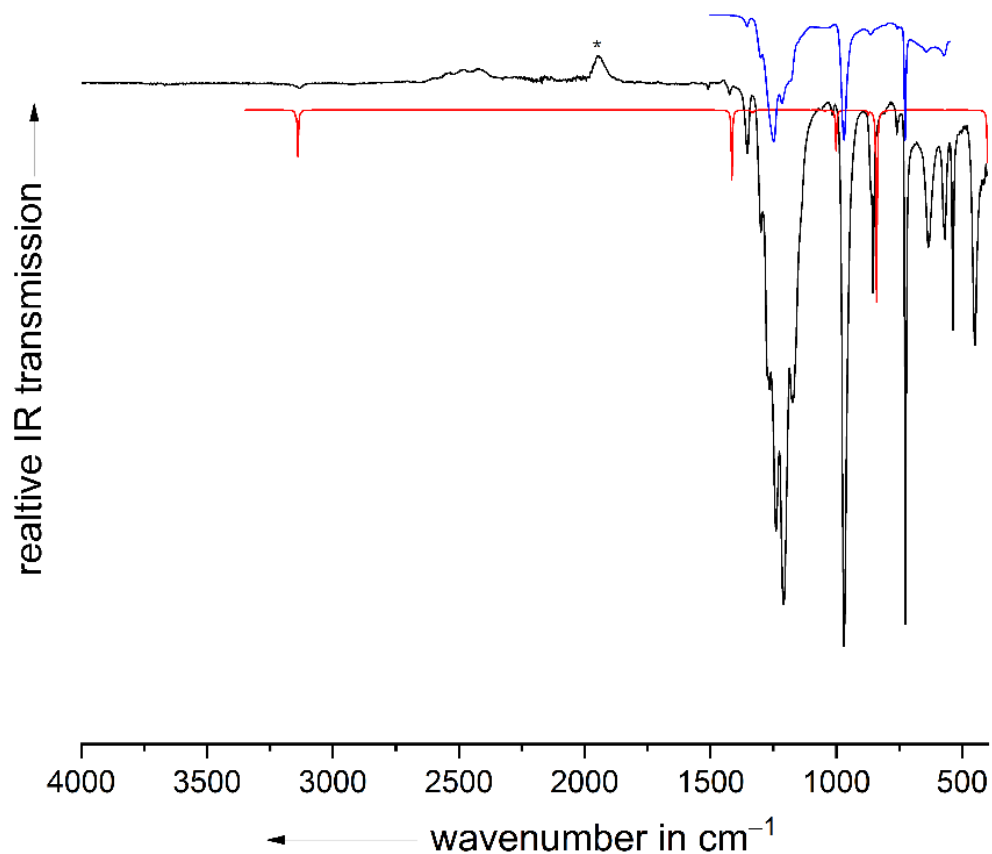


Figure S28: Comparison of the ATR-IR spectrum (diamond) of crystalline  $[\text{Fc}]^+[\text{F}\{\text{Al}(\text{OR}^{\text{F}})_3\}_2]^-$  (32 scans, black line) with the B3LYP(D3BJ)/def2-TZVPP calculated IR spectrum of  $[\text{Fc}]^+$  (red line) scaled by 0.9657 and the IR spectrum of  $[\text{NO}]^+[\text{F}\{\text{Al}(\text{OR}^{\text{F}})_3\}_2]^-$  (blue line; to show the expectation spectrum of the anion bands). Bands marked with “\*” are artefacts of the diamond window.

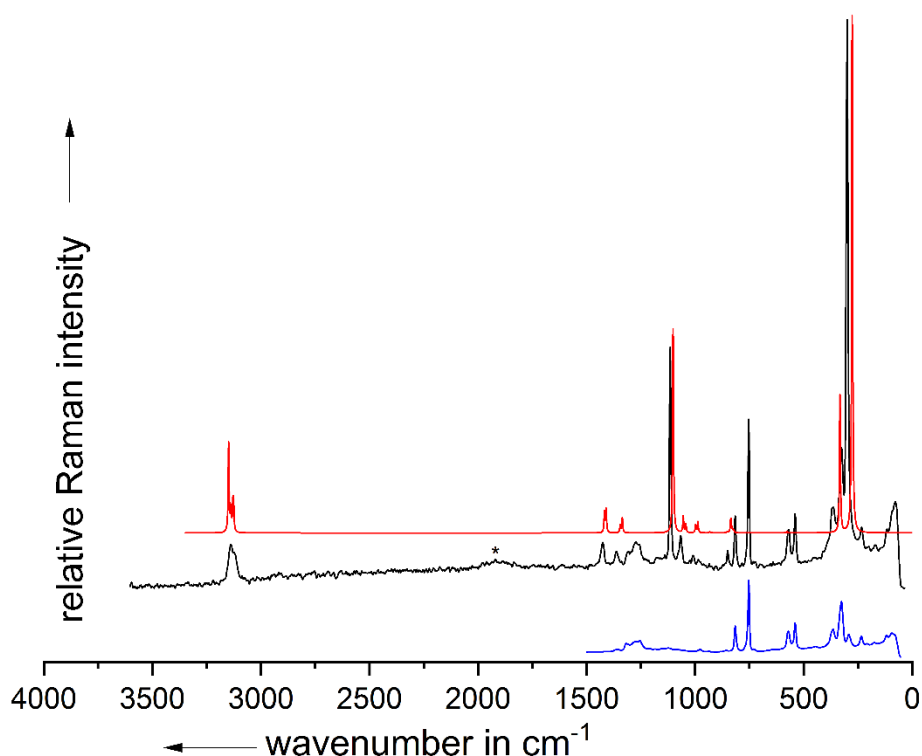


Figure S29: Comparison of the Raman spectrum of crystalline  $[\text{Fc}]^+[\text{F}\{\text{Al}(\text{OR}^{\text{F}})_3\}_2]^-$  (1000 scans, 50 mW, black line) with the B3LYP(D3BJ)/def2-TZVPP calculated Raman spectrum of  $[\text{Fc}]^+$  (red line) scaled by 0.9657 and the Raman spectrum of  $[\text{NO}]^+[\text{F}\{\text{Al}(\text{OR}^{\text{F}})_3\}_2]^-$  (blue line; to show the expectation spectrum of the anion bands). Bands marked with "\*" are artefacts of the spectrometer.

### 2.3.3 Synthesis and Characterization of $[\text{Fc}(\text{CO})]^{2+}([\text{F}\{\text{Al}(\text{OR}^{\text{F}})_3\}_2]^-)_2$

$[\text{Fc}]^+[\text{F}\{\text{Al}(\text{OR}^{\text{F}})_3\}_2]^-$  (70 mg, 42  $\mu\text{mol}$ , 1.0 eq.) and [naphthalene<sup>F</sup>] $[\text{F}\{\text{Al}(\text{OR}^{\text{F}})_3\}_2]^-$  (81 mg, 46  $\mu\text{mol}$ , 1.1 eq.) were filled in a YOUNG NMR tube and 4FB (1 mL) was added. The solution was cooled to  $-78^\circ\text{C}$  and the tube was evacuated. Afterwards, carbon monoxide pressure (2 bar) was added and the colour of the previously dark green solution faded to a lighter green-brown. The product was washed with 6FB (2x 3 mL) to remove naphthalene<sup>F</sup> and the product was isolated as a brownish solid (96 mg, 71 %, 30  $\mu\text{mol}$ ). Despite many attempts, the product could not be obtained as single crystals suitable for scXRD.

#### Vibrational Spectroscopy

ATR IR (ZnSe)  $\tilde{\nu} / \text{cm}^{-1}$  = 3133 (vw), 2131 (vw), 1662 (vw), 1524 (vw), 1519 (vw), 1480 (vw), 1415 (vw), 1354 (vw), 1300 (w), 1265 (s), 1243 (vs), 1215 (vs), 1215 (vs), 1215 (vs), 1127 (w), 1048 (vw), 972 (vs), 951 (m), 881 (vw), 863 (vw), 855 (vw), 801 (vw), 760 (vw), 746 (vw), 727 (s), 683 (vw), 634 (vw), 593 (vw), 568 (vw).

#### NMR Spectroscopy

$^1\text{H}$ -NMR (400 MHz, 4FB, 298 K):  $\delta$  = 7.57 (s, 10H) ppm. Additionally, small impurities of  $[\text{Fc}]^+$  were observed at 35.1 ppm.

$^{13}\text{C}$ -NMR (101 MHz, 4FB, 298 K):  $\delta$  = 78.2 (m, 12C, anion -  $\text{OC}(\text{CF}_3)_3$ ), 98.1 (s, 10C,  $^1J_{\text{C-H}}$  = 194 Hz), 120.6 (q, 36C, anion -  $\text{OC}(\text{CF}_3)_3$ ), 198.8 (s, 1C, CO) ppm.

$^{19}\text{F}$ -NMR (376 MHz, 4FB, 298 K):  $\delta$  =  $-76.3$  (s, 108F, anion -  $\text{OC}(\text{CF}_3)_3$ ),  $-184.9$  (s, 2F, anion - Al-F-Al) ppm.

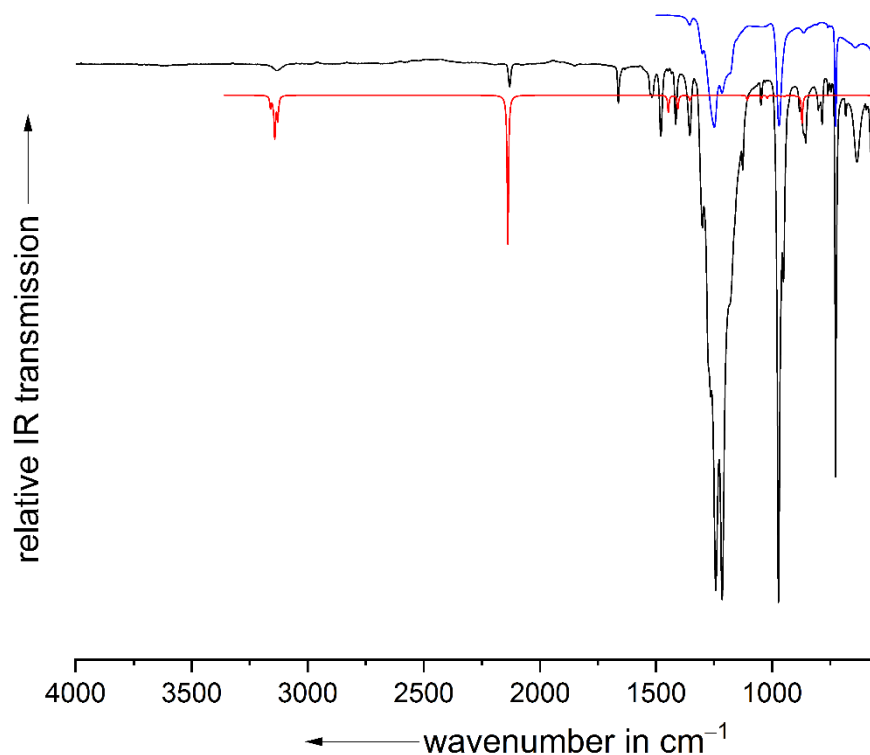


Figure S30: Comparison of the measured IR spectrum of  $[\text{Fc}(\text{CO})]^{2+}([\text{F}(\text{Al}(\text{OR}^{\text{F}})_3)_2]^-)_2$  (32 scans, black line) with the B3LYP(D3BJ)/def2-TZVPP calculated spectrum of  $[\text{Fc}(\text{CO})]^{2+}$  (red line) scaled by 0.968 according to Duncan *et al.* and the IR spectrum of  $[\text{NO}]^+[\text{F}(\text{Al}(\text{OR}^{\text{F}})_3)_2]^-$  (blue line; to show the expectation spectrum of the anion bands).

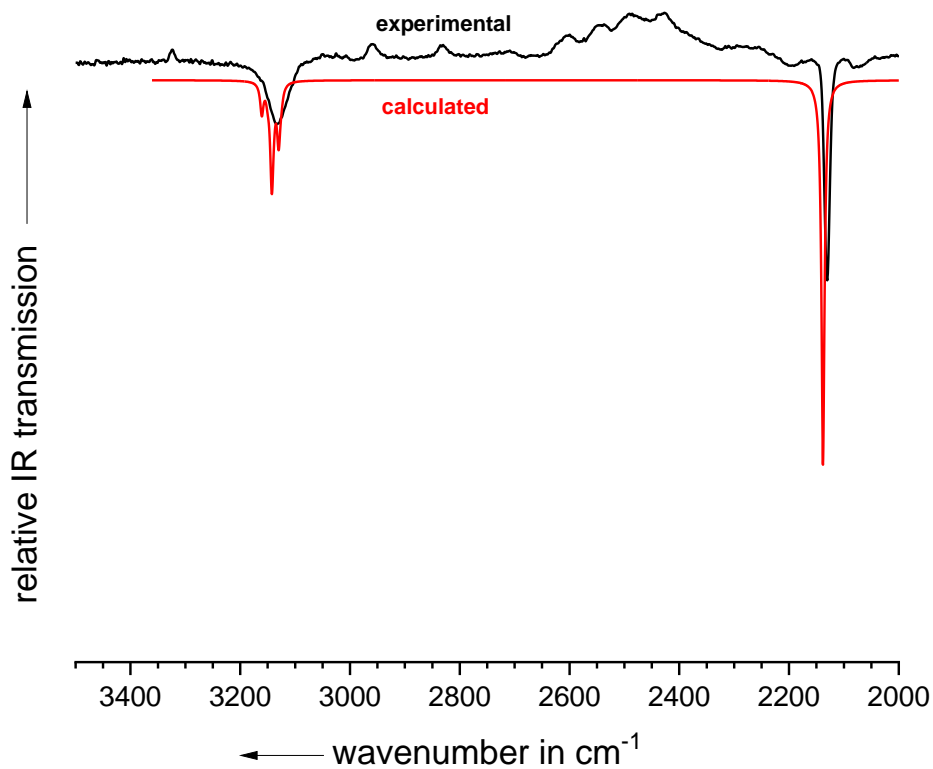


Figure S31: Comparison of the measured IR spectrum of  $[\text{Fc}(\text{CO})]^{2+}([\text{F}(\text{Al}(\text{OR}^{\text{F}})_3)_2]^-)_2$  (32 scans, black line) with the B3LYP(D3BJ)/def2-TZVPP calculated spectrum of  $[\text{Fc}(\text{CO})]^{2+}$  (red line) scaled by 0.968 according to Duncan *et al.* in the range of 3500–2000  $\text{cm}^{-1}$ .

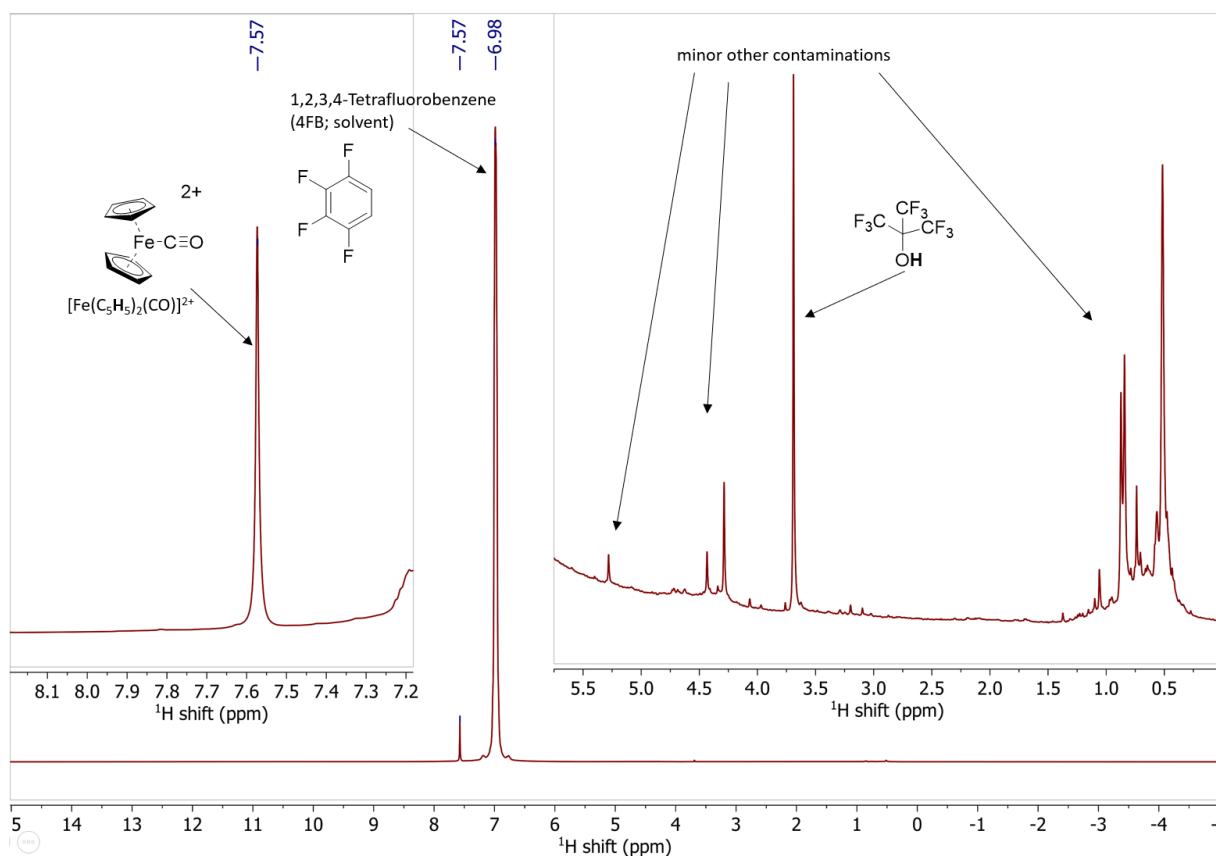


Figure S32:  $^1\text{H}$  NMR spectrum of  $[\text{Fc}(\text{CO})]^{2+}([\text{F}\{\text{Al}(\text{OR}^{\text{F}})_3\}_2]^-)_2$  in 1,2,3,4-tetrafluorobenzene (4FB) at room temperature.

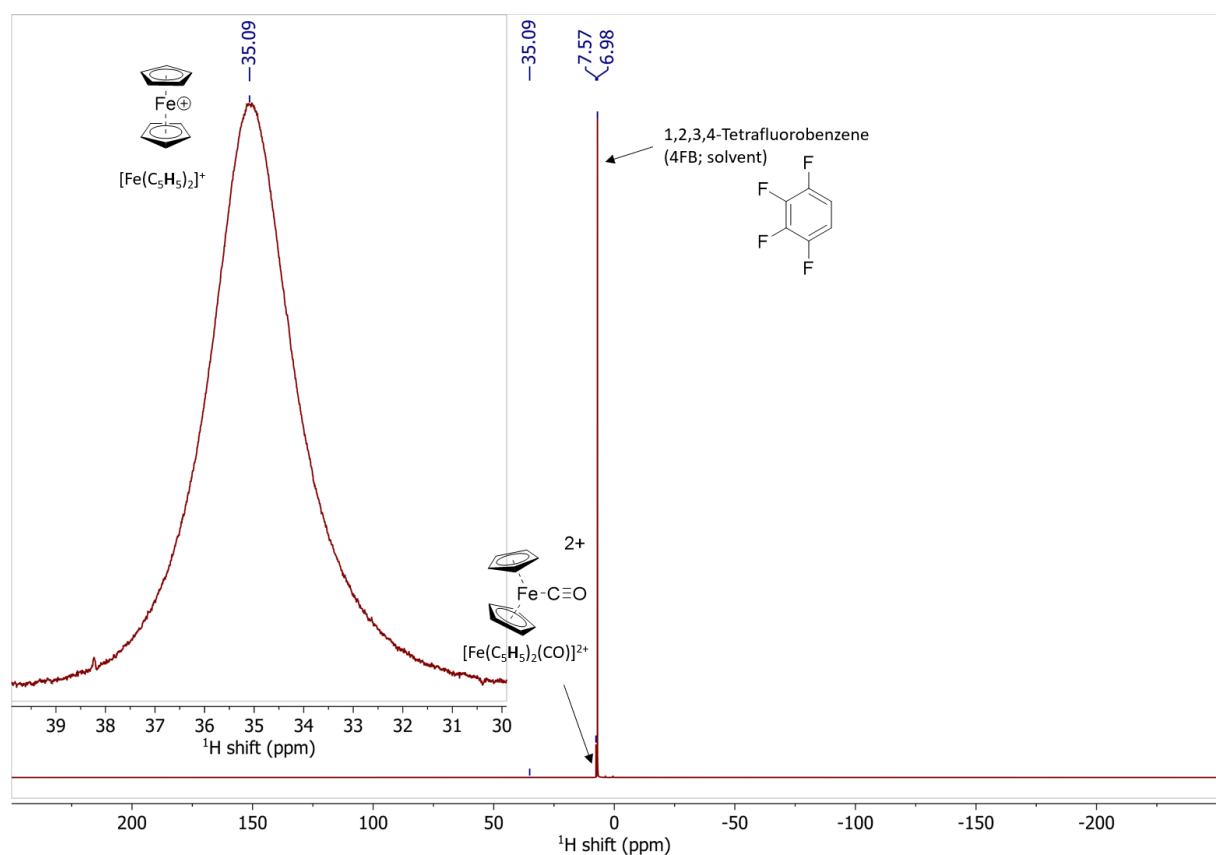


Figure S33:  $^1\text{H}$  NMR spectrum of  $[\text{Fc}(\text{CO})]^{2+}([\text{F}\{\text{Al}(\text{OR}^{\text{F}})_3\}_2]^-)_2$  in 1,2,3,4-tetrafluorobenzene (4FB) at room temperature with a wider sweep range.

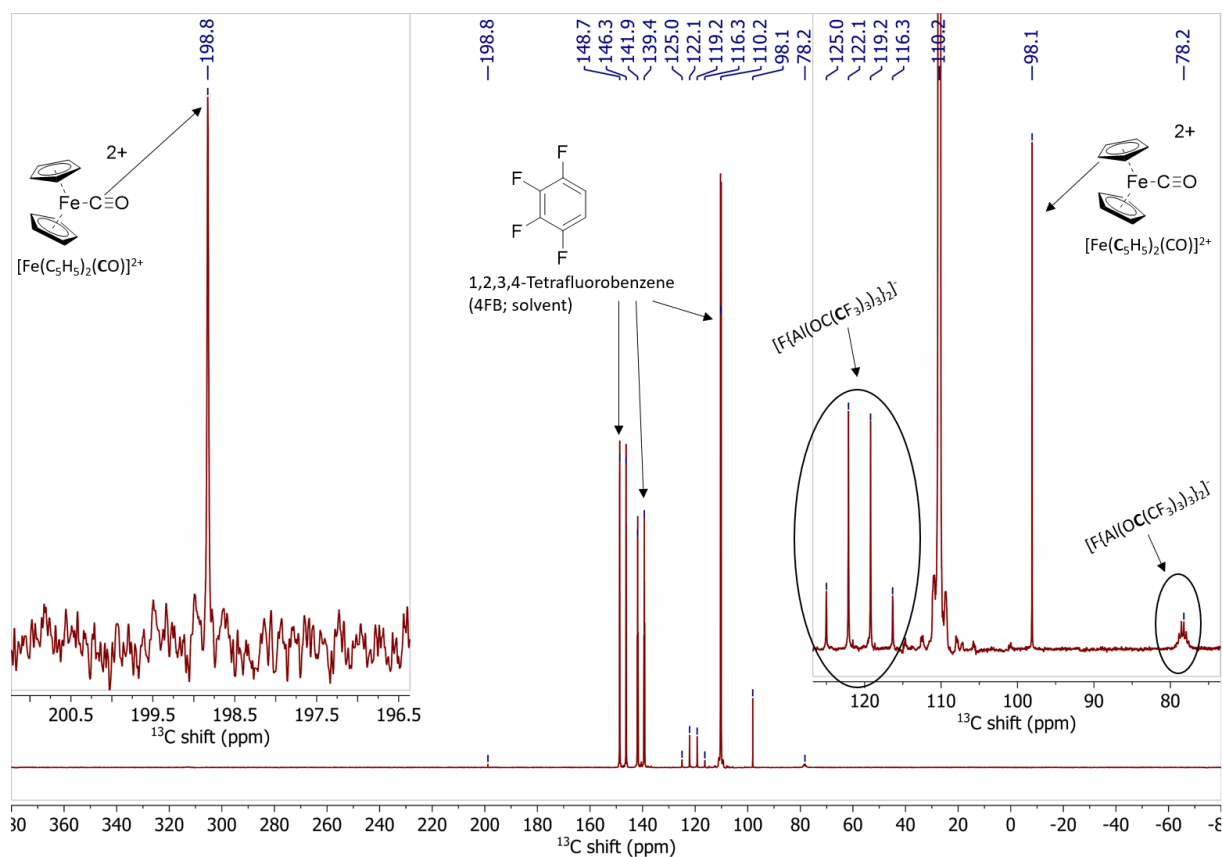


Figure S34:  $^{13}\text{C}$  NMR spectrum of  $[\text{Fc}(\text{CO})]^{2+}([\text{FAl}(\text{OR}^{\text{F}})_3]_2)^{-}$  in 1,2,3,4-tetrafluorobenzene (4FB) at room temperature.

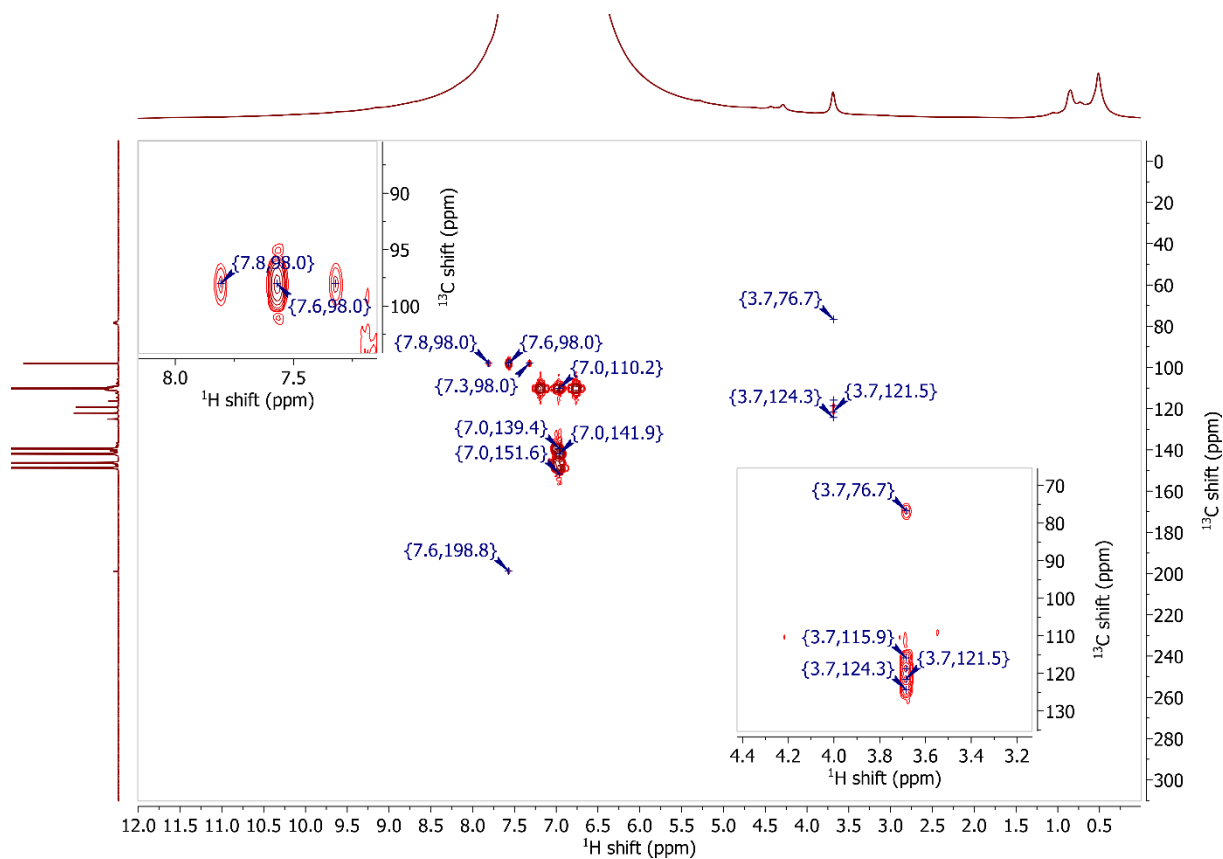


Figure S35:  $^1\text{H}$   $^{13}\text{C}$  HMBC NMR spectrum of  $[\text{Fc}(\text{CO})]^{2+}([\text{FAl}(\text{OR}^{\text{F}})_3]_2)^{-}$  in 1,2,3,4-tetrafluorobenzene (4FB) at room temperature.

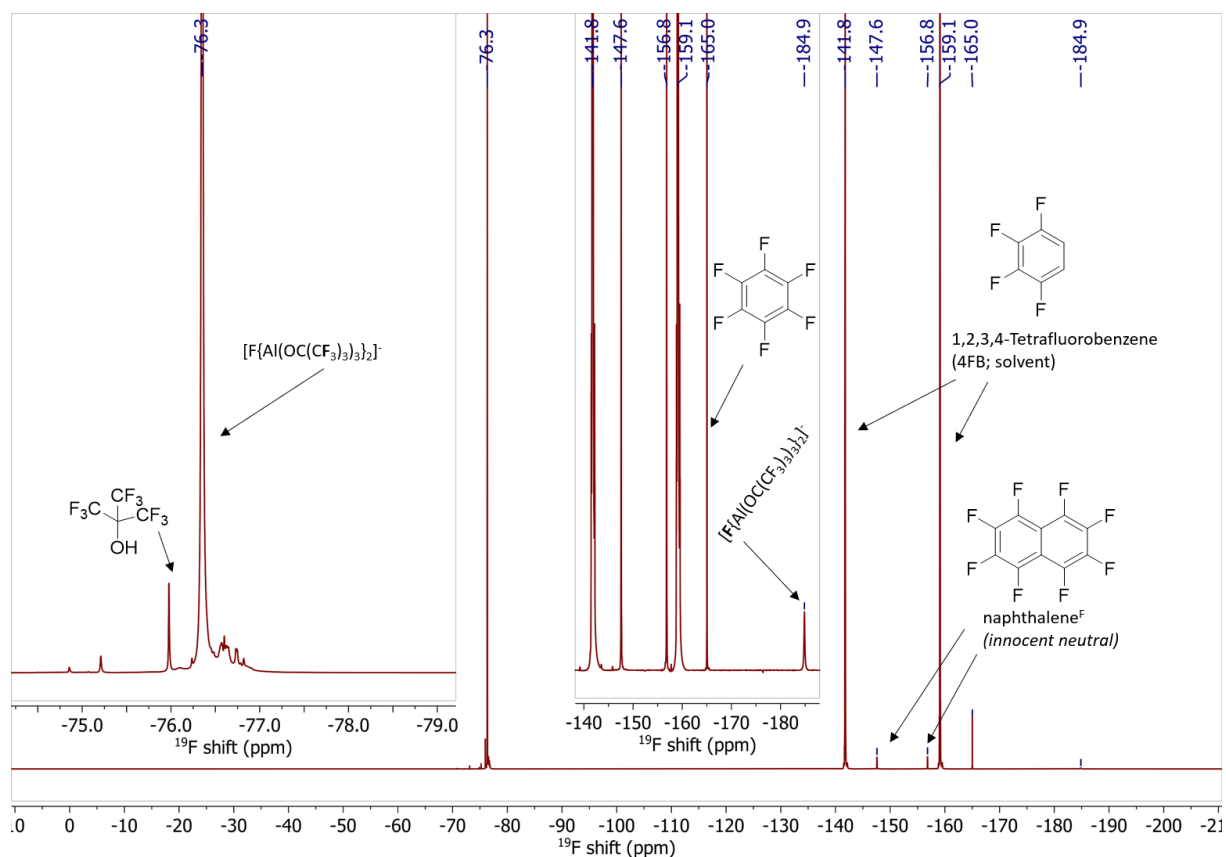


Figure S36:  $^{19}\text{F}$  NMR spectrum of  $[\text{Fc}(\text{CO})]^{2+}([\text{F}\{\text{Al}(\text{OR}^{\text{F}})_3\}_2]^-)_2$  in 1,2,3,4-tetrafluorobenzene (4FB) at room temperature.

## 2.4 Anthracene

### 2.4.1 Cyclic Voltammetry of Anthracene

The second deelectronation wave of the anthracene is largely overlapped with the beginning solvent decomposition. Therefore, no extensive electrochemical study was conducted and the obtained half-wave potential of  $E_{1/2} = +2.18 \text{ V}$  vs.  $\text{Fc}^{+/0}$  should be handled with care, this potential is however supported by the calculated value (see section 4.3).

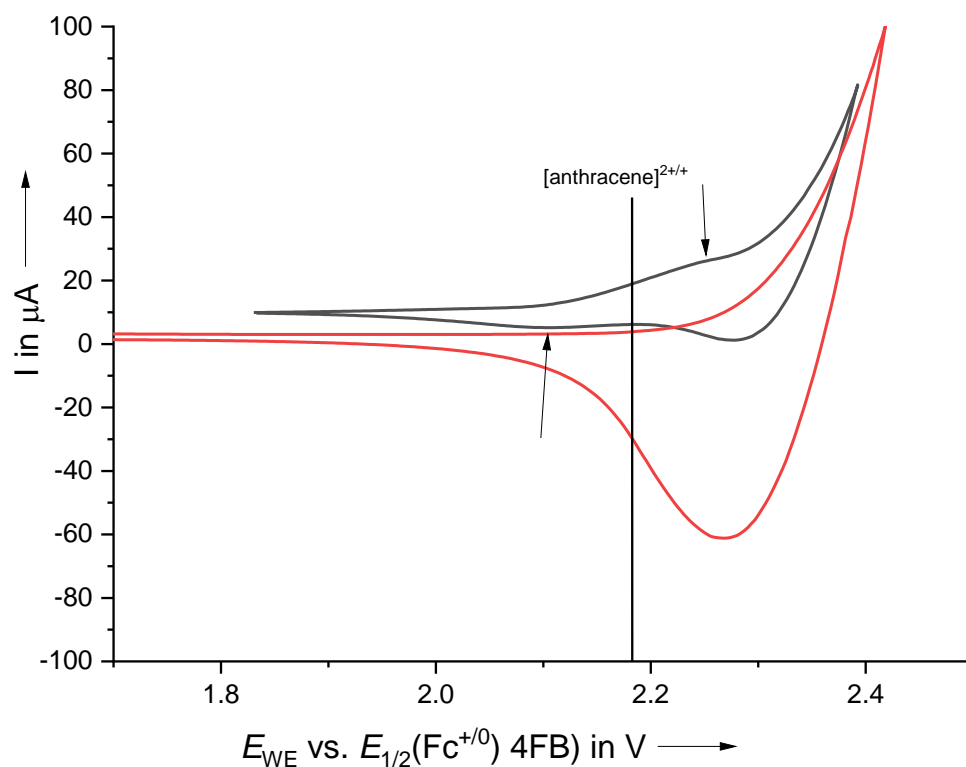
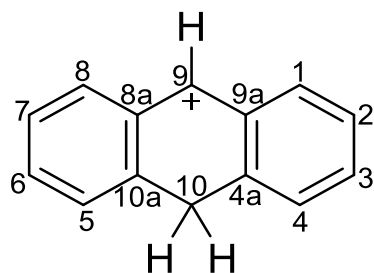


Figure S37: Cyclic voltammogram (2<sup>nd</sup> cycle) at 100 mV s<sup>-1</sup> of anthracene (10 mM) in 1,2,3,4-tetrafluorobenzene using [NBu<sub>4</sub>]<sup>+</sup>[Al(OR<sup>F</sup>)<sub>4</sub>]<sup>-</sup> (100 mM) as supporting electrolyte (black line) in comparison to the solvent window (red line).

#### 2.4.2 Attempts to Prepare the Anthracene Dication

Anthracene (9.0 mg, 50 μmol, 1.0 eq.) and [naphthalene<sup>F</sup>]<sup>+</sup>[F{Al(OR<sup>F</sup>)<sub>3</sub>}<sub>2</sub>]<sup>-</sup> (21 mg, 120 μmol, 2.4 eq.) were placed in a YOUNG NMR tube and 3FB (0.7 mL) was added. Upon shaking, the solution turned from green to yellow. The NMR spectroscopic characterization showed the expected signals for the protonated anthracene 9,10-dihydroanthracene-9-ylum instead.

#### NMR



<sup>1</sup>H-NMR (400 MHz, 3FB, 298 K): 9,10-dihydroanthracene-9-ylum δ = 9.88 (s, 1H, 9-CH), 8.60 (m, 2H, 1,8-CH), 8.43 (2m, 2H, 3,6-CH), 8.26 (m, 2H, 4,5-CH), 8.04 (m, 2H, 2,7-CH), 5.18 (s, 2H, 10-CH<sub>2</sub>) ppm.

<sup>13</sup>C-NMR (101 MHz, 3FB, 298 K): 9,10-dihydroanthracene-9-ylum δ = 181.8 (s, 1C, 9-CH), 154.6 (s, 2C, 4a,10a-CH), 146.3 (s, 2C, 3,6-CH), 141.4 (s, 2C, 1,8-CH), 133.6 (s, 2C, 8a,9a-C), 130.8 (s, 2C, 2,7-CH), 38.1 (s, 1C, CH<sub>2</sub>) ppm.

<sup>19</sup>F-NMR (377 MHz, 3FB, 298 K): δ = -75.8 (s, 54F, F-{Al(OC(CF<sub>3</sub>)<sub>3</sub>)<sub>3</sub>}<sub>2</sub>), -184.6 (s, br, 1F, F-{Al(OC(CF<sub>3</sub>)<sub>3</sub>)<sub>3</sub>}<sub>2</sub>) ppm.



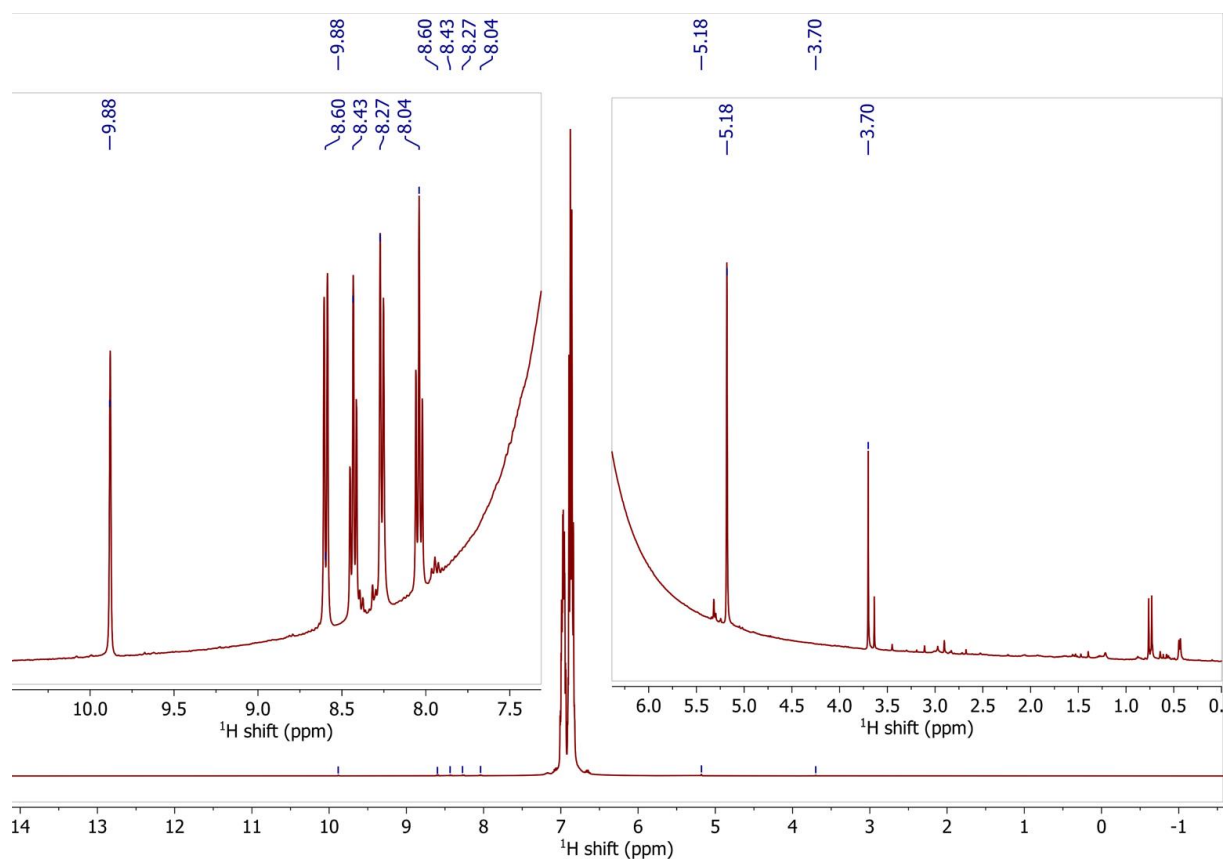


Figure S38:  $^1\text{H}$  NMR spectrum of the deelectronation reaction of anthracene in 1,2,3-Trifluorobenzene (3FB) at room temperature.

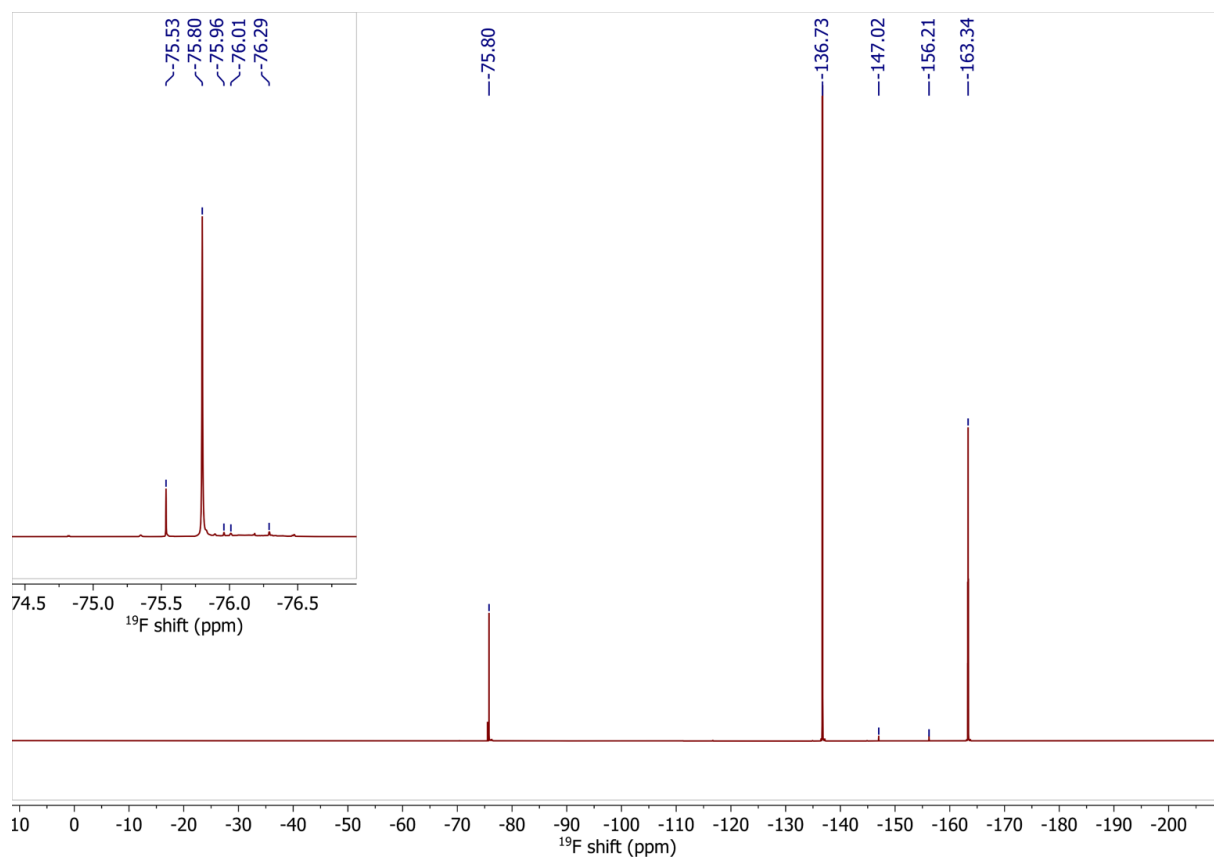


Figure S39:  $^{19}\text{F}$  NMR spectrum of the deelectronation reaction of anthracene in 1,2,3-Trifluorobenzene (3FB) at room temperature.

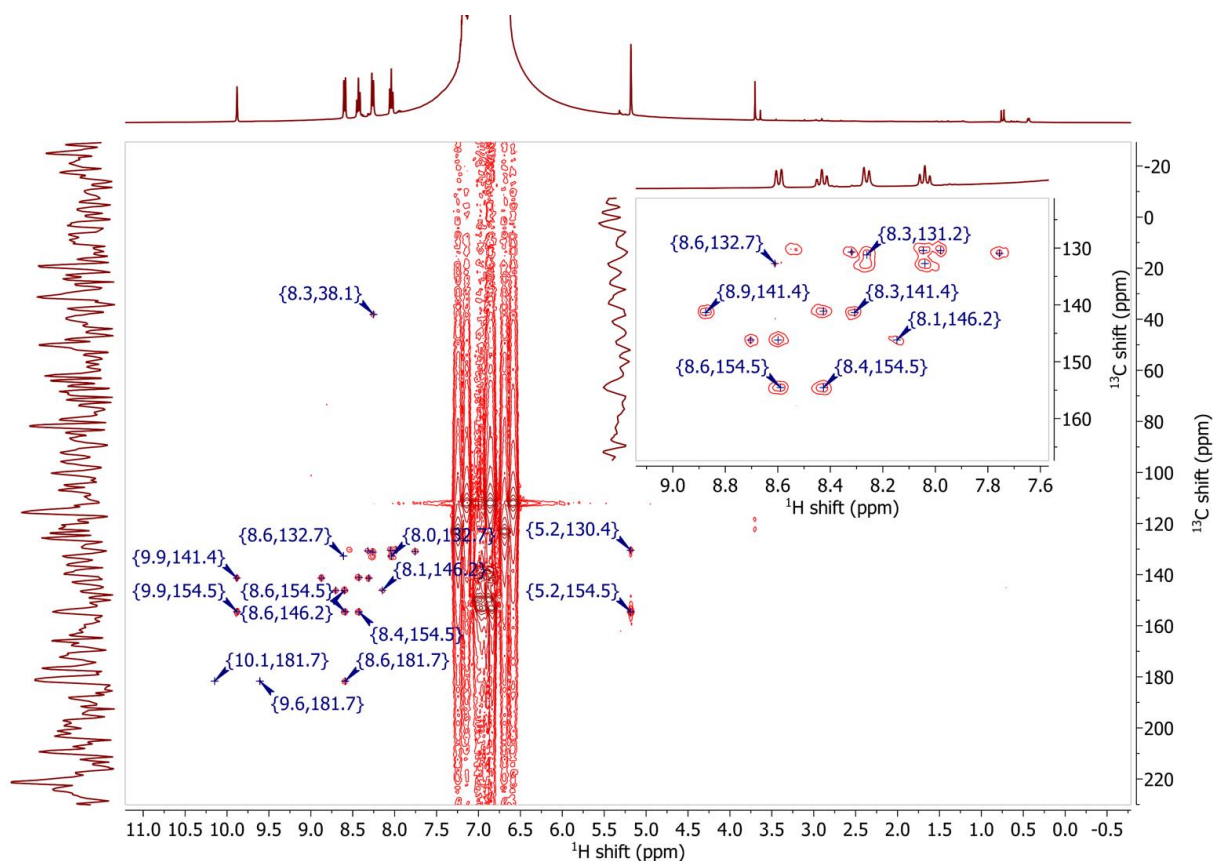


Figure S40:  $^1\text{H}$ - $^{13}\text{C}$  HMBC NMR spectrum of the deelectronation reaction of anthracene in 1,2,3-Trifluorobenzene (3FB) at room temperature.

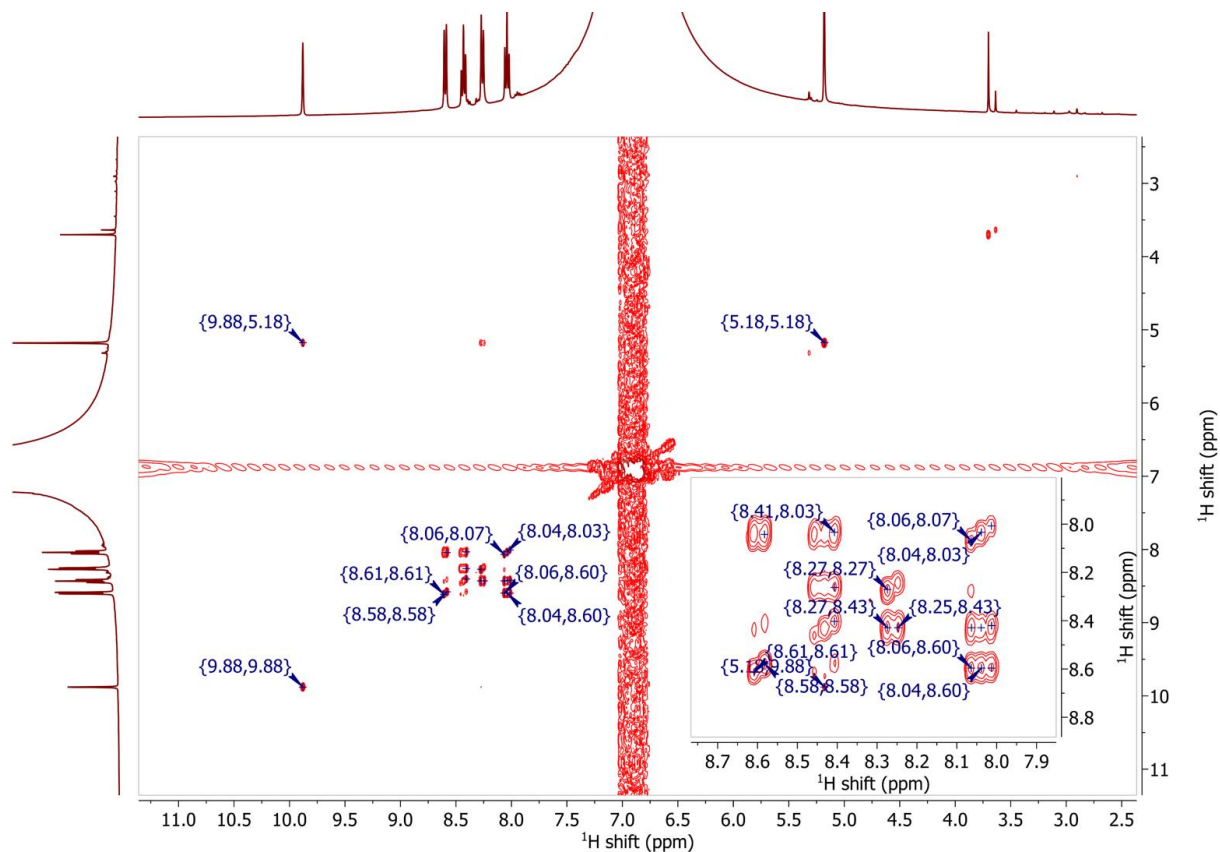


Figure S41:  $^1\text{H}$  COSY NMR spectrum of the deelectronation reaction of anthracene in 1,2,3-Trifluorobenzene (3FB) at room temperature.

## 2.5 Tetracene

### 2.5.1 Cyclic Voltammetry of Tetracene

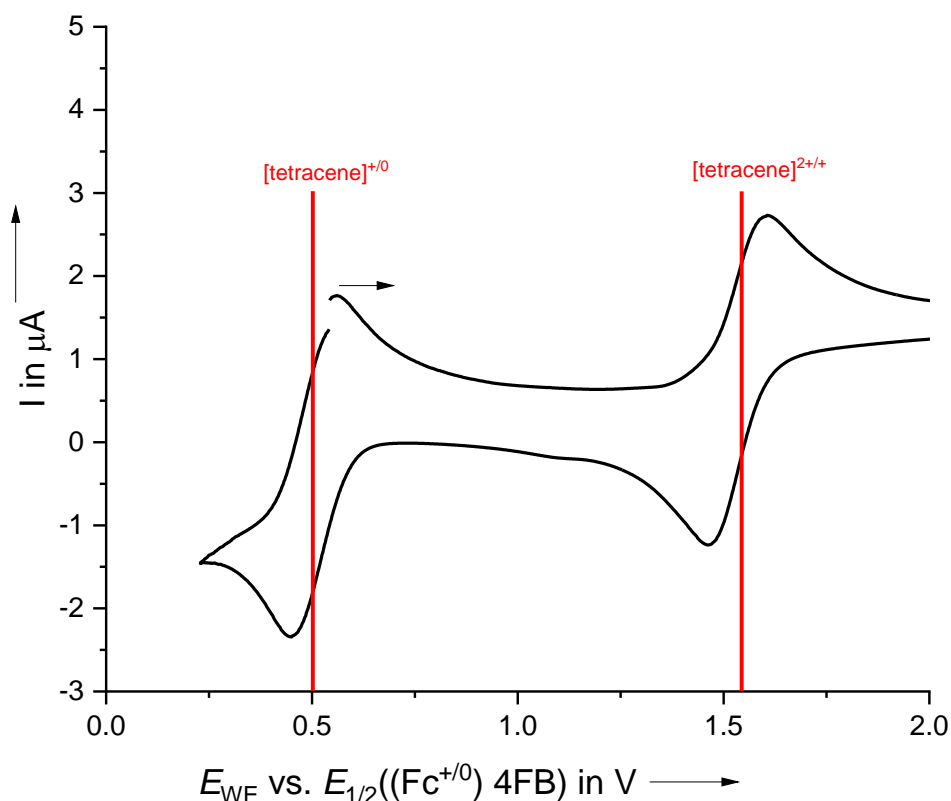


Figure S42: Cyclic voltammogram (2<sup>nd</sup> cycle) at 100 mV s<sup>-1</sup> of [tetracene]<sup>+</sup>[F{Al(OR<sup>F</sup>)<sub>3</sub>]<sub>2</sub>]<sup>-</sup> (10 mM) in 1,2,3,4-tetrafluorobenzene using [NBu<sub>4</sub>]<sup>+</sup>[Al(OR<sup>F</sup>)<sub>4</sub>]<sup>-</sup> (100 mM) as supporting electrolyte.

### 2.5.2 Deelectronation Towards the Tetracene Dication

[Naphthalene]<sup>F</sup><sup>+</sup>[F{Al(OR<sup>F</sup>)<sub>3</sub>]<sub>2</sub>]<sup>-</sup> (40 mg, 23 μmol, 2.0 eq.) and tetracene (2.6 mg, 12 μmol, 1.0 eq.) were dissolved in 5FB (1.5 mL) and the reaction solution was slowly evaporated over days in a glove box. A black solid and green crystals of [tetracene]<sup>2+</sup>([F{Al(OR<sup>F</sup>)<sub>3</sub>]<sub>2</sub>)<sup>-</sup>)<sub>2</sub>·(5FB)<sub>3</sub> were obtained. No yield was determined.

#### scXRD

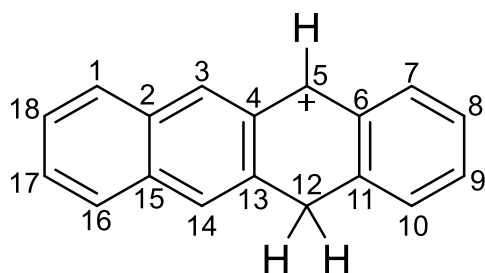
*C*2/*c*, *a* = 18.809(3) Å, *b* = 20.800(6) Å, *c* = 29.904(8) Å, α = 90°, β = 90.516(19)°, γ = 90°, *V* = 11699(5) Å<sup>3</sup>, *Z* = 4.

#### NMR Spectroscopy

For NMR spectroscopic experiments, a fresh solution was prepared:

[Tetracene]<sup>+</sup>[F{Al(OR<sup>F</sup>)<sub>3</sub>]<sub>2</sub>]<sup>-</sup> (6.1 mg, 3.5 μmol, 1.0 eq.) and [Naphthalene]<sup>F</sup><sup>+</sup>[F{Al(OR<sup>F</sup>)<sub>3</sub>]<sub>2</sub>]<sup>-</sup> filled in a YOUNG NMR tube and 5FB (0.7 mL) was added. Because the product was not soluble in 5FB, the precipitate was dissolved in 3FB (0.7 mL). Besides other decomposition products, the protonated tetracene 5,12-dihydropentacene-5-ylum is the main product.

Also, the direct use of 4FB as solvent yielded the same signals of protonated tetracene.



$^1\text{H}$  NMR (400 MHz, 3FB, 298 K): 5,12-dihydrotetracene-5-ylum  $\delta$  = 9.77 (s, 1H, 5-CH), 9.20 (s, 1H, 3-CH), 8.47 (d, 1H, 7-CH), 8.32 (s, 1H, 14-CH), 8.30 (s, 1H, 9-CH), 8.29 (s, 1H, 1-CH), 8.10 (d, 1H, 10-CH), 8.06 (d, 1H, 17-CH), 8.05 (s, 1H, 16-CH), 7.92 (t, 1H, 8-CH), 7.79 (m, 1H, 18-CH), 5.05 (s, 2H, 12-CH<sub>2</sub>) ppm.

$^{13}\text{C}$  NMR (101 MHz, 3FB, 298 K): 5,12-dihydrotetracene-5-ylum  $\delta$  = 180.5 (s, 1C, 5-CH), 153.0 (s, 1C, 11-C), 150.3 (s, 1C, 3-CH), 145.6 (s, 1C, 9-CH), 142.2 (s, 1C, 15-C), 141.3 (s, 1C, 7-C), 139.4 (s, 1C, 13-C), 138.8 (s, 1C, 17-CH), 133.1 (s, 1C, 1-CH), 133.0 (s, 1C, 6-C), 132.9 (s, 1C, 2-C), 132.3 (s, 1C, 4-C), 130.5 (s, 1C, 10-CH), 130.2 (s, 1C, 8-CH), 129.4 (s, 1C, 14-CH), 129.2 (s, 1C, 18-CH), 128.2 (s, 1C, 16-CH), 35.6 (s, 1C, 12-CH<sub>2</sub>) ppm.

$^{19}\text{F}$  NMR (377 MHz, 3FB, 298 K):  $\delta$  = -75.8 (s, 54F, F-{Al(OC(CF<sub>3</sub>)<sub>3</sub>)<sub>3</sub>}<sub>2</sub>), -184.6 (s, br, 1F, F-{Al(OC(CF<sub>3</sub>)<sub>3</sub>)<sub>3</sub>}<sub>2</sub>) ppm.

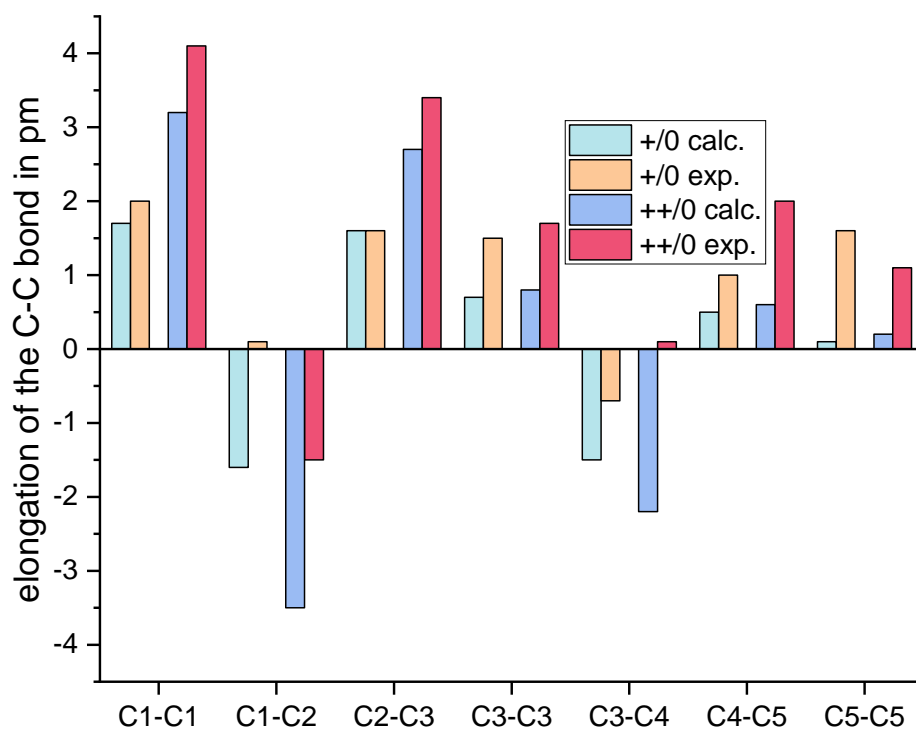


Figure S43: Comparison of the calculated differences (B3LYP(D3BJ)/def2-TZVPP) in the bond lengths with the experimental values obtained from scXRD from tetracene upon deelectronation.

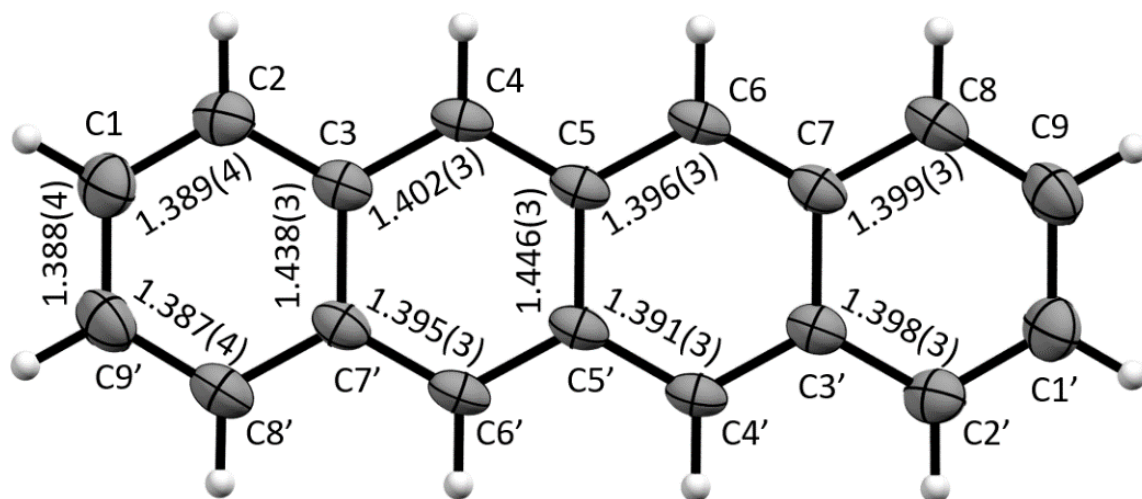


Figure S44: Molecular structure of  $[\text{tetracene}]^{2+}([\text{F}(\text{Al}(\text{OR}^{\text{f}})_3)_2]^-)_2 \cdot (4\text{FB})_3$  in solid-state. Counterions and solvent molecules omitted for clarity. Ellipsoids shown at 50% probability, Colour code: carbon – grey, hydrogen – white. Distances are given in Å.

## 2.6 Pentacene

### 2.5.1 Cyclic Voltammetry of Pentacene

Table S4: Key data of the electrochemical transition  $[\text{pentacene}]^+ \rightarrow [\text{pentacene}]^{++}$  at different scan rates (20-1000  $\text{mV s}^{-1}$ ) with of  $[\text{pentacene}]^+ [\text{F}[\text{Al}(\text{OR}^{\text{F}})_3]_2]^-$  (10 mM) in 1,2,3,4-tetrafluorobenzene using  $[\text{NBu}_4]^+ [\text{Al}(\text{OR}^{\text{F}})_4]^-$  (100 mM) as supporting electrolyte.

Scan rate in $\text{mV s}^{-1}$	Electronation potential in V	Deelectronation potential in V	Half-wave potential in V	Current at anodic peak potential in $\mu\text{A}$ (first cycle)	Peak difference in V	Corrected half-wave potential
20	1.128	1.226	1.177	4.01	0.098	1.1646
50	1.123	1.231	1.177	5.67	0.108	1.1646
100	1.112	1.24	1.176	6.66	0.128	1.1636
200	1.103	1.243	1.173	9.32	0.14	1.1606
500	1.093	1.259	1.176	14.4	0.166	1.1636
1000	1.086	1.277	1.1815	21.11	0.191	1.1691

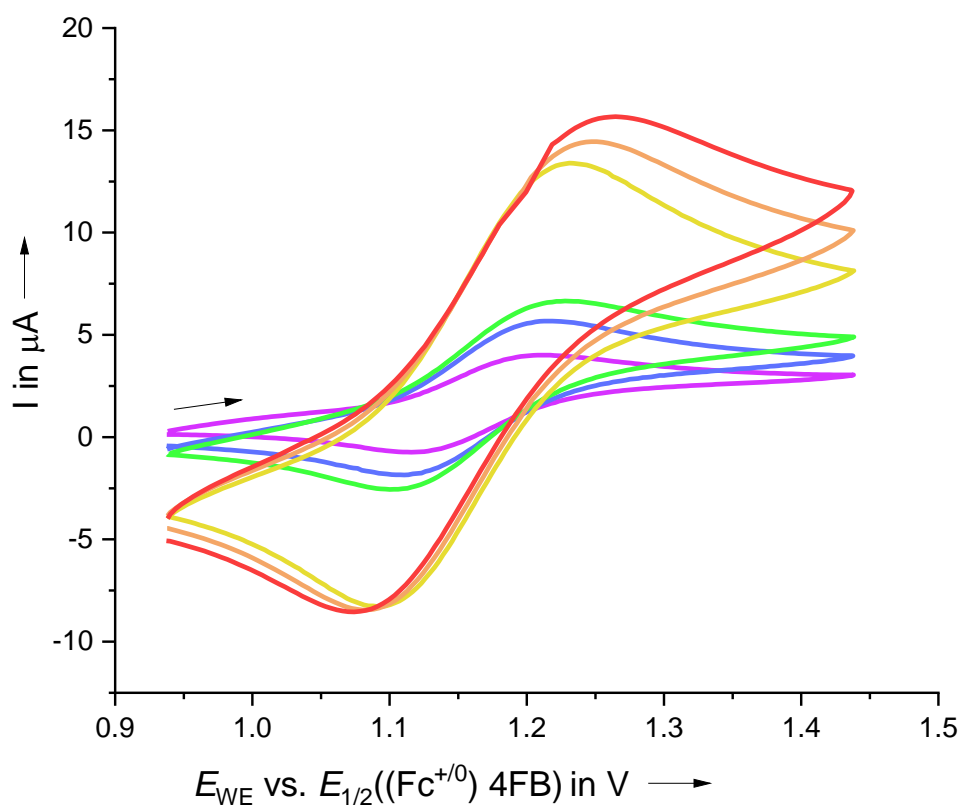


Figure S45: Cyclic voltammograms (2<sup>nd</sup> cycle, 6<sup>th</sup> cycle for 100  $\text{mV s}^{-1}$ ) at different scan rates (purple (20  $\text{mV s}^{-1}$ )  $\rightarrow$  green (100  $\text{mV s}^{-1}$ )  $\rightarrow$  red (1000  $\text{mV s}^{-1}$ )) of  $[\text{pentacene}]^+ [\text{F}[\text{Al}(\text{OR}^{\text{F}})_3]_2]^-$  (10 mM) in 1,2,3,4-tetrafluorobenzene using  $[\text{NBu}_4]^+ [\text{Al}(\text{OR}^{\text{F}})_4]^-$  (100 mM) as supporting electrolyte.

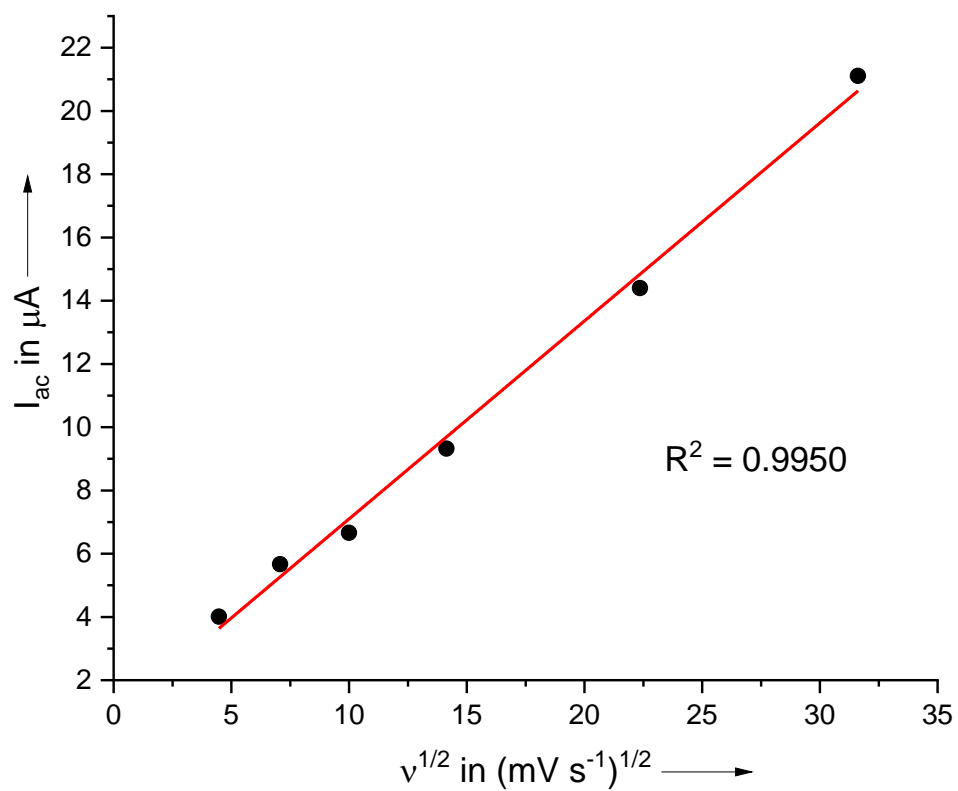


Figure S46: Linear fit of the anodic peak current  $I_{ac}$  of the **first** cycle against the square root of the scan rate  $v^{1/2}$  of [Pentacene]<sup>++/+.</sup>

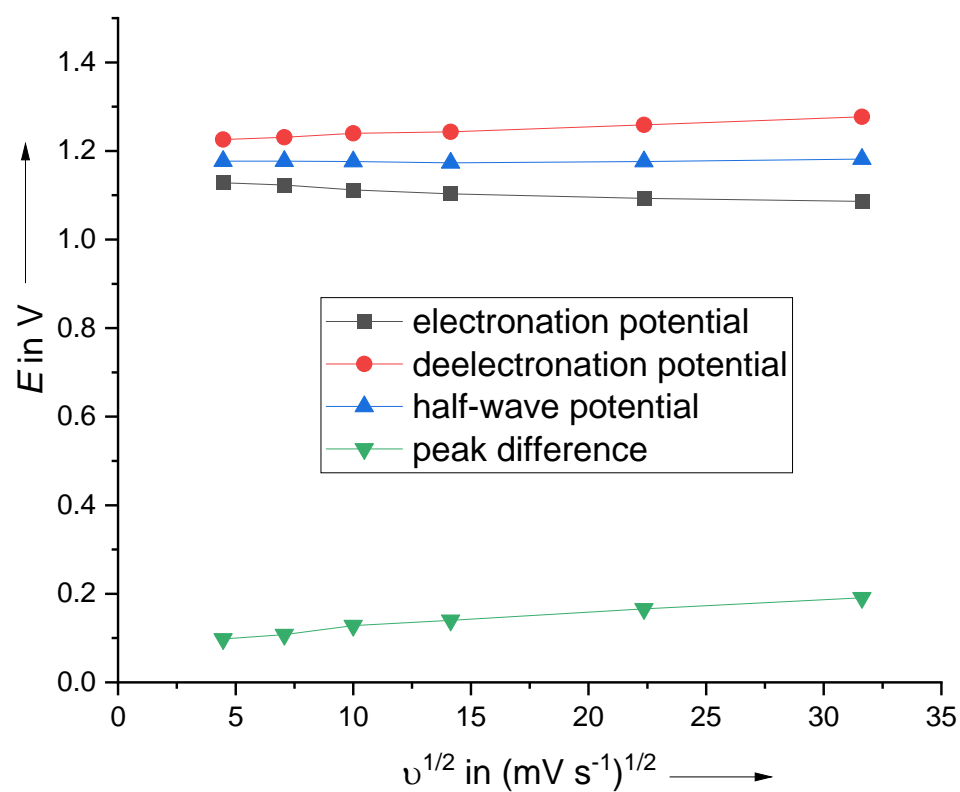
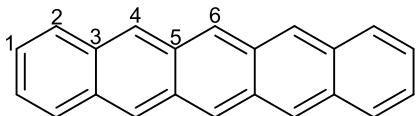


Figure S47: Electronation-, deelectronation- and half-wave potential & peak difference against the square root of the scan rate  $v^{1/2}$  of [Pentacene]<sup>++/+.</sup>

## 2.6.2 Synthesis and Characterization of [Pentacene]<sup>2+</sup>([F{Al(OR<sup>F</sup>)<sub>3</sub>}<sub>2</sub>]<sup>-</sup>)<sub>2</sub>

[Pentacene]<sup>+</sup>[F{Al(OR<sup>F</sup>)<sub>3</sub>}<sub>2</sub>]<sup>-</sup> (16 mg, 8.8 μmol, 1.0 eq.) and [naphthalene<sup>F</sup>]<sup>+</sup>[F{Al(OR<sup>F</sup>)<sub>3</sub>}<sub>2</sub>]<sup>-</sup> (20 mg, 11 μmol, 1.2 eq.) were dissolved in 1,2,3-trifluorobenzene (1.0 mL). Slow evaporation of the solvent in a glovebox led to the crystallization of [pentacene]<sup>2+</sup>([F{Al(OR<sup>F</sup>)<sub>3</sub>}<sub>2</sub>]<sup>-</sup>)<sub>2</sub>. The product was washed afterwards with pentafluorobenzene (2x 1.0 mL).



### scXRD

$P\bar{1}$ ,  $a = 10.581(6)$  Å,  $b = 14.274(6)$  Å,  $c = 16.784(6)$  Å,  $\alpha = 95.455(12)^\circ$ ,  $\beta = 95.58(2)^\circ$ ,  $\gamma = 96.76(3)^\circ$ ,  $V = 2490.8(19)$  Å<sup>3</sup>,  $Z = 1$ .

### NMR

<sup>1</sup>H-NMR (300.18 MHz, 3FB, 298 K):  $\delta = 9.75$  (s, 2H, 6-CH), 9.48 (s, 4H, 4-CH), 8.56-8.44 (m, AA'BB', 1,2-CH) ppm.

<sup>13</sup>C-NMR (75.48 MHz, 3FB, 298 K):  $\delta = 169.9$  (s, <sup>1</sup>J<sub>C-H</sub> = 172.5 Hz, 2C, 6-CH), 162.5 (s, <sup>1</sup>J<sub>C-H</sub> = 172.5 Hz, 4C, 4-CH), 144.7 (s, <sup>1</sup>J<sub>C-H</sub> = 172.0 Hz, 4C, 1-CH), 143.1 (s, <sup>1</sup>J<sub>C-H</sub> = 168.0 Hz, 4C, 2-CH), 139.4 (s, 4C, 3-C), 134.5 (s, 4C, 5-C) ppm.

<sup>19</sup>F-NMR (282 MHz, 3FB, 298 K):  $\delta = -75.9$  (s, 54F, F-{Al(OC(CF<sub>3</sub>)<sub>3</sub>)<sub>3</sub>}<sub>2</sub>), -184.6 (s, br, 1F, F-{Al(OC(CF<sub>3</sub>)<sub>3</sub>)<sub>3</sub>}<sub>2</sub>) ppm.

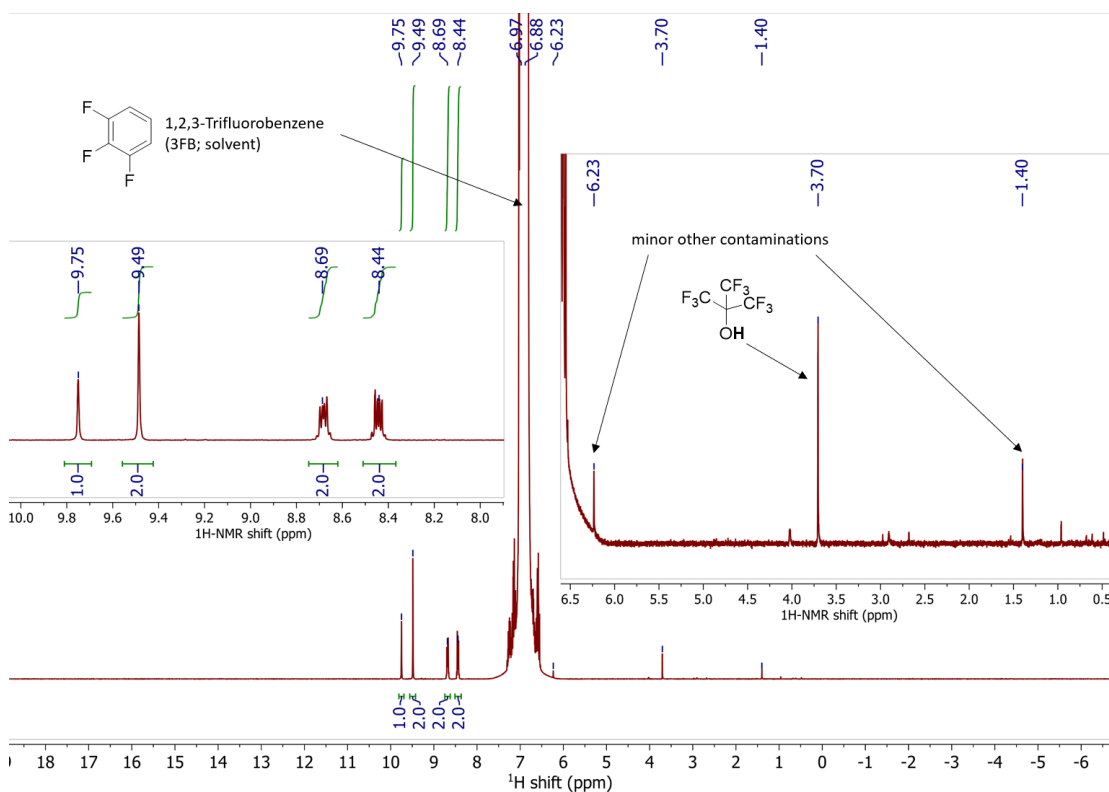


Figure S48: <sup>1</sup>H NMR spectrum of [pentacene]<sup>2+</sup>([F{Al(OR<sup>F</sup>)<sub>3</sub>}<sub>2</sub>]<sup>-</sup>)<sub>2</sub> in 1,2,3-trifluorobenzene (3FB) at room temperature.



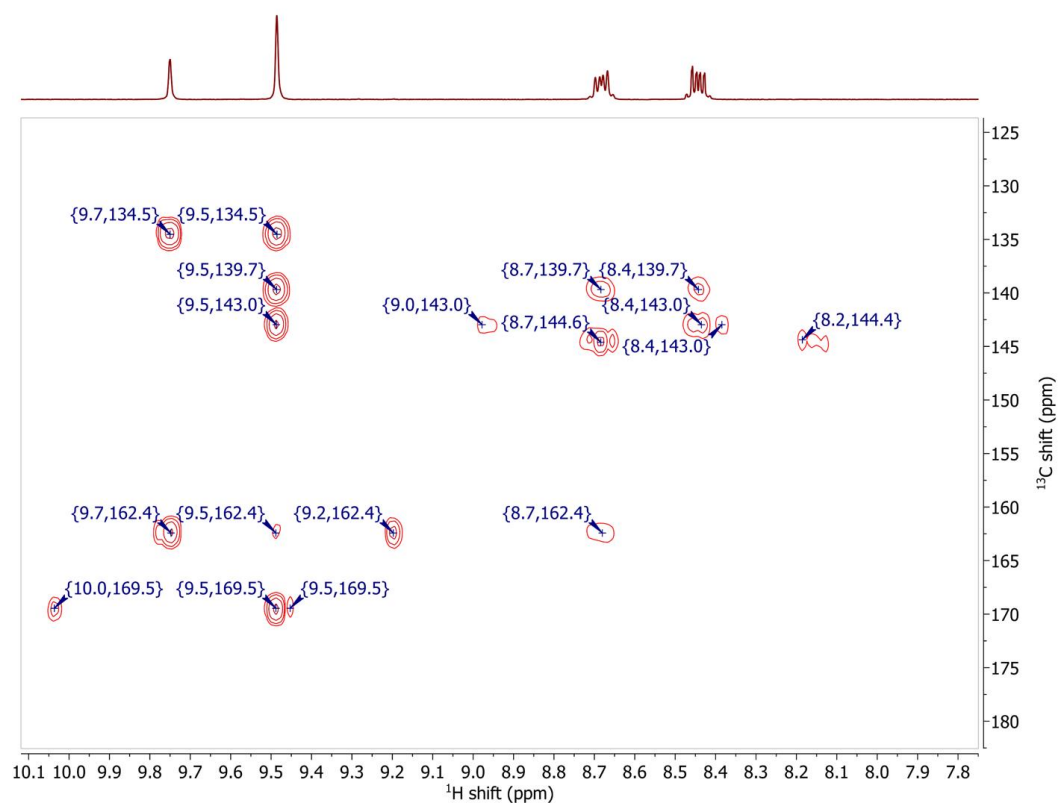


Figure S49: HMBC NMR spectrum of  $[\text{pentacene}]^{2+}([\text{F}\{\text{Al}(\text{OR}^{\text{F}})_3\}_2]^-)_2$  in 1,2,3-trifluorobenzene (3FB) at room temperature.

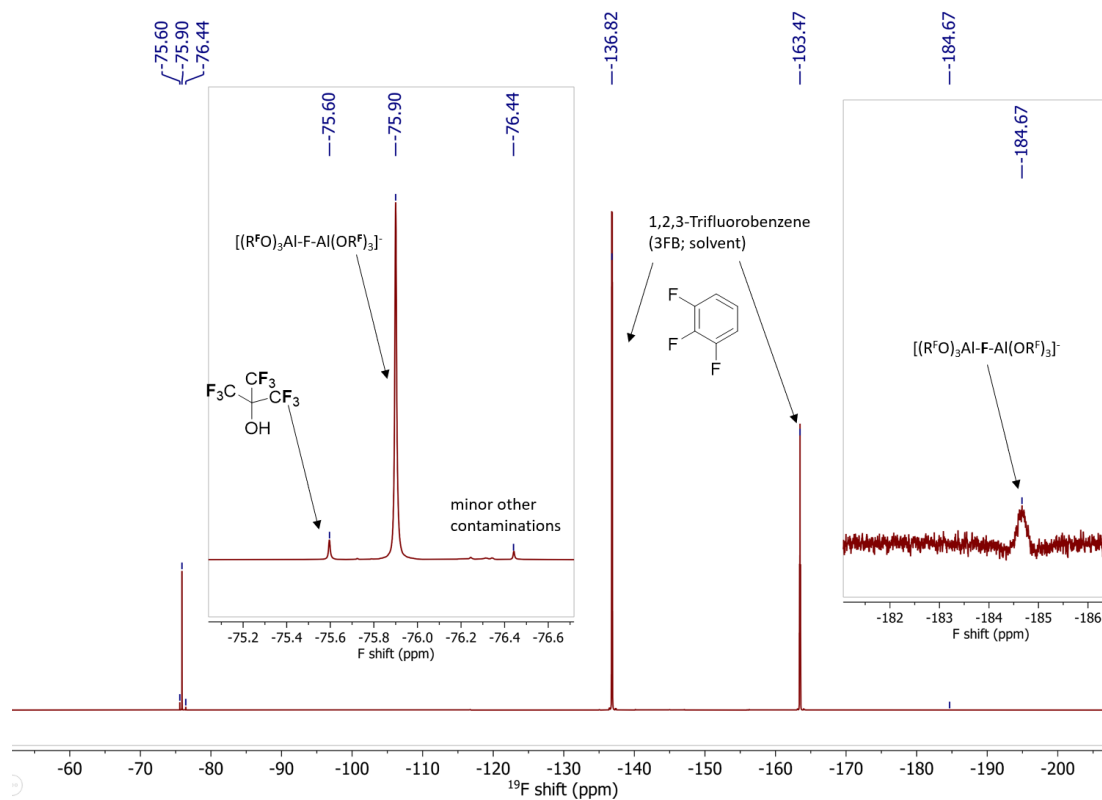


Figure S50:  $^{19}\text{F}$  NMR spectrum of  $[\text{pentacene}]^{2+}([\text{F}\{\text{Al}(\text{OR}^{\text{F}})_3\}_2]^-)_2$  in 1,2,3-trifluorobenzene (3FB) at room temperature.

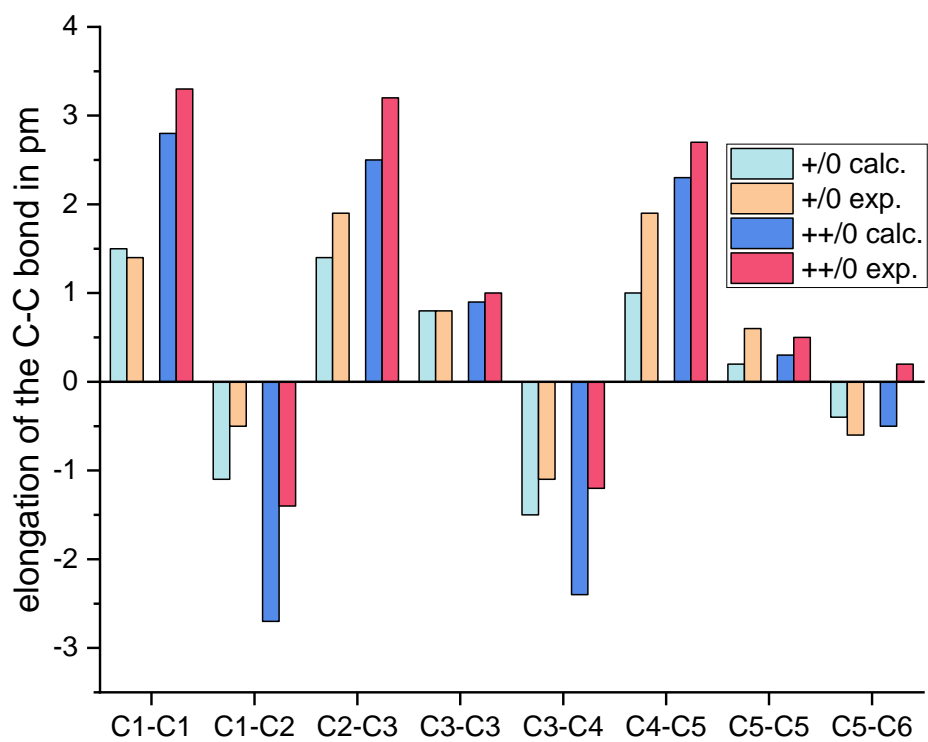


Figure S51: Comparison of the calculated differences (B3LYP(D3BJ)/def2-TZVPP) in the bond lengths with the experimental values obtained from scXRD from pentacene upon deelectronation.

## 2.7 Naphthalene<sup>Cl</sup>

### 2.7.1 Cyclic Voltammetry of Naphthalene<sup>Cl</sup>

Table S5: Key data of the electrochemical transition naphthalene<sup>Cl</sup> → [naphthalene<sup>Cl</sup>]<sup>+</sup> at different scan rates (20-1000 mV s<sup>-1</sup>) with of naphthalene<sup>Cl</sup> (10 mM) in 1,2,3,4-tetrafluorobenzene using [NBu<sub>4</sub>]<sup>+</sup>[Al(OR<sup>F</sup>)<sub>4</sub>]<sup>-</sup> (100 mM) as supporting electrolyte.

Scan rate in mV s <sup>-1</sup>	Electronation potential in V	Deelectronation potential in V	Half-wave potential in V	Current at anodic peak potential in μA	Peak difference in V	Corrected half-wave potential
20	1.739	1.879	1.809	5.51	0.14	1.7931
50	1.727	1.885	1.806	8.42	0.158	1.7901
100	1.712	1.904	1.808	10.93	0.192	1.7921
200	1.677	1.935	1.806	11.74	0.258	1.7901
500	1.638	1.968	1.803	16.39	0.33	1.7871
1000	1.605	2.003	1.804	21.11	0.398	1.7881

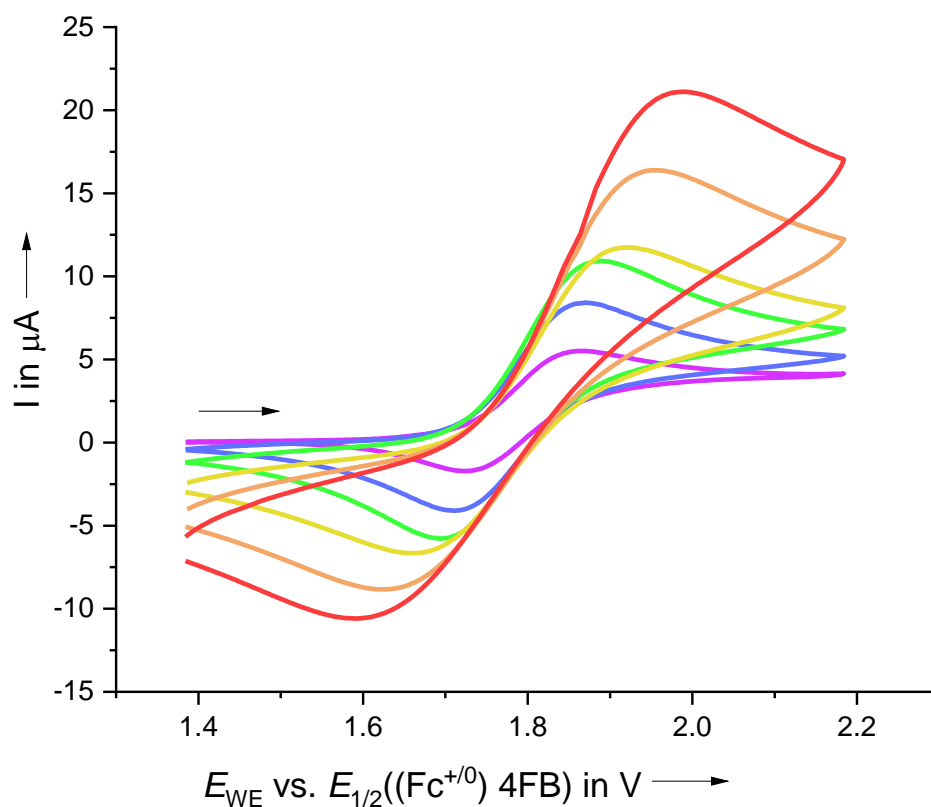


Figure S52: Cyclic voltammograms (2<sup>nd</sup> cycle) at different scan rates (purple (20 mV s<sup>-1</sup>) → green (100 mV s<sup>-1</sup>) → red (1000 mV s<sup>-1</sup>)) of naphthalene<sup>Cl</sup> (10 mM) in 1,2,3,4-tetrafluorobenzene using [NBu<sub>4</sub>]<sup>+</sup>[Al(OR<sup>F</sup>)<sub>4</sub>]<sup>-</sup> (100 mM) as supporting electrolyte.

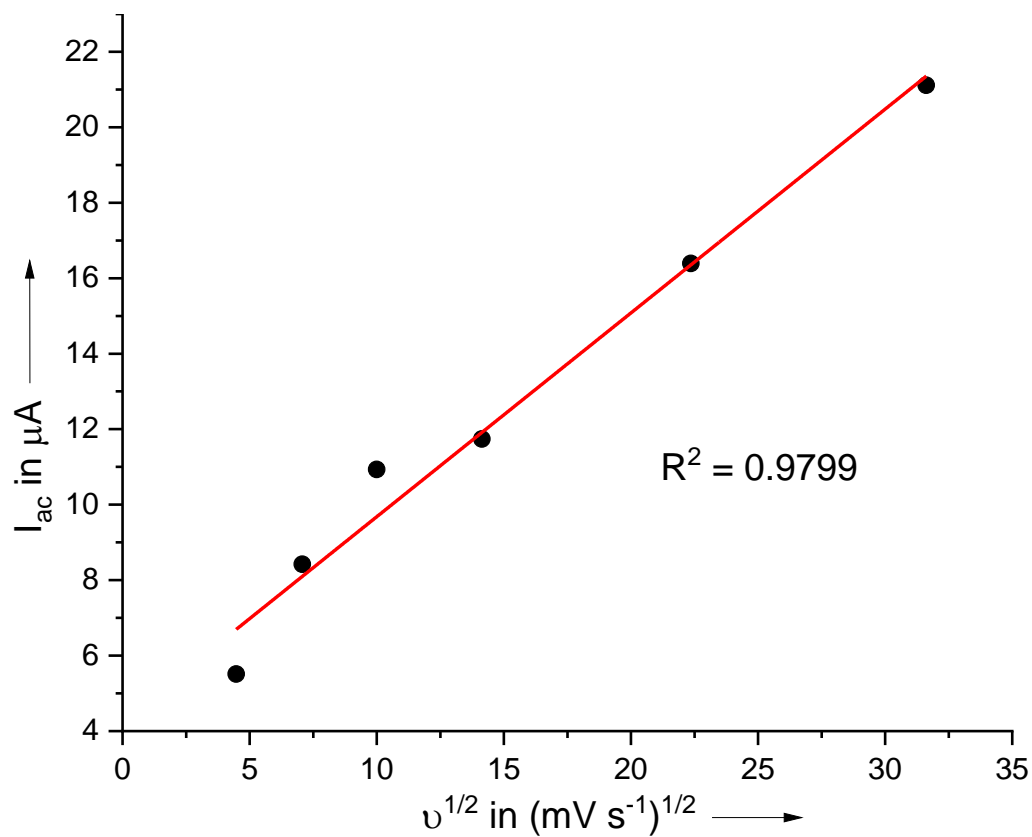


Figure S53: Linear fit of the anodic peak current  $I_{ac}$  against the square root of the scan rate  $v^{1/2}$  of [naphthalene<sup>Cl</sup>]<sup>+/0</sup>.

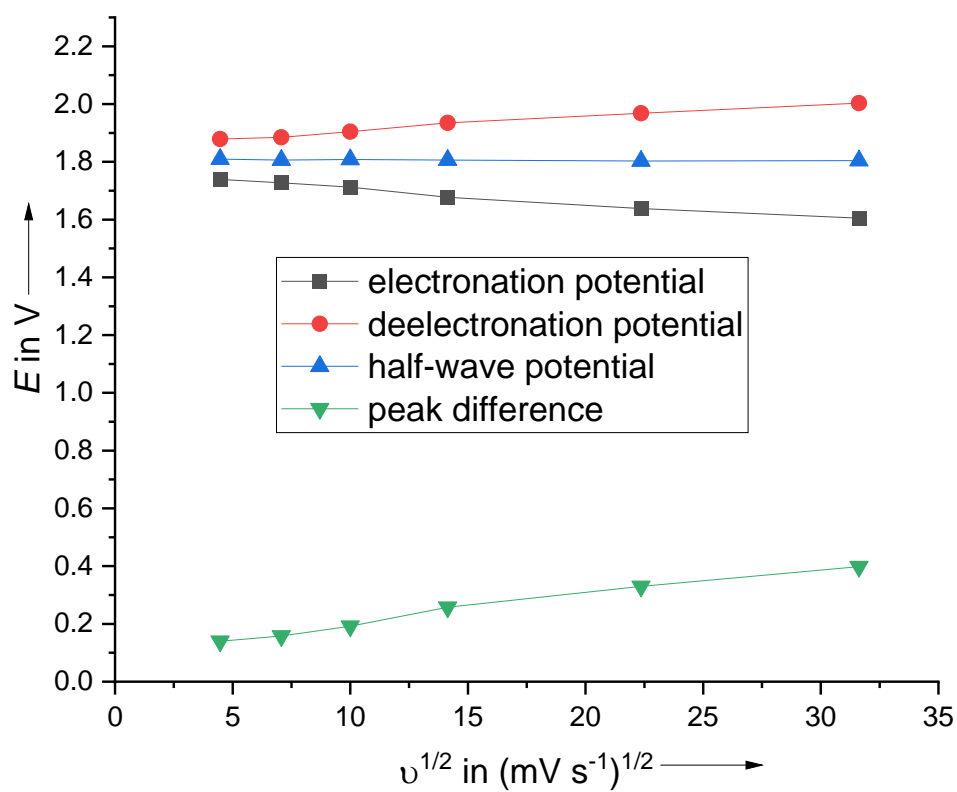


Figure S54: Electronation-, deelectronation- and half-wave potential & peak difference against the square root of the scan rate  $v^{1/2}$  of [naphthalene<sup>Cl</sup>]<sup>+/0</sup>.

## 2.7.2 Chemical Deelectronation and Structural Characterization of [Naphthalene<sup>Cl</sup>]<sup>+</sup>

[Naphthalene<sup>F</sup>]<sup>+</sup>[F{Al(OR<sup>F</sup>)<sub>3</sub>}<sub>2</sub>]<sup>-</sup> (60 mg, 34  $\mu$ mol, 1.0 eq.) and naphthalene<sup>Cl</sup> (16 mg, 37  $\mu$ mol, 1.1 eq.) were solved in 4FB in a glove box and the solution was evaporated over the course of days leading to a homogenous set of brown single crystals of [naphthalene<sup>Cl</sup>]<sup>+</sup>[F{Al(OR<sup>F</sup>)<sub>3</sub>}<sub>2</sub>]<sup>-</sup>·(4FB) suitable for scXRD. The crystals were washed with hexafluorobenzene (2 x 3 mL) to remove excess naphthalene<sup>Cl</sup> and naphthalene<sup>F</sup> (42 mg, 65 %, 22  $\mu$ mol).

### Vibrational Spectroscopy

Raman  $\tilde{\nu}$  / cm<sup>-1</sup> = 1492 (m), 1317 (m), 1292 (vs), 819 (w), 425 (w), 295 (w), 220 (w).

### scXRD

$P\bar{1}$ ,  $a = 10.542(3)$  Å,  $b = 13.614(3)$  Å,  $c = 34.876(8)$  Å,  $\alpha = 95.557(15)^\circ$ ,  $\beta = 93.394(16)^\circ$ ,  $\gamma = 110.032(12)^\circ$ ,  $V = 4657(2)$  Å<sup>3</sup>,  $Z = 3$ .

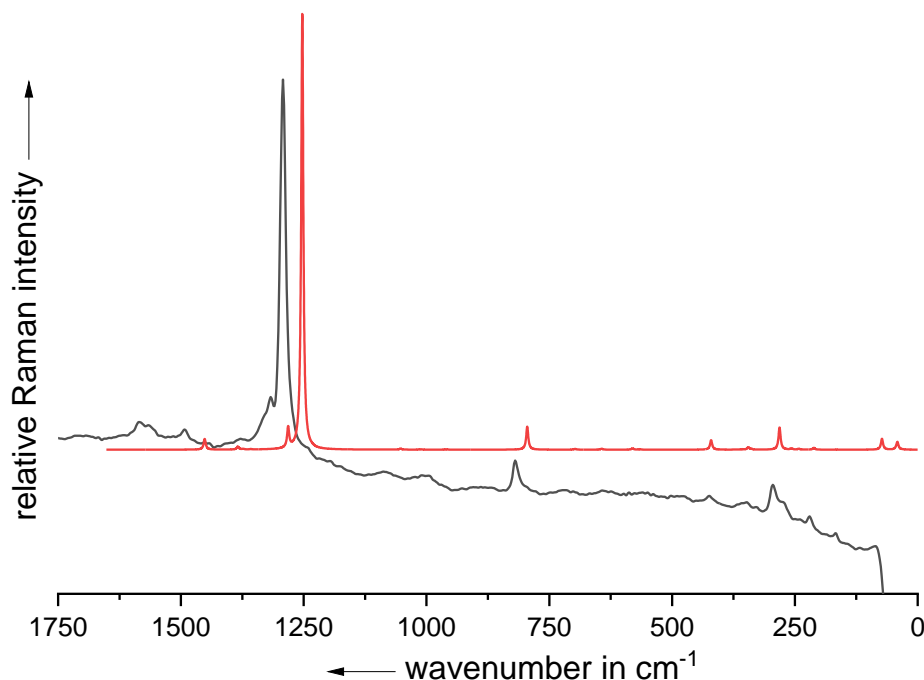
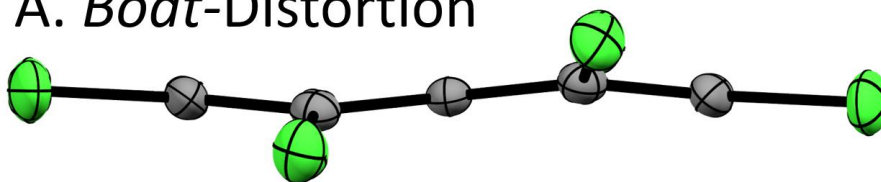


Figure S55: Comparison of the measured Raman spectrum of [naphthalene<sup>Cl</sup>]<sup>+</sup>[F{Al(OR<sup>F</sup>)<sub>3</sub>}<sub>2</sub>]<sup>-</sup> (black line, 10,000 scans, 20 mW) with the B3LYP(D3BJ)/def2-TZVPP calculated spectrum of [naphthalene<sup>Cl</sup>]<sup>+</sup> (red line) scaled by 0.9657.

## A. Boat-Distortion



## B. Twist-Distortion

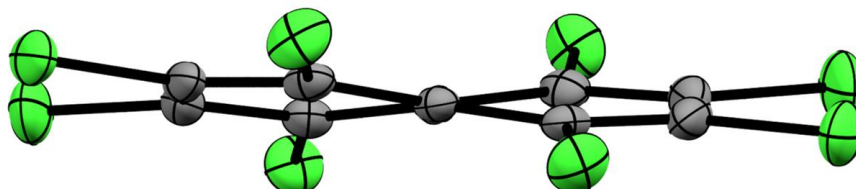


Figure S56: Boat-Twist-Isomerism of  $[\text{naphthalene}^{\text{Cl}}]^+$  in  $[\text{naphthalene}^{\text{Cl}}]^+[\text{F}\{\text{Al}(\text{OR}^{\text{F}})_3\}_2]^- \cdot (4\text{FB})$ .

The values in % in the following figures are giving the actual intramolecular distances divided by the doubled Van-der-Waals radius of a chlorine atom (175 pm).<sup>[28]</sup>

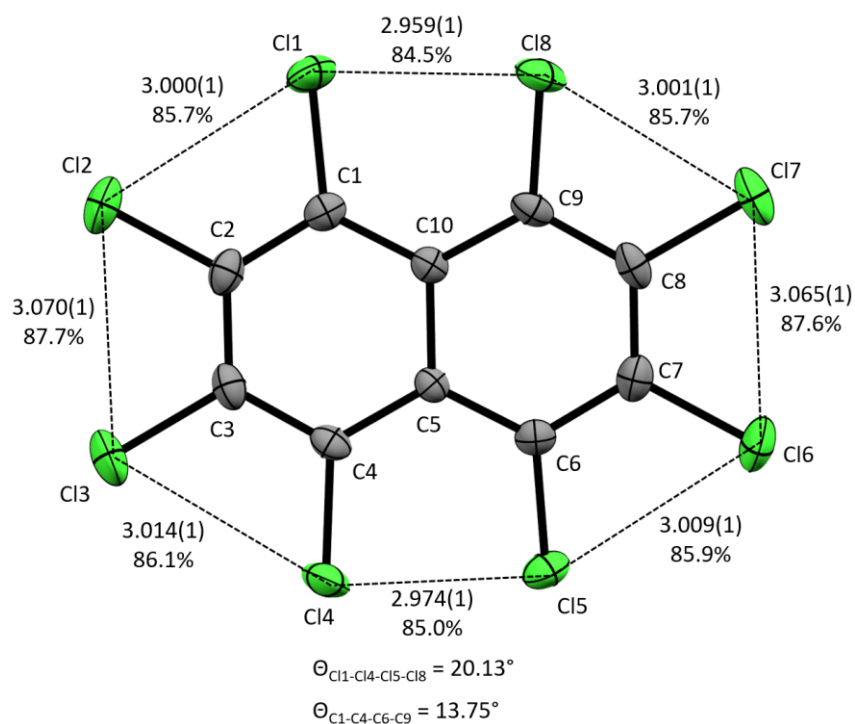


Figure S57: Intramolecular chlorine-chlorine distances in the *boat*-isomer of  $[\text{naphthalene}^{\text{Cl}}]^+$  in  $[\text{naphthalene}^{\text{Cl}}]^+[\text{F}\{\text{Al}(\text{OR}^{\text{F}})_3\}_2]^- \cdot (4\text{FB})$ .

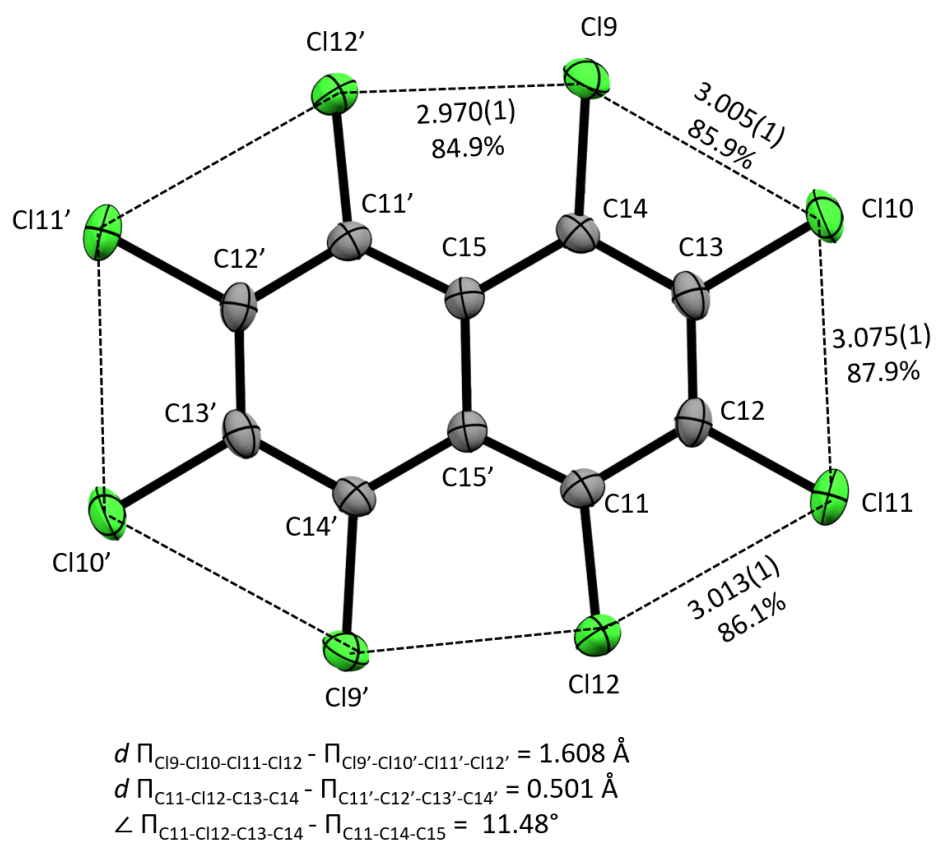


Figure S58: Intramolecular chlorine-chlorine distances in the *twist*-isomer of [naphthalene<sup>Cl</sup>]<sup>+</sup> in [naphthalene<sup>Cl</sup>]<sup>+</sup>[F{Al(OR<sup>F</sup>)<sub>3</sub>}<sub>2</sub>]<sup>-</sup>·(4FB).

## 2.8 Copper

### 2.8.1 Cyclic Voltammetry

For the determination of  $E^{\circ'}(\text{Cu}^+/\text{Cu}_{\text{metal}}, 4\text{FB})$  the reference electrode was a copper wire immersed in a solution of  $\text{Cu}^+[\text{F}\{\text{Al}(\text{OR}^{\text{F}})_3\}_2]^-$  (10 mM) and  $[\text{NBu}_4]^+[\text{Al}(\text{OR}^{\text{F}})_4]^-$  (100 mM) as supporting electrolyte in 4FB and separated from the test solution by a glass frit. The test solution contained  $\text{Fc}^+[\text{Al}(\text{OR}^{\text{F}})_4]^-$  (10 mM) and  $[\text{NBu}_4]^+[\text{pf}]^-$  (100 mM) as supporting electrolyte. The negative value of the potential of ferrocene against this reference results the  $E_{1/2}$  for 10 mM  $\text{Cu}^+/\text{Cu}_{\text{metal}}$ , which is at  $E_{1/2} = +1.35$  V vs.  $\text{Fc}^{+/0}$ , this value has to be corrected by 0.118 V to yield the formal potential of  $E^{\circ'} = +1.47$  V vs.  $\text{Fc}^{+/0}$  for 1 M  $\text{Cu}^+/\text{Cu}_{\text{metal}}$ .

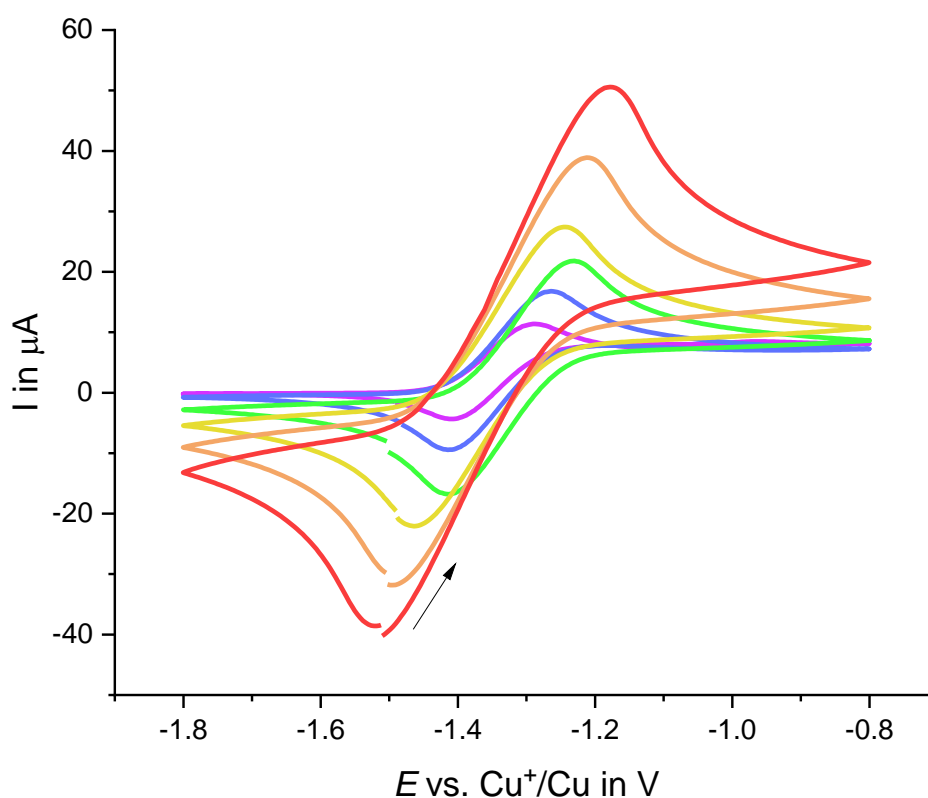


Figure S59: Cyclic voltammograms (2<sup>nd</sup> cycle) at different scan rates (purple (20 mV s<sup>-1</sup>) → green (100 mV s<sup>-1</sup>) → red (1000 mV s<sup>-1</sup>)) of Fc (10 mM) in 1,2,3,4-tetrafluorobenzene using  $[\text{NBu}_4]^+[\text{Al}(\text{OR}^{\text{F}})_4]^-$  (100 mM) as supporting electrolyte measured with a compartment reference electrode filled with 10 mM  $\text{Cu}[\text{F}\{\text{Al}(\text{OR}^{\text{F}})_3\}_2]$  and  $[\text{NBu}_4]^+[\text{Al}(\text{OR}^{\text{F}})_4]^-$  (100 mM) in 1,2,3,4-tetrafluorobenzene and a copper metal electrode.

### 2.9.2 Chemical Deelectronation of Elemental Copper and Structural Characterization of $[\text{CuF}\{\text{Al}(\text{OR}^{\text{F}})_3\}_2]$

$[\text{Naphthalene}^{\text{F}}]^+[\text{F}\{\text{Al}(\text{OR}^{\text{F}})_3\}_2]^-$  (30 mg, 0.017 mmol) and Cu powder (5.4 mg, 0.085 mmol, 5.0 eq.) were suspended in 5FB (1 mL) and stirred at RT for 24 h. Then the solution was filtrated and the solvent of the filtrate was evaporated slowly in the glovebox to produce colourless crystals of  $[\text{CuF}\{\text{Al}(\text{OR}^{\text{F}})_3\}_2]$ . Neutral naphthalene<sup>F</sup> was removed in high-vacuum yielding analytically pure  $[\text{CuF}\{\text{Al}(\text{OR}^{\text{F}})_3\}_2]$  as a white microcrystalline powder (19 mg, 73 %, 12 μmol).

#### scXRD

$P\bar{1}$ ,  $a = 10.565(4)$  Å,  $b = 10.725(4)$  Å,  $c = 22.179(6)$  Å,  $\alpha = 82.617(9)^\circ$ ,  $\beta = 87.180(11)^\circ$ ,  $\gamma = 61.723(11)^\circ$ ,  $V = 2194.7(13)$  Å<sup>3</sup>,  $Z = 2$ .



### Vibrational Spectroscopy

ATR-IR (Diamond, crystals)  $\tilde{\nu} / \text{cm}^{-1} = 1364$  (vw), 1302 (vw), 1244 (vs), 1213 (vs), 1184 (s), 1142 (w), 1082 (vw), 1034 (vw), 971 (s), 901 (vw), 847 (vw), 788 (vw), 759 (vw), 742 (vw), 726 (vs), 590 (w), 572 (w), 538 (w), 503 (vw), 454 (vw).

Raman  $\tilde{\nu} / \text{cm}^{-1} = 1313$  (s), 1290 (s), 789 (s), 760 (s), 749 (s), 573 (vs), 540 (vs), 362 (vs), 328 (vs), 292 (vs), 249 (vs), 226 (vs).

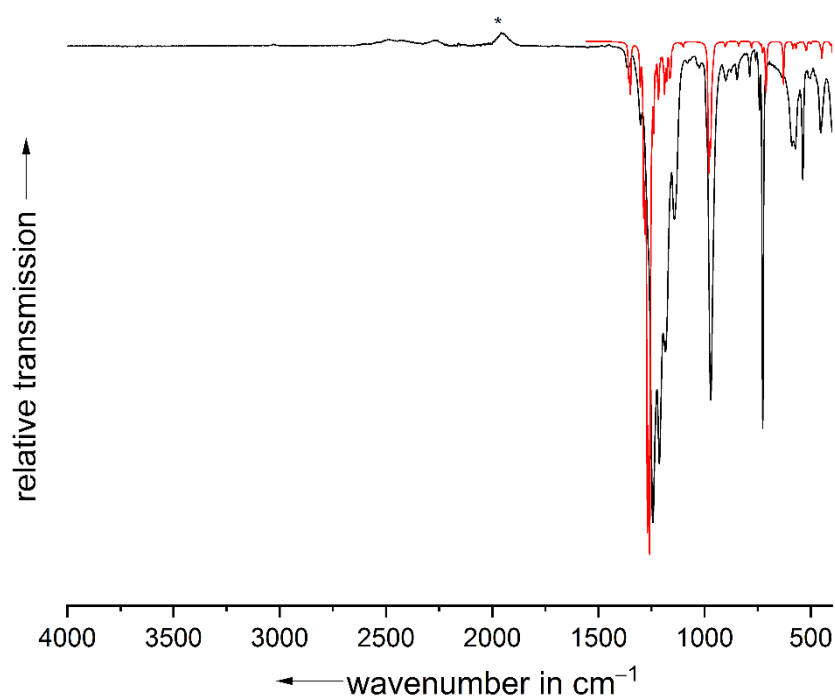


Figure S60: Comparison of the ATR-IR spectrum (Diamond) of  $[\text{Cu}(\text{F}\{\text{Al}(\text{OR}^{\text{F}})_3\}_2)]$  powder (32 scans, black line) with the B3LYP(D3BJ)/def2-SVP calculated IR spectrum of  $[\text{Cu}(\text{F}\{\text{Al}(\text{OR}^{\text{F}})_3\}_2)]$  (red line) scaled by 0.9671. Bands marked with “\*” are artefacts of the diamond window.

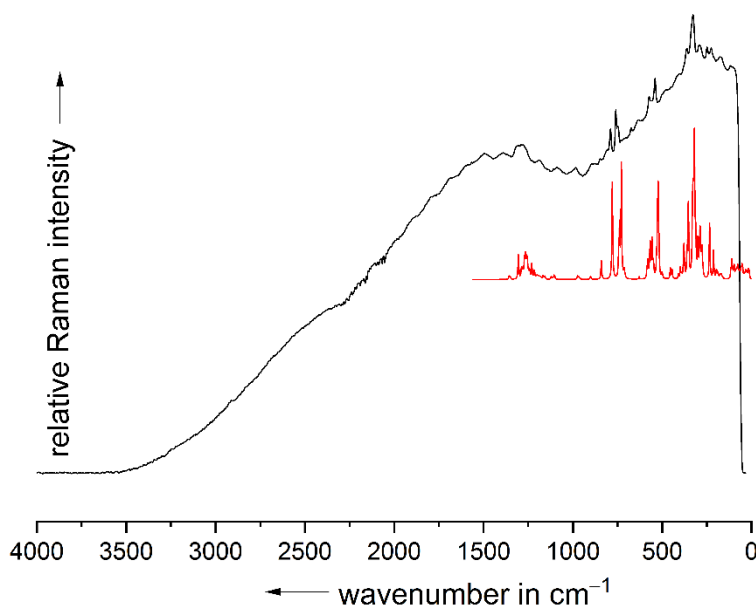


Figure S61: Raman spectrum of  $[\text{Cu}(\text{F}\{\text{Al}(\text{OR}^{\text{F}})_3\}_2)]$  (10,000 scans, 20 mW, black line) with the B3LYP(D3BJ)/def2-SVP calculated Raman spectrum of  $[\text{Cu}(\text{F}\{\text{Al}(\text{OR}^{\text{F}})_3\}_2)]$  (red line) scaled by 0.9671.

## 2.9 White Phosphorous

### 2.9.1 Chemical Deelectronation of $\text{P}_4$ Towards $[\text{P}_9]^+$

Important remark: Despite its much lower potential, also  $[\text{NO}]^+$  is able to convert  $\text{P}_4$  to  $[\text{P}_9]^+$  through the intermediate formation of  $[\text{P}_4\text{NO}]^+$ .<sup>[29]</sup> As nitrogen monoxide is deelectronated by  $[\text{naphthalene}^{\text{F}}]^+$  in 4FB, even catalytic amounts of  $[\text{NO}]^+$  have to be ruled out in the reaction. Therefore, the  $[\text{naphthalene}^{\text{F}}]^+[\text{F}\{\text{Al}(\text{OR}^{\text{F}})_3\}_2]^-$  used in the following reaction was prepared by the method 1a (see chapter 2.1.2).

$[\text{Naphthalene}^{\text{F}}]^+[\text{F}\{\text{Al}(\text{OR}^{\text{F}})_3\}_2]^-$  (25 mg, 14  $\mu\text{mol}$ , 1.0 eq.) and  $\text{P}_4$  (3.5 mg, 28  $\mu\text{mol}$ , 2.0 eq.) were dissolved in 5FB (0.7 mL) in an NMR tube. A green solution was formed and let sit for 10 min at ambient temperature. Then the reaction mixture was sonicated for 1.5 h. The solution turned yellow and was characterized by NMR spectroscopy.

#### NMR Spectroscopy

$^1\text{H}$  NMR (400.17 MHz, 5FB, 298 K): no signal.  $^{19}\text{F}$  NMR (376.5 MHz, 5FB, 298 K):  $\delta = -76.1$  (s, 54 F,  $[\text{F}\{\text{Al}(\text{OR}^{\text{F}})_3\}_2]^-$ ),  $-147.9$  (m, 4 F,  $\text{C}_{10}\text{F}_8$ ),  $-157.2$  (m, 4F,  $\text{C}_{10}\text{F}_8$ ),  $-184.8$  (s, 1 F,  $[\text{F}\{\text{Al}(\text{OR}^{\text{F}})_3\}_2]^-$ ) ppm.

$^{31}\text{P}$  NMR (121.5 MHz, 5FB, 298 K):  $\delta = 124.2$  (m, 4 P,  $\text{P}_A$ ,  $[\text{P}_9]^+$ ),  $69.0$  (m, 1 P,  $\text{P}_B$ ,  $[\text{P}_9]^+$ ),  $-263.3$  (m, 4 P,  $\text{P}_C$ ,  $[\text{P}_9]^+$ ),  $-516.1$  (s, 4 P, residual excess  $\text{P}_4$ ) ppm.

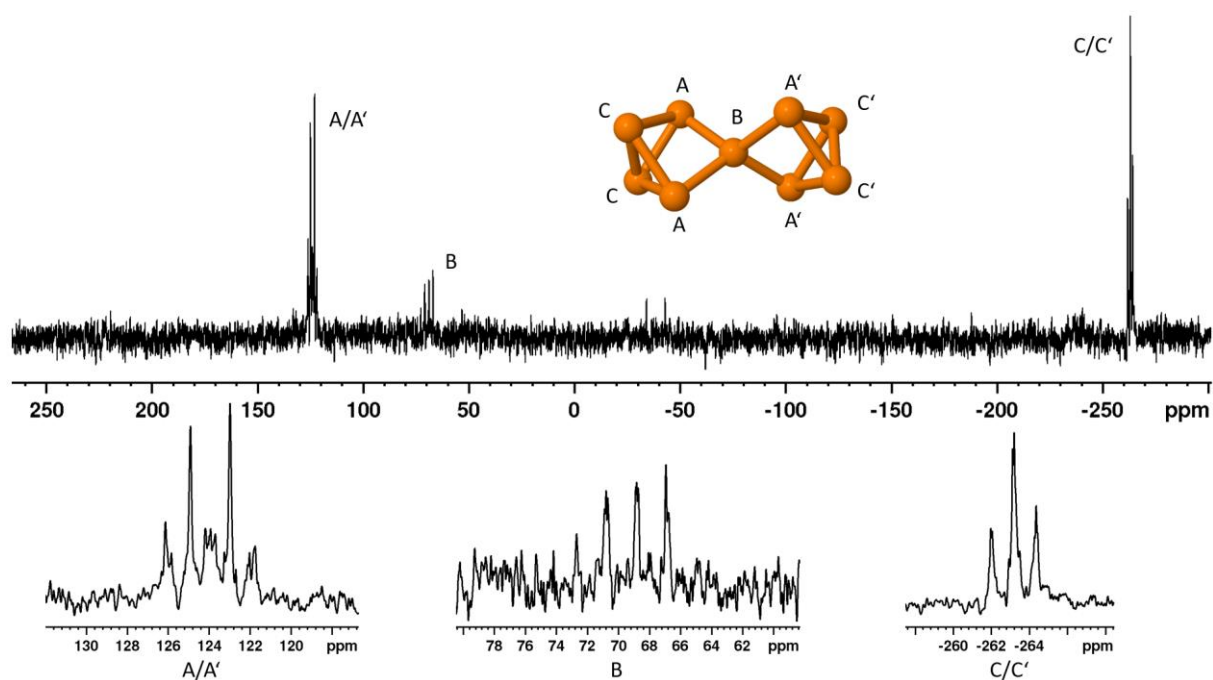


Figure S62:  $^{31}\text{P}$  NMR spectrum of the reaction of  $[\text{naphthalene}]^+[\text{F}\{\text{Al}(\text{OR}^{\text{F}})_3\}_2]^-$  with 2.0 eq. of  $\text{P}_4$  resulting in the formation of  $[\text{P}_9]^+[[\text{F}\{\text{Al}(\text{OR}^{\text{F}})_3\}_2]^-]$ .

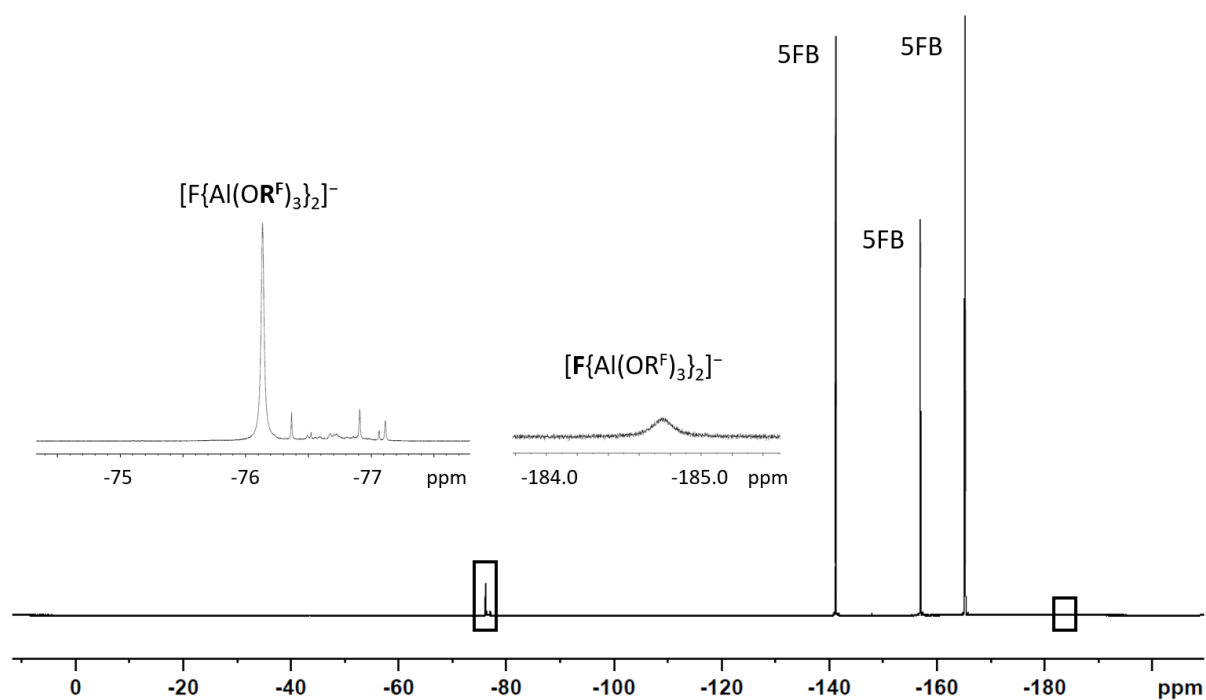


Figure S63:  $^{19}\text{F}$  NMR spectrum of the reaction of  $[\text{naphthalene}]^+[\text{F}\{\text{Al}(\text{OR}^{\text{F}})_3\}_2]^-$  with 2.0 eq. of  $\text{P}_4$  resulting in the formation of  $[\text{P}_9]^+[[\text{F}\{\text{Al}(\text{OR}^{\text{F}})_3\}_2]^-]$ .

### 3. scXRD Data Tables

Table S6: Crystallographic data tables for [naphthalene<sup>F</sup>]<sup>+</sup> [F{Al(OR<sup>F</sup>)<sub>3</sub>}<sub>2</sub>]<sup>-</sup>·(5FB), [naphthalene<sup>F</sup>]<sup>+</sup> [F{Al(OR<sup>F</sup>)<sub>3</sub>}<sub>2</sub>]<sup>-</sup>·(6FB) and [naphthalene<sup>F</sup>]<sup>+</sup> [F{Al(OR<sup>F</sup>)<sub>3</sub>}<sub>2</sub>]<sup>-</sup>·(naphthalene<sup>F</sup>).

	[naphthalene <sup>F</sup> ] <sup>+</sup> [F{Al(OR <sup>F</sup> ) <sub>3</sub> } <sub>2</sub> ] <sup>-</sup> ·(5FB)	[naphthalene <sup>F</sup> ] <sup>+</sup> [F{Al(OR <sup>F</sup> ) <sub>3</sub> } <sub>2</sub> ] <sup>-</sup> ·(6FB)	[naphthalene <sup>F</sup> ] <sup>+</sup> [F{Al(OR <sup>F</sup> ) <sub>3</sub> } <sub>2</sub> ] <sup>-</sup> ·(naphthalene <sup>F</sup> )
CCDC number	2323250	2323246	2323252
Empirical formula	C <sub>40</sub> HAl <sub>2</sub> F <sub>68</sub> O <sub>6</sub>	C <sub>40</sub> Al <sub>2</sub> F <sub>69</sub> O <sub>6</sub>	C <sub>44</sub> Al <sub>2</sub> F <sub>71</sub> O <sub>6</sub>
Formula weight	1923.37	1941.36	2027.40
Temperature [K]	100(2)	100(2)	100(2)
Crystal system	triclinic	triclinic	triclinic
Space group (number)	<i>P</i> $\bar{1}$ (2)	<i>P</i> $\bar{1}$ (2)	<i>P</i> $\bar{1}$ (2)
<i>a</i> [Å]	10.359(3)	10.3239(17)	13.197(5)
<i>b</i> [Å]	11.891(3)	11.885(2)	13.902(4)
<i>c</i> [Å]	13.295(3)	13.278(3)	36.579(13)
$\alpha$ [°]	107.296(12)	107.402(6)	84.884(7)
$\beta$ [°]	108.150(8)	108.255(5)	84.184(9)
$\gamma$ [°]	100.836(12)	100.577(6)	63.547(11)
Volume [Å <sup>3</sup> ]	1413.0(6)	1405.6(5)	5970(4)
<i>Z</i>	1	1	4
$\rho_{\text{calc}}$ [gcm <sup>-3</sup> ]	2.260	2.293	2.255
$\mu$ [mm <sup>-1</sup> ]	0.327	0.332	0.323
<i>F</i> (000)	927	935	3908
Crystal size [mm <sup>3</sup> ]	0.127×0.119×0.081	0.228×0.183×0.074	0.120×0.116×0.047
Crystal colour	green	green	green
Crystal shape	plate	plate	block
Radiation	MoK $\alpha$ ( $\lambda$ =0.71073 Å)	MoK $\alpha$ ( $\lambda$ =0.71073 Å)	MoK $\alpha$ ( $\lambda$ =0.71073 Å)
2 $\theta$ range [°]	3.77 to 54.29 (0.78 Å)	3.49 to 56.77 (0.75 Å)	3.28 to 50.30 (0.84 Å)
Index ranges	-13 ≤ <i>h</i> ≤ 13 -15 ≤ <i>k</i> ≤ 15 -17 ≤ <i>l</i> ≤ 17	-13 ≤ <i>h</i> ≤ 13 -15 ≤ <i>k</i> ≤ 15 -17 ≤ <i>l</i> ≤ 17	-15 ≤ <i>h</i> ≤ 15 -16 ≤ <i>k</i> ≤ 16 -43 ≤ <i>l</i> ≤ 43
Reflections collected	22133	35355	169544
Independent reflections	6197 <i>R</i> <sub>int</sub> = 0.0268 <i>R</i> <sub>sigma</sub> = 0.0268	7009 <i>R</i> <sub>int</sub> = 0.0441 <i>R</i> <sub>sigma</sub> = 0.0328	21294 <i>R</i> <sub>int</sub> = 0.0763 <i>R</i> <sub>sigma</sub> = 0.0600

Completeness to $\theta = 25.242^\circ$	99.7 %	99.9 %	99.5 %
Data / Restraints / Parameters	6197/1943/574	7009/1731/529	21294/34989/2597
Goodness-of-fit on $F^2$	1.043	1.047	1.025
Final $R$ indexes [ $I \geq 2\sigma(I)$ ]	$R_1 = 0.0321$ $wR_2 = 0.0734$	$R_1 = 0.0350$ $wR_2 = 0.0740$	$R_1 = 0.0527$ $wR_2 = 0.1213$
Final $R$ indexes [all data]	$R_1 = 0.0459$ $wR_2 = 0.0810$	$R_1 = 0.0523$ $wR_2 = 0.0826$	$R_1 = 0.0989$ $wR_2 = 0.1447$
Largest peak/hole [ $\text{e}\text{\AA}^{-3}$ ]	0.32/-0.29	0.40/-0.37	0.58/-0.37

Table S7: Crystallographic data tables for  $[\text{Fe}(\text{sc})_2]^+[\text{F}\{\text{Al}(\text{OR}^{\text{F}})_3\}_2]^-$ ,  $[\text{Fe}(\text{sc})_2]^{2+}([\text{F}\{\text{Al}(\text{OR}^{\text{F}})_3\}_2]^-)_2 \cdot (4\text{FB})_3$  and  $[\text{Fc}]^+[\text{F}\{\text{Al}(\text{OR}^{\text{F}})_3\}_2]^-$ .

	$[\text{Fe}(\text{sc})_2]^+[\text{F}\{\text{Al}(\text{OR}^{\text{F}})_3\}_2]^-$	$[\text{Fe}(\text{sc})_2]^{2+}([\text{F}\{\text{Al}(\text{OR}^{\text{F}})_3\}_2]^-)_2 \cdot (4\text{FB})_3$	$[\text{Fc}]^+[\text{F}\{\text{Al}(\text{OR}^{\text{F}})_3\}_2]^-$
CCDC number	2323251	2323254	2323253
Empirical formula	$\text{C}_{42}\text{H}_{20}\text{Al}_2\text{B}_2\text{F}_{55}\text{FeN}_{12}\text{O}_6$	$\text{C}_{84}\text{H}_{26}\text{Al}_4\text{B}_2\text{F}_{122}\text{FeN}_{12}\text{O}_{12}$	$\text{C}_{34}\text{H}_{10}\text{Al}_2\text{F}_{55}\text{FeO}_6$
Formula weight	1965.13	3898.56	1669.23
Temperature [K]	100(2)	100(2)	100(2)
Crystal system	triclinic	triclinic	monoclinic
Space group (number)	$P\bar{1}$ (2)	$P\bar{1}$ (2)	$P2_1/c$ (14)
$a$ [Å]	12.616(3)	12.344(2)	10.513(3)
$b$ [Å]	14.712(2)	14.699(3)	18.004(3)
$c$ [Å]	19.020(5)	18.545(4)	13.813(4)
$\alpha$ [°]	77.082(11)	77.130(16)	90
$\beta$ [°]	71.115(15)	72.296(15)	103.709(18)
$\gamma$ [°]	89.325(10)	88.16(2)	90
Volume [Å <sup>3</sup> ]	3248.5(13)	3122.6(11)	2540.0(11)
$Z$	2	1	2
$\rho_{\text{calc}}$ [gcm <sup>-3</sup> ]	2.009	2.073	2.183
$\mu$ [mm <sup>-1</sup> ]	0.475	0.394	0.581
$F(000)$	1922	1896	1618
Crystal size [mm <sup>3</sup> ]	0.206×0.192×0.138	0.259×0.165×0.139	0.243×0.238×0.148
Crystal colour	red	brown	red
Crystal shape	block	plate	block
Radiation	$\text{MoK}_\alpha$ ( $\lambda=0.71073$ Å)	$\text{MoK}_\alpha$ ( $\lambda=0.71073$ Å)	$\text{MoK}_\alpha$ ( $\lambda=0.71073$ Å)
$2\theta$ range [°]	2.85 to 52.04 (0.81 Å)	2.84 to 55.16 (0.77 Å)	3.79 to 55.97 (0.76 Å)
Index ranges	$-15 \leq h \leq 15$ $-18 \leq k \leq 18$ $-22 \leq l \leq 23$	$-16 \leq h \leq 16$ $-19 \leq k \leq 19$ $-24 \leq l \leq 24$	$-13 \leq h \leq 13$ $-23 \leq k \leq 23$ $-18 \leq l \leq 18$

Reflections collected	48836	107082	83050
Independent reflections	12772 $R_{\text{int}} = 0.0399$ $R_{\text{sigma}} = 0.0375$	14387 $R_{\text{int}} = 0.0555$ $R_{\text{sigma}} = 0.0290$	6101 $R_{\text{int}} = 0.0377$ $R_{\text{sigma}} = 0.0147$
Completeness to $\theta = 25.242^\circ$	99.7 %	99.8 %	99.9 %
Data / Restraints / Parameters	12772/5901/1093	14387/11923/1465	6101/3666/612
Goodness-of-fit on $F^2$	1.062	1.113	1.039
Final $R$ indexes [ $I \geq 2\sigma(I)$ ]	$R_1 = 0.0484$ $wR_2 = 0.1326$	$R_1 = 0.0523$ $wR_2 = 0.1392$	$R_1 = 0.0262$ $wR_2 = 0.0593$
Final $R$ indexes [all data]	$R_1 = 0.0684$ $wR_2 = 0.1465$	$R_1 = 0.0616$ $wR_2 = 0.1454$	$R_1 = 0.0314$ $wR_2 = 0.0617$
Largest peak/hole [ $\text{e}\text{\AA}^{-3}$ ]	0.69/-0.59	0.93/-0.42	0.41/-0.25

Table S8: Crystallographic data tables for [Tetracene]<sup>2+</sup>([F{Al(OR<sup>F</sup>)<sub>3</sub>}<sub>2</sub>]<sup>-</sup>)<sub>2</sub>·(4FB)<sub>3</sub> and [Pentacene]<sup>2+</sup>([F{Al(OR<sup>F</sup>)<sub>3</sub>}<sub>2</sub>]<sup>-</sup>)<sub>2</sub>.

	[Tetracene] <sup>2+</sup> ([F{Al(OR <sup>F</sup> ) <sub>3</sub> } <sub>2</sub> ] <sup>-</sup> ) <sub>2</sub> ·(4FB) <sub>3</sub>	[Pentacene] <sup>2+</sup> ([F{Al(OR <sup>F</sup> ) <sub>3</sub> } <sub>2</sub> ] <sup>-</sup> ) <sub>2</sub>
CCDC number	2241459	2323249
Empirical formula	C <sub>84</sub> H <sub>15</sub> Al <sub>4</sub> F <sub>125</sub> O <sub>12</sub>	C <sub>70</sub> H <sub>14</sub> Al <sub>4</sub> F <sub>110</sub> O <sub>12</sub>
Formula weight	3698.88	3244.73
Temperature [K]	100(2)	100(2)
Crystal system	monoclinic	triclinic
Space group (number)	<i>C</i> 2/ <i>c</i> (15)	<i>P</i> $\bar{1}$ (2)
<i>a</i> [Å]	18.809(3)	10.581(6)
<i>b</i> [Å]	20.800(6)	14.274(6)
<i>c</i> [Å]	29.904(8)	16.784(6)
$\alpha$ [°]	90	95.455(12)
$\beta$ [°]	90.516(19)	95.58(2)
$\gamma$ [°]	90	96.76(3)
Volume [Å <sup>3</sup> ]	11699(5)	2490.8(19)
<i>Z</i>	4	2
$\rho_{\text{calc}}$ [gcm <sup>-3</sup> ]	2.100	2.163
$\mu$ [mm <sup>-1</sup> ]	0.298	0.313
<i>F</i> (000)	7168	1572
Crystal size [mm <sup>3</sup> ]	0.146×0.066×0.061	0.148×0.137×0.044
Crystal colour	green	brown
Crystal shape	needle	plate
Radiation	MoK $\alpha$ ( $\lambda$ =0.71073 Å)	MoK $\alpha$ ( $\lambda$ =0.71073 Å)
2 $\theta$ range [°]	2.92 to 54.35 (0.78 Å)	3.58 to 54.38 (0.78 Å)
Index ranges	-23 ≤ <i>h</i> ≤ 24 -26 ≤ <i>k</i> ≤ 26 -38 ≤ <i>l</i> ≤ 37	-13 ≤ <i>h</i> ≤ 13 -14 ≤ <i>k</i> ≤ 18 -21 ≤ <i>l</i> ≤ 21
Reflections collected	80686	64884
Independent reflections	12953 <i>R</i> <sub>int</sub> = 0.0432 <i>R</i> <sub>sigma</sub> = 0.0301	11038 <i>R</i> <sub>int</sub> = 0.0533 <i>R</i> <sub>sigma</sub> = 0.0350
Completeness to $\theta$ = 25.242°	99.9 %	99.9 %



Data / Restraints / Parameters	12953/12939/1518	11038/8109/1010
Goodness-of-fit on $F^2$	1.020	1.018
Final $R$ indexes [ $I \geq 2\sigma(I)$ ]	$R_1 = 0.0378$ $wR_2 = 0.0938$	$R_1 = 0.0416$ $wR_2 = 0.0988$
Final $R$ indexes [all data]	$R_1 = 0.0572$ $wR_2 = 0.1069$	$R_1 = 0.0683$ $wR_2 = 0.1131$
Largest peak/hole [ $\text{e}\text{\AA}^{-3}$ ]	0.55/-0.30	0.33/-0.42

Table S 9: Crystallographic data tables for [naphthalene<sup>Cl</sup>]<sup>+</sup>[F{Al(OR<sup>F</sup>)<sub>3</sub>}<sub>2</sub>]<sup>-</sup>·(4FB) and [CuF{Al(OR<sup>F</sup>)<sub>3</sub>}<sub>2</sub>].

	[naphthalene <sup>Cl</sup> ] <sup>+</sup> [F{Al(OR <sup>F</sup> ) <sub>3</sub> } <sub>2</sub> ] <sup>-</sup> ·(4FB)	[CuF{Al(OR <sup>F</sup> ) <sub>3</sub> } <sub>2</sub> ]
CCDC number	2323248	2323247
Empirical formula	C <sub>40</sub> H <sub>2</sub> Al <sub>2</sub> Cl <sub>8</sub> F <sub>59</sub> O <sub>6</sub>	C <sub>24</sub> Al <sub>2</sub> CuF <sub>55</sub> O <sub>6</sub>
Formula weight	2036.98	1546.74
Temperature [K]	100(2)	100(2)
Crystal system	triclinic	triclinic
Space group (number)	<i>P</i> $\bar{1}$ (2)	<i>P</i> $\bar{1}$ (2)
<i>a</i> [Å]	10.542(3)	10.565(4)
<i>b</i> [Å]	13.614(3)	10.725(4)
<i>c</i> [Å]	34.876(8)	22.179(6)
$\alpha$ [°]	95.557(15)	82.617(9)
$\beta$ [°]	93.394(16)	87.180(9)
$\gamma$ [°]	110.032(12)	61.723(11)
Volume [Å <sup>3</sup> ]	4657(2)	2194.7(13)
<i>Z</i>	3	2
$\rho_{\text{calc}}$ [gcm <sup>-3</sup> ]	2.179	2.341
$\mu$ [mm <sup>-1</sup> ]	0.617	0.815
<i>F</i> (000)	2949	1484
Crystal size [mm <sup>3</sup> ]	0.183×0.169×0.121	0.207×0.189×0.156
Crystal colour	blue	colourless
Crystal shape	block	block
Radiation	MoK $\alpha$ ( $\lambda$ =0.71073 Å)	MoK $\alpha$ ( $\lambda$ =0.71073 Å)
2 $\theta$ range [°]	3.21 to 54.34 (0.78 Å)	3.70 to 61.19 (0.70 Å)
Index ranges	-13 ≤ <i>h</i> ≤ 13 -17 ≤ <i>k</i> ≤ 17 -42 ≤ <i>l</i> ≤ 44	-15 ≤ <i>h</i> ≤ 15 -15 ≤ <i>k</i> ≤ 15 -31 ≤ <i>l</i> ≤ 31
Reflections collected	213034	172583
Independent reflections	20686 <i>R</i> <sub>int</sub> = 0.0529 <i>R</i> <sub>sigma</sub> = 0.0247	13457 <i>R</i> <sub>int</sub> = 0.0858 <i>R</i> <sub>sigma</sub> = 0.0275
Completeness to $\theta$ = 25.242°	100.0 %	99.8 %

Data / Restraints / Parameters	20686/24807/2164	13457/8161/920
Goodness-of-fit on $F^2$	1.028	1.051
Final $R$ indexes [ $I \geq 2\sigma(I)$ ]	$R_1 = 0.0327$ $wR_2 = 0.0694$	$R_1 = 0.0371$ $wR_2 = 0.0943$
Final $R$ indexes [all data]	$R_1 = 0.0444$ $wR_2 = 0.0749$	$R_1 = 0.0435$ $wR_2 = 0.0980$
Largest peak/hole [ $\text{e}\text{\AA}^{-3}$ ]	0.45/−0.37	0.95/−0.71

## 4. DFT Calculations

### 4.1 Born-Fajans-Haber Cycles of Deelectronation Reactions in Solution

The structures of all particles were calculated at the B3LYP(D3BJ)/def2-TZVPP level of theory. Solvation energies were calculated with COSMO RS (parameterization BP\_TZVPD\_FINE\_22).<sup>[30]</sup> The sublimation Gibbs energy was taken from the handbook of Chemistry and physics<sup>[31]</sup> and the ionization energies of ferrocene and the acenes from ref. <sup>[32]</sup> and the electron affinity of PtF<sub>6</sub> from ref. <sup>[33]</sup>

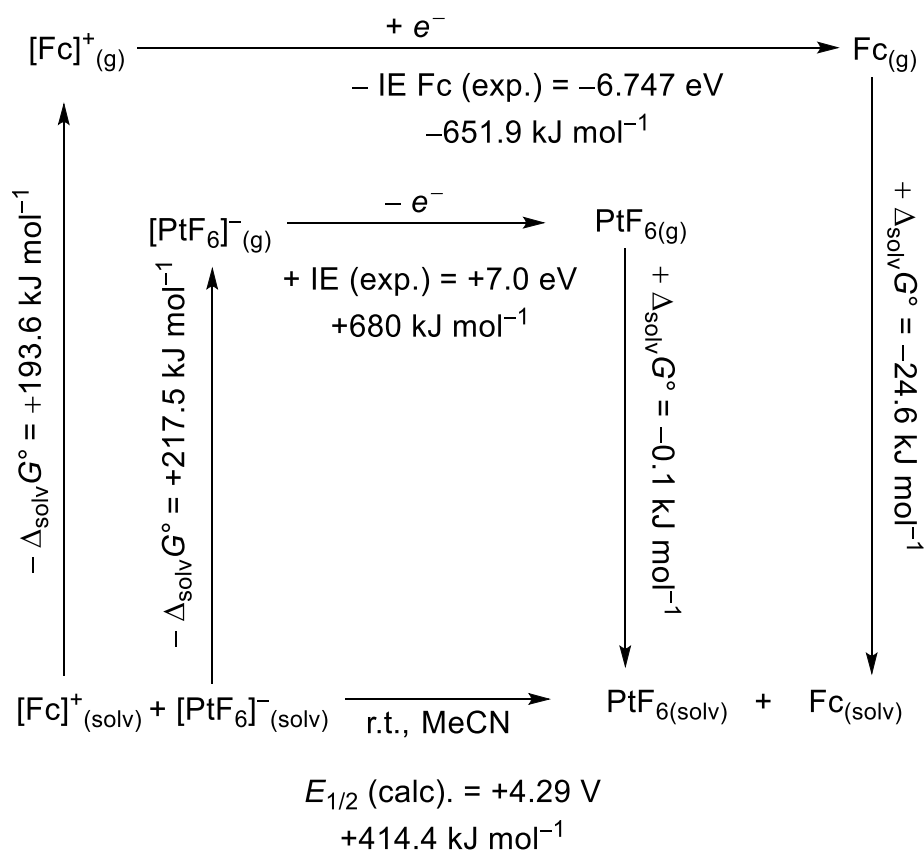


Figure S64: Born-Fajans-Haber cycle of the electron transfer between [PtF<sub>6</sub>]<sup>−</sup> and ferrocene in MeCN.

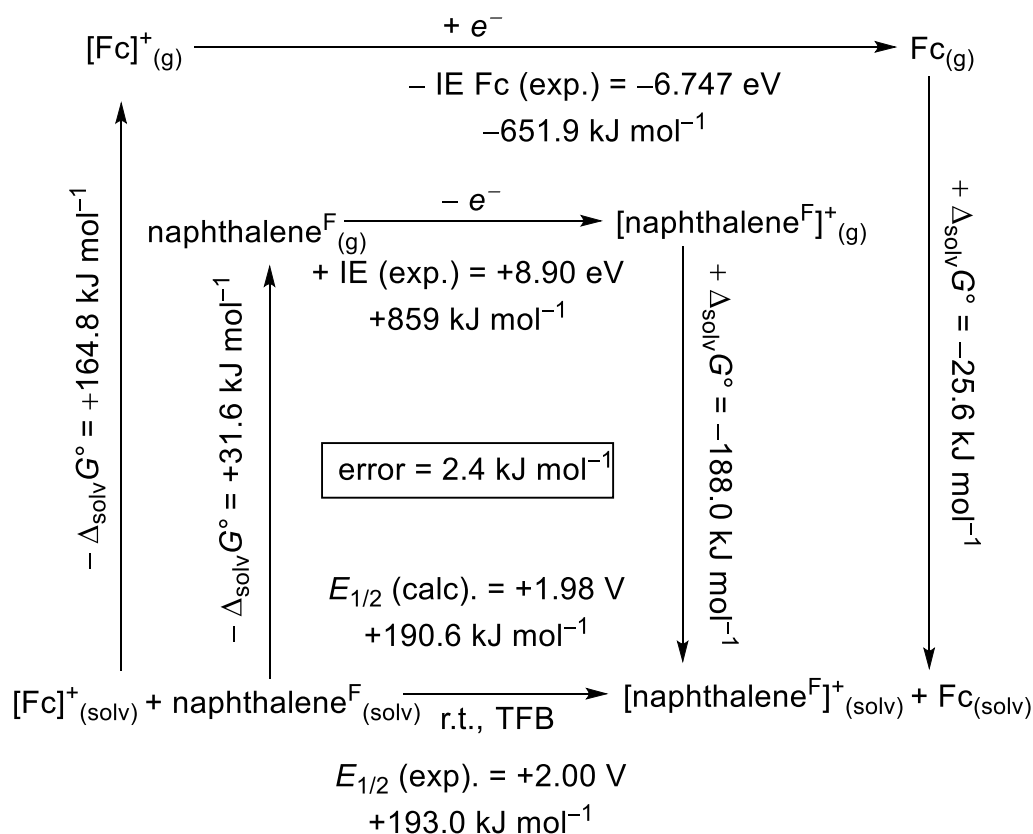


Figure S65: Born-Fajans-Haber cycle of the electron transfer between naphthalene<sup>F</sup> and ferrocene in 4FB.

#### 4.2 Born-Fajans-Haber Cycles of Deelectronation Reactions in Solid-State

The evaluated values for the experimental ionization energies and fusion/sublimation energies were taken from NIST. Molecular volumes were either directly taken from the salts or calculated from the sizes of the anions. The lattice energies as well as the entropy in solid-state were taken from the volume-based thermodynamics discussed in ref. [34]. Additional values for the gas-phase reaction were DFT-calculated using B3LYP(D3BJ)/def2-TZVPP level of theory.

$$U_{latt} = 2 \left( \left( \frac{117.3\ kJ\ nm\ mol^{-1}}{V_m(in\ nm)} \right) + 51.9\ kJ\ mol^{-1} \right)$$

$$H_{latt} = U_{latt} + 2(298\ K * 0.00813\ kJ\ K^{-1}\ mol^{-1})$$

$$S_{latt} = (1.36 * V_m(in\ nm^3)) + 0.015\ kJ\ K^{-1}\ mol^{-1}$$

Table S10: Calculation of the solid-state reaction enthalpy of the deelectronation of naphthalene<sup>F</sup> with [NO]<sup>+</sup>[WCA]<sup>-</sup>.

	[F{Al(OR <sup>F</sup> ) <sub>3</sub> } <sub>2</sub> ] <sup>-</sup>	[Al(OR <sup>F</sup> ) <sub>4</sub> ] <sup>-</sup>	[SbF <sub>6</sub> ] <sup>-</sup>
V <sub>m</sub> (NO) in nm <sup>3</sup>	0.01	0.01	0.01
V <sub>m</sub> (naphthalene <sup>F</sup> ) in nm <sup>3</sup>	0.213	0.213	0.213
V <sub>m</sub> (WCA) in nm <sup>3</sup>	1.05	0.723	0.121
V <sub>m</sub> (NO-WCA) in nm <sup>3</sup>	1.06	0.733	0.128
V <sub>m</sub> (naphthalene <sup>F</sup> -WCA) in nm <sup>3</sup>	1.265	0.936	0.334
U <sub>latt</sub> (NO-WCA) in kJ mol <sup>-1</sup>	333.8	364.0	569.3
U <sub>latt</sub> (naphthalene <sup>F</sup> -WCA) in kJ mol <sup>-1</sup>	320.7	343.6	441.9
ΔH <sub>sub</sub> (NO) in kJ mol <sup>-1</sup>	0	0	0
ΔH <sub>sub</sub> (naphthalene <sup>F</sup> ) in kJ mol <sup>-1</sup>	-70	-70	-70
H <sub>latt</sub> (NO-WCA) in kJ mol <sup>-1</sup>	338.8	368.9	574.3
H <sub>latt</sub> (naphthalene <sup>F</sup> -WCA) in kJ mol <sup>-1</sup>	325.7	348.6	446.9
ΔH(phase-change) in kJ mol <sup>-1</sup>	83.2	90.4	197.4
IE (NO) in eV	9.2642	9.2642	9.2642
IE (naphthalene <sup>F</sup> ) in eV	8.87	8.87	8.87
ΔH <sub>rxn(g)</sub> in kJ mol <sup>-1</sup>	-38.0	-38.0	-38.0
ΔH <sub>rxn(s)</sub> in kJ mol <sup>-1</sup>	+45.1	+52.3	+159.3
ΔG <sub>sub</sub> (NO) in kJ mol <sup>-1</sup>	0	0	0
ΔG <sub>sub</sub> (naphthalene <sup>F</sup> ) in kJ mol <sup>-1</sup>	-26.7	-26.7	-26.7
S <sub>s</sub> (NO-WCA) in kJ mol <sup>-1</sup>	1.456	1.011	0.189
S <sub>s</sub> (naphthalene <sup>F</sup> -WCA) in kJ mol <sup>-1</sup>	1.735	1.288	0.469
S <sub>gas</sub> (WCA) in kJ mol <sup>-1</sup>	1.975	1.333	0.377
S <sub>gas</sub> (naphthalene <sup>F</sup> ) in kJ mol <sup>-1</sup>	0.493	0.493	0.493
S <sub>gas</sub> ([naphthalene <sup>F</sup> ] <sup>+</sup> ) in kJ mol <sup>-1</sup>	0.493	0.493	0.493
S <sub>gas</sub> (NO) in kJ mol <sup>-1</sup>	0.200	0.200	0.200
S <sub>gas</sub> ([NO] <sup>+</sup> ) in kJ mol <sup>-1</sup>	0.198	0.198	0.198
ΔS <sub>latt</sub> (NO-WCA) in kJ mol <sup>-1</sup>	0.717	0.519	0.386
ΔS <sub>latt</sub> (naphthalene <sup>F</sup> -WCA) in kJ mol <sup>-1</sup>	0.733	0.538	0.401
ΔΔS <sub>latt</sub> in kJ mol <sup>-1</sup>	0.016	0.019	0.015
ΔS <sub>rxn(g)</sub> in kJ mol <sup>-1</sup>	0.002	0.002	0.002
ΔG <sub>rxn(g)</sub> in kJ mol <sup>-1</sup>	-38.6	-38.6	-38.6
ΔG <sub>phase-transfer</sub> (NO-WCA+naphthalene <sup>F</sup> ) in kJ mol <sup>-1</sup>	151.7	240.9	485.8
ΔG <sub>phase-transfer</sub> (naphthalene <sup>F</sup> -WCA+NO) in kJ mol <sup>-1</sup>	107.0	188.2	327.3
<b>ΔG<sub>rxn(s)</sub> in kJ mol<sup>-1</sup></b>	<b>6.1</b>	<b>14.1</b>	<b>119.9</b>

Table S11: Calculation of the solid-state reaction enthalpy of the deelectronation of ferrocene with  $[\text{NO}]^+[\text{WCA}]^-$ .

	$[\text{F}\{\text{Al}(\text{OR}^{\text{F}})_3\}_2]^-$	$[\text{Al}(\text{OR}^{\text{F}})_4]^-$	$[\text{SbF}_6]^-$
$V_{\text{m}}(\text{NO})$ in $\text{nm}^3$	0.01	0.01	0.01
$V_{\text{m}}(\text{Fc})$ in $\text{nm}^3$	0.204	0.204	0.204
$V_{\text{m}}(\text{WCA})$ in $\text{nm}^3$	1.05	0.723	0.121
$V_{\text{m}}(\text{Fc-WCA})$ in $\text{nm}^3$	1.06	0.733	0.128
$V_{\text{m}}(\text{Fc-WCA})$ in $\text{nm}^3$	1.27	0.927	0.318
$\Delta U_{\text{latt}}(\text{Fc-WCA})$ in $\text{kJ mol}^{-1}$	333.9	364.0	569.3
$\Delta U_{\text{latt}}(\text{Fc-WCA})$ in $\text{kJ mol}^{-1}$	320.4	344.4	447.5
$\Delta H_{\text{sub}}(\text{NO})$ in $\text{kJ mol}^{-1}$	0	0	0
$\Delta H_{\text{sub}}(\text{Fc})$ in $\text{kJ mol}^{-1}$	-73	-73	-73
$\Delta H_{\text{latt}}(\text{Fc-WCA})$ in $\text{kJ mol}^{-1}$	338.8	368.9	574.3
$\Delta H_{\text{latt}}(\text{Fc-WCA})$ in $\text{kJ mol}^{-1}$	325.4	349.4	452.5
$\Delta \Delta H_{\text{latt}}(\text{Fc-WCA})$ in $\text{kJ mol}^{-1}$	86.4	92.6	194.8
IE (NO) in eV	9.2642	9.2642	9.2642
IE (Fc) in eV	6.747	6.747	6.747
$\Delta H_{\text{rxn(g)}}$ in $\text{kJ mol}^{-1}$	-242.9	-242.9	-242.9
$\Delta H_{\text{rxn(s)}}$ in $\text{kJ mol}^{-1}$	-156.4	-150.3	-48.1
$\Delta G_{\text{sub}}(\text{NO})$ in $\text{kJ mol}^{-1}$	0	0	0
$\Delta G_{\text{sub}}(\text{Fc})$ in $\text{kJ mol}^{-1}$	-20.5	-20.5	-20.5
$S_{\text{s}}(\text{NO-WCA})$ in $\text{kJ mol}^{-1}$	1.457	1.012	0.189
$S_{\text{(s)}}(\text{Fc-WCA})$ in $\text{kJ mol}^{-1}$	1.742	1.276	0.447
$S_{\text{gas}}(\text{WCA})$ in $\text{kJ mol}^{-1}$	1.976	1.333	0.377
$S_{\text{gas}}(\text{Fc})$ in $\text{kJ mol}^{-1}$	0.427	0.427	0.427
$S_{\text{gas}}([\text{Fc}]^+)$ in $\text{kJ mol}^{-1}$	0.433	0.433	0.433
$S_{\text{gas}}(\text{NO})$ in $\text{kJ mol}^{-1}$	0.200	0.200	0.200
$S_{\text{gas}}([\text{NO}]^+)$ in $\text{kJ mol}^{-1}$	0.198	0.198	0.198
$\Delta S_{\text{latt}}(\text{NO-WCA})$ in $\text{kJ mol}^{-1}$	0.717	0.519	0.386
$\Delta S_{\text{latt}}(\text{Fc-WCA})$ in $\text{kJ mol}^{-1}$	0.666	0.490	0.362
$\Delta \Delta S_{\text{latt}}$ in $\text{kJ mol}^{-1}$	-0.051	-0.029	-0.024
$\Delta S_{\text{rxn(g)}}$ in $\text{kJ mol}^{-1}$	0.007	0.007	0.007
$\Delta G_{\text{rxn(g)}}$ in $\text{kJ mol}^{-1}$	-245.0	-245.0	-245.0
$\Delta G_{\text{phase-transfer}}(\text{NO-WCA} + \text{Fc})$ in $\text{kJ mol}^{-1}$	145.5	234.7200715	479.6
$\Delta G_{\text{phase-transfer}}(\text{Fc-WCA} + \text{NO})$ in $\text{kJ mol}^{-1}$	126.8	203.3	344.4
<b><math>\Delta G_{\text{rxn(s)}}</math> in <math>\text{kJ mol}^{-1}</math></b>	<b>-226.2</b>	<b>-213.6</b>	<b>-109.8</b>
<b><math>-\Delta G_{\text{rxn(s)}}</math> in eV</b>	<b>2.344</b>	<b>2.214</b>	<b>1.138</b>

### 4.3 Solvation Energies of the Dications

The difference of the half-wave potentials of the first and second deelectronation are defined as  $E_{1/2}(1)$  and  $E_{1/2}(2)$ . The difference between these potentials is defined as  $\Delta E_{1/2}$ . In the experiments (Table S13), its value is in each case strongly different between  $\text{SO}_2$  and 4FB. Fortunately, this difference in the  $\Delta E_{1/2}$  values between 4FB and  $\text{SO}_2$ , defined as  $\Delta\Delta E_{1/2}$  is only dependent from the solvation energies of each the neutral and dicationic substrate in both solvents, defined as  $\Delta\Delta\Delta G_{\text{solv}}$  (Table S12). Division of this value by twice the Faraday constant gives the calculated  $\Delta\Delta E_{1/2}$ .

$$\Delta\Delta E_{1/2} = \frac{\left( \left( \Delta G_{\text{solv},\text{SO}_2}(S^{2+}) - \Delta G_{\text{solv},\text{SO}_2}(S^0) \right) - \left( \Delta G_{\text{solv},4\text{FB}}(S^{2+}) - \Delta G_{\text{solv},4\text{FB}}(S^0) \right) \right)}{2 F}$$

Table S12: Solvation Energies of the substrate in its neutral and dicationic form in  $\text{SO}_2$  and 4FB and the differences in solvation energies.

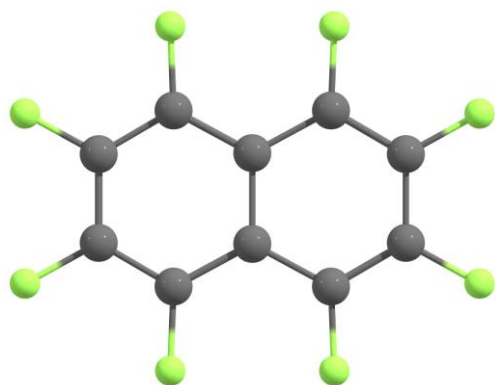
	$\Delta G_{\text{solv}} S^0$ 4FB (in kJ mol <sup>-1</sup> )	$\Delta G_{\text{solv}} S^{2+}$ 4FB (in kJ mol <sup>-1</sup> )	$\Delta\Delta G_{\text{solv}}$ 4FB (in kJ mol <sup>-1</sup> )	$\Delta G_{\text{solv}} S^0$ $\text{SO}_2$ (in kJ mol <sup>-1</sup> )	$\Delta G_{\text{solv}} S^{2+}$ $\text{SO}_2$ (in kJ mol <sup>-1</sup> )	$\Delta\Delta G_{\text{solv}}$ $\text{SO}_2$ (in kJ mol <sup>-1</sup> )	$\Delta\Delta\Delta G_{\text{solv}}$ (in kJ mol <sup>-1</sup> )	$\Delta\Delta E_{1/2}$ $\text{SO}_2$ -4FB (calc. in V)
Anthracene	-43	-547	-504	-45	-658	-613	109	0.56
Thianthrene	-49	-552	-504	-52	-662	-610	107	0.55
Nickelocene	-28	-576	-548	-30	-698	-668	121	0.63
Fe(sc) <sub>2</sub>	-74	-477	-403	-77	-560	-483	80	0.41

Table S13: Experimental half-wave potentials of the first and second deelectronation as well as the  $\Delta E_{1/2}$  values in 4FB and  $\text{SO}_2$  in comparison with the calculated  $\Delta E_{1/2}$  values.

	$E_{1/2}(1)$ 4FB (exp. in V vs. $\text{Fc}^{+/0}$ )	$E_{1/2}(2)$ 4FB (exp. in V vs. $\text{Fc}^{+/0}$ )	$\Delta E_{1/2}$ 4FB (exp. in V)	$\Delta E_{1/2}$ $\text{SO}_2$ (exp. in V)	$\Delta\Delta E_{1/2}$ $\text{SO}_2$ - 4FB (exp. in V)	$\Delta\Delta E_{1/2}$ $\text{SO}_2$ -4FB (calc. in V)	$\Delta\Delta\Delta G_{\text{solv}}$ (in kJ mol <sup>-1</sup> )
Anthracene	+0.86	+2.18	1.32	0.77	0.55	0.56	109
Thianthrene	+0.83	+1.96	1.13	0.58	0.55	0.55	107
Nickelocene	-0.33	+1.17	1.6	0.91	0.69	0.63	121
Fe(sc) <sub>2</sub>	-0.33	+1.87	2.20	1.8	0.4	0.41	80



#### 4.4 Coordinates of the DFT-Optimized Structures



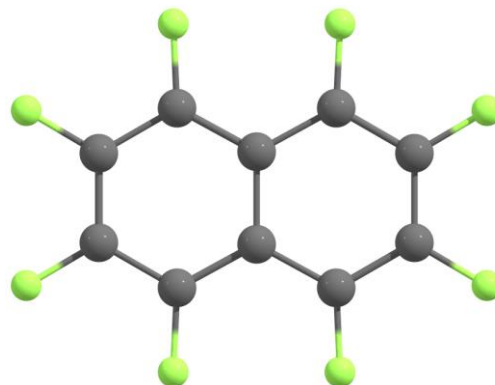
Naphthalene<sup>F</sup>

Method: (RI-)B3LYP(D3BJ)/def2-TZVPP  
Symmetry: d2h

Cartesian coordinates in Ångström:

C	-2.4246102	0.7024970	0.0000000
C	-2.4246102	-0.7024970	0.0000000
C	-1.2428972	-1.3934718	0.0000000
C	0.0000000	-0.7186466	0.0000000
C	0.0000000	0.7186466	0.0000000
C	-1.2428972	1.3934718	0.0000000
C	1.2428972	-1.3934718	0.0000000
C	2.4246102	-0.7024970	0.0000000
C	2.4246102	0.7024970	0.0000000
C	1.2428972	1.3934718	0.0000000
F	1.2949649	2.7269762	0.0000000
F	3.5888098	-1.3459061	0.0000000
F	3.5888098	1.3459061	0.0000000
F	1.2949649	-2.7269762	0.0000000
F	-3.5888098	-1.3459061	0.0000000
F	-1.2949649	-2.7269762	0.0000000
F	-1.2949649	2.7269762	0.0000000
F	-3.5888098	1.3459061	0.0000000

SCF energy GE00PT = -1179.762927981 H  
ZPE = 215.1 kJ/mol  
FREEH energy = 252.15 kJ/mol  
FREEH entropy = 0.48128 kJ/mol/K



[Naphthalene<sup>F</sup>]<sup>+</sup>

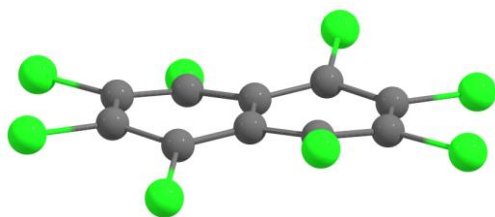
Method: (RI-)B3LYP(D3BJ)/def2-TZVPP  
Symmetry: d2h

Cartesian coordinates in Ångström:

C	-2.4529950	0.6931471	0.0000000
C	-2.4529950	-0.6931471	0.0000000
C	-1.2374134	-1.3924575	0.0000000
C	0.0000000	-0.7172604	0.0000000
C	0.0000000	0.7172604	0.0000000
C	-1.2374134	1.3924575	0.0000000
C	1.2374134	-1.3924575	0.0000000
C	2.4529950	-0.6931471	0.0000000
C	2.4529950	0.6931471	0.0000000
C	1.2374134	1.3924575	0.0000000
F	1.2961654	2.6978837	0.0000000
F	3.5803774	-1.3556795	0.0000000
F	3.5803774	1.3556795	0.0000000
F	1.2961654	-2.6978837	0.0000000
F	-3.5803774	-1.3556795	0.0000000
F	-1.2961654	-2.6978837	0.0000000
F	-1.2961654	2.6978837	0.0000000
F	-3.5803774	1.3556795	0.0000000

SCF energy GE00PT = -1179.454509081 H  
ZPE = 216.6 kJ/mol  
FREEH energy = 253.50 kJ/mol  
FREEH entropy = 0.48169 kJ/mol/K

Boat-Isomer of [Naphthalene<sup>Cl</sup>]<sup>+</sup>



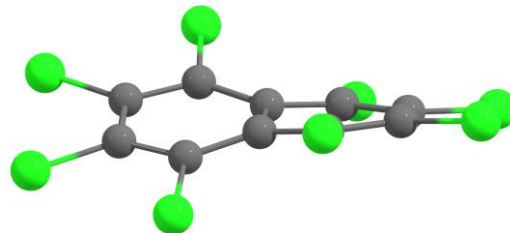
Method: (RI-)B3LYP(D3BJ)/def2-TZVPP  
Symmetry: c2h

Cartesian coordinates in Ångström:

Cl	1.4302782	-0.4037953	-3.0519931
Cl	3.1781128	-2.3467410	-1.5377122
Cl	3.1781128	-2.3467410	1.5377122
Cl	1.4302782	-0.4037953	3.0519931
C	1.0877412	-0.6343410	-1.4005352
C	2.0078571	-1.4394829	-0.6966561
C	2.0078571	-1.4394829	0.6966561
C	1.0877412	-0.6343410	1.4005352
C	-0.0000000	-0.0000000	0.7249858
Cl	-1.4302782	0.4037953	3.0519931
Cl	-3.1781128	2.3467410	1.5377122
Cl	-3.1781128	2.3467410	-1.5377122
Cl	-1.4302782	0.4037953	-3.0519931
C	-1.0877412	0.6343410	1.4005352
C	-2.0078571	1.4394829	0.6966561
C	-2.0078571	1.4394829	-0.6966561
C	-1.0877412	0.6343410	-1.4005352
C	-0.0000000	-0.0000000	-0.7249858

SCF energy GE0OPT = -4061.994297964 H  
ZPE = 182.0 kJ/mol  
FREEH energy = 225.87 kJ/mol  
FREEH entropy = 0.57991 kJ/mol/K

Twist-Isomer of [Naphthalene<sup>Cl</sup>]<sup>+</sup>

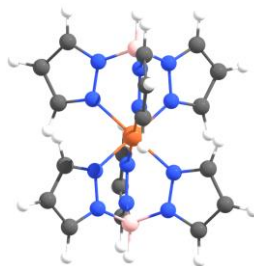
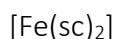


Method: (RI-)B3LYP(D3BJ)/def2-TZVPP  
Symmetry: d2

Cartesian coordinates in Ångström:

C	0.1481393	-0.6826165	-2.4627992
C	-0.1481393	0.6826165	-2.4627992
C	-0.2198274	1.3860544	-1.2434581
C	0.0000000	0.7215969	0.0000000
C	0.0000000	-0.7215969	0.0000000
C	0.2198274	-1.3860544	-1.2434581
C	-0.2198274	-1.3860544	1.2434581
C	0.2198274	1.3860544	1.2434581
C	0.1481393	0.6826165	2.4627992
C	-0.1481393	-0.6826165	2.4627992
Cl	-0.7156717	-3.0117965	1.3305761
Cl	0.7156717	3.0117965	1.3305761
Cl	0.7156717	-3.0117965	-1.3305761
Cl	0.3902695	-1.4933144	-3.9396515
Cl	-0.3902695	1.4933144	-3.9396515
Cl	-0.7156717	3.0117965	-1.3305761
Cl	0.3902695	1.4933144	3.9396515
Cl	-0.3902695	-1.4933144	3.9396515

SCF energy GE0OPT = -4061.997044520 H  
ZPE = 182.2 kJ/mol  
FREEH energy = 225.96 kJ/mol  
FREEH entropy = 0.56053 kJ/mol/K

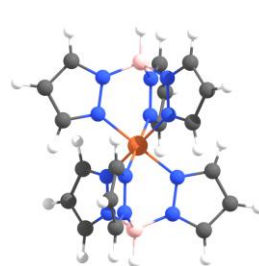
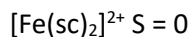


Method: (RI-)B3LYP(D3BJ)/def2-TZVPP  
Symmetry: d3d

Cartesian coordinates in Ångström:

Fe	0.0000000	0.0000000	0.0000000
N	-1.3892739	0.8020977	1.1840927
N	-1.2429907	0.7176410	2.5263861
N	1.3892739	0.8020977	1.1840927
N	1.2429907	0.7176410	2.5263861
N	0.0000000	-1.6041953	1.1840927
N	-0.0000000	-1.4352820	2.5263861
C	-2.5248068	1.4576979	0.9519345
H	-2.8435136	1.6417033	-0.0590153
C	-3.1322527	1.8084070	2.1653505
H	-4.0549171	2.3411075	2.3098051
C	-2.2810989	1.3169930	3.1398682
H	-2.3392323	1.3505564	4.2135739
B	0.0000000	-0.0000000	3.0897737
H	0.0000000	-0.0000000	4.2856127
C	2.5248068	1.4576979	0.9519345
H	2.8435136	1.6417033	-0.0590153
C	3.1322527	1.8084070	2.1653505
H	4.0549171	2.3411075	2.3098051
C	2.2810989	1.3169930	3.1398682
H	2.3392323	1.3505564	4.2135739
C	0.0000000	-2.9153958	0.9519345
H	0.0000000	-3.2834066	-0.0590153
C	-0.0000000	-3.6168139	2.1653505
H	0.0000000	-4.6822150	2.3098051
C	0.0000000	-2.6339861	3.1398682
H	0.0000000	-2.7011128	4.2135739
N	1.3892739	-0.8020977	-1.1840927
N	1.2429907	-0.7176410	-2.5263861
N	-1.3892739	-0.8020977	-1.1840927
N	-1.2429907	-0.7176410	-2.5263861
N	0.0000000	1.6041953	-1.1840927
N	-0.0000000	1.4352820	-2.5263861
C	2.5248068	-1.4576979	-0.9519345
H	2.8435136	-1.6417033	0.0590153
C	3.1322527	-1.8084070	-2.1653505
H	4.0549171	-2.3411075	-2.3098051
C	2.2810989	-1.3169930	-3.1398682
H	2.3392323	-1.3505564	-4.2135739
B	0.0000000	0.0000000	-3.0897737
H	0.0000000	0.0000000	-4.2856127
C	-2.5248068	-1.4576979	-0.9519345
H	-2.8435136	-1.6417033	0.0590153
C	-3.1322527	-1.8084070	-2.1653505
H	-4.0549171	-2.3411075	-2.3098051
C	-2.2810989	-1.3169930	-3.1398682
H	-2.3392323	-1.3505564	-4.2135739
C	0.0000000	2.9153958	-0.9519345
H	0.0000000	3.2834066	0.0590153
C	0.0000000	3.6168139	-2.1653505
H	0.0000000	4.6822150	-2.3098051
C	0.0000000	2.6339861	-3.1398682
H	-0.0000000	2.7011128	-4.2135739

SCF energy GE0OPT = -2668.416019594 H  
ZPE = 1064. kJ/mol  
FREEH energy = 1130.94 kJ/mol  
FREEH entropy = 0.68939 kJ/mol/K

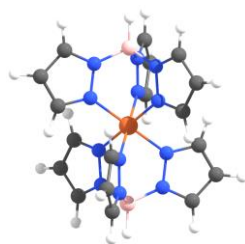
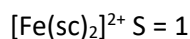


Method: (RI-)B3LYP(D3BJ)/def2-TZVPP  
Symmetry: c1

Cartesian coordinates in Ångström:

Fe	21.5717449	9.3215446	8.6095452
N	20.1761075	9.2007055	9.9737925
N	20.3791511	8.4556356	11.0922079
N	22.8905862	9.5444516	10.0354040
N	22.8282134	8.7683035	11.1494201
N	21.8078034	7.4358933	8.7346759
N	21.8581513	6.8331412	9.9583574
C	18.9428548	9.7251777	10.0533399
H	18.5616078	10.3588415	9.2722087
C	18.3420175	9.3188113	11.2376761
H	17.3596624	9.5698527	11.5956538
C	19.2881038	8.5090319	11.8657636
H	19.2447787	7.9747130	12.7995978
B	21.7162697	7.7086202	11.2364993
H	21.7761711	7.0580922	12.2261127
C	23.9492079	10.3595900	10.1668380
H	24.1960038	11.0710433	9.3988364
C	24.5770632	10.1115656	11.3804599
H	25.4483101	10.5982788	11.7807868
C	23.8346776	9.0891284	11.9712708
H	23.9669635	8.5788028	12.9101600
C	21.9521835	6.4712712	7.7963254
H	21.9434026	6.7200181	6.7503694
C	22.0954819	5.2476611	8.4146554
H	22.2291049	4.2856682	7.9526429
C	22.0296251	5.5239660	9.7931527
H	22.0956391	4.8614976	10.6402518
N	22.9673824	9.4423838	7.2452978
N	22.7643388	10.1874536	6.1268824
N	20.2529034	9.0986378	7.1836865
N	20.3152763	9.8747860	6.0696703
N	21.3356867	11.2071958	8.4844146
N	21.2853388	11.8099481	7.2607331
C	24.2006345	8.9179102	7.1657500
H	24.5818808	8.2842453	7.9468806
C	24.8014719	9.3242768	5.9814140
H	25.7838263	9.0732337	5.6234355
C	23.8553867	10.1340581	5.3533274
H	23.8987134	10.6683800	4.4194949
B	21.4272202	10.9344692	5.9825912
H	21.3673188	11.5849972	4.9929779
C	19.1942814	8.2834999	7.0522527
H	18.9474856	7.5720464	7.8202541
C	18.5664254	8.5315250	5.8386311
H	17.6951776	8.0448130	5.4383050
C	19.3088120	9.5539612	5.2478197
H	19.1765268	10.0642860	4.3089299
C	21.1913068	12.1718179	9.4227652
H	21.2000867	11.9230707	10.4687212
C	21.0480097	13.3954282	8.8044354
H	20.9143883	14.3574212	9.2664480
C	21.1138657	13.1191233	7.4259381
H	21.0478513	13.7815918	6.5788390

SCF energy GE0OPT = -2667.791298699 H  
ZPE = 1065. kJ/mol  
FREEH energy = 1130.94 kJ/mol  
FREEH entropy = 0.69464 kJ/mol/K

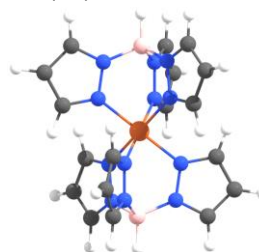
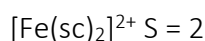


Method: (RI-)B3LYP(D3BJ)/def2-TZVPP  
Symmetry: c1

Cartesian coordinates in Ångström:

Fe	21.5717487	9.3215478	8.6095471
N	20.1874268	9.2029233	9.9566955
N	20.3827886	8.4388562	11.0639049
N	22.8795568	9.5445136	10.0184668
N	22.8309094	8.7507851	11.1209229
N	21.8121256	7.4052633	8.7325912
N	21.8617702	6.8049899	9.9511955
C	18.9634691	9.7581646	10.0489015
H	18.5924477	10.4082050	9.2766458
C	18.3643365	9.3473834	11.2280504
H	17.3890800	9.6135448	11.5945488
C	19.2982282	8.5117791	11.8419751
H	19.2514605	7.9742815	12.7740080
B	21.7203498	7.6823584	11.2137461
H	21.7773006	7.0516166	12.2155773
C	23.9206743	10.3873034	10.1620843
H	24.1523457	11.1129209	9.4029626
C	24.5491351	10.1335678	11.3698581
H	25.4094360	10.6330451	11.7781684
C	23.8264448	9.0884390	11.9466376
H	23.9635893	8.5750627	12.8833530
C	21.9554655	6.4486591	7.7949030
H	21.9471851	6.6957981	6.7483071
C	22.0989747	5.2192799	8.4162814
H	22.2321051	4.2603924	7.9481736
C	22.0338387	5.4899101	9.7836751
H	22.0992219	4.8301148	10.6323137
N	22.9560691	9.4401643	7.2623967
N	22.7607087	10.2042293	6.1551858
N	20.2639391	9.0985841	7.2006283
N	20.3125866	9.8923121	6.0981716
N	21.3313723	11.2378323	8.4865004
N	21.2817293	11.8381034	7.2678950
C	24.1800160	8.8849009	7.1701804
H	24.5510334	8.2348559	7.9424342
C	24.7791432	9.2956661	5.9910231
H	25.7543875	9.0294787	5.6245112
C	23.8452647	10.1312942	5.3771108
H	23.8920396	10.6688020	4.4450843
B	21.4231508	10.9607335	6.0053457
H	21.3662016	11.5914743	5.0035137
C	19.2228364	8.2557779	7.0569999
H	18.9912023	7.5301192	7.8160936
C	18.5943439	8.5095482	5.8492498
H	17.7340278	8.0100877	5.4409511
C	19.3170245	9.5546875	5.2724772
H	19.1798517	10.0680949	4.3357831
C	21.1880321	12.1944387	9.4241865
H	21.1963124	11.9473019	10.4707829
C	21.0445209	13.4238162	8.8028054
H	20.9114031	14.3827064	9.2709113
C	21.1096417	13.1531811	7.4354120
H	21.0442299	13.8129707	6.5867712

SCF energy GE0OPT = -2667.828313957 H  
ZPE = 1070. kJ/mol  
FREEH energy = 1135.06 kJ/mol  
FREEH entropy = 0.68987 kJ/mol/K



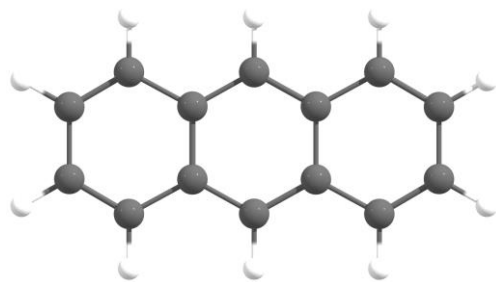
Method: (RI-)B3LYP(D3BJ)/def2-TZVPP  
Symmetry: c1

Cartesian coordinates in Ångström:

Fe	21.5717798	9.3216773	8.6096313
N	20.1861491	9.1637274	9.9805101
N	20.3903749	8.3612370	11.0601991
N	22.8862654	9.5075094	10.0445657
N	22.8405459	8.6725076	11.1178081
N	21.8374014	7.2107015	8.7507563
N	21.8767452	6.6645099	9.9969123
C	18.9724438	9.7374455	10.1036099
H	18.6080259	10.4211230	9.3576644
C	18.3832022	9.2939672	11.2746084
H	17.4155569	9.5600831	11.6612326
C	19.3144509	8.4265593	11.8502924
H	19.2709140	7.8610205	12.7658990
B	21.7303733	7.5896914	11.2118017
H	21.7805107	7.0043224	12.2418075
C	23.9106627	10.3662095	10.2200199
H	24.1259766	11.1238668	9.4877975
C	24.5378809	10.0771365	11.4192238
H	25.3891936	10.5748495	11.8484098
C	23.8283167	9.0003932	11.9561442
H	23.9701224	8.4579773	12.8757783
C	21.9865507	6.2067373	7.8733322
H	21.9877826	6.3995197	6.8138161
C	22.1234742	5.0011037	8.5525010
H	22.2584132	4.0202505	8.1329531
C	22.0480479	5.3373147	9.9008620
H	22.1052847	4.7198662	10.7812713
N	22.9573231	9.4793859	7.2386415
N	22.7531005	10.2817662	6.1588668
N	20.2571984	9.1359282	7.1747501
N	20.3029028	9.9709707	6.1015404
N	21.3064499	11.4326712	8.4684642
N	21.2671486	11.9788347	7.2222937
C	24.1706057	8.9048724	7.1151115
H	24.5350149	8.2212856	7.8611443
C	24.7594591	9.3474751	5.9435868
H	25.7266668	9.0804905	5.5564672
C	23.8285529	10.2154550	5.3682100
H	23.8720423	10.7807876	4.4524741
B	21.4132459	11.0536006	6.0074156
H	21.3631067	11.6389545	4.9774012
C	19.2326325	8.2774077	6.9993866
H	19.0173366	7.5196969	7.7315574
C	18.6052222	8.5667248	5.8003415
H	17.7537376	8.0692073	5.3712701
C	19.3148985	9.6433678	5.2633727
H	19.1730345	10.1858838	4.3438065
C	21.1577327	12.4367094	9.3458771
H	21.1567634	12.2439832	10.4054043
C	21.0208956	13.6423367	8.6666812
H	20.8861269	14.6232216	9.0862095
C	21.0960632	13.3060601	7.3183211
H	21.0387764	13.9234824	6.4378969

SCF energy GE0OPT = -2667.781978292 H  
ZPE = 1060. kJ/mol  
FREEH energy = 1128.96 kJ/mol  
FREEH entropy = 0.72904 kJ/mol/K

# Anthracene



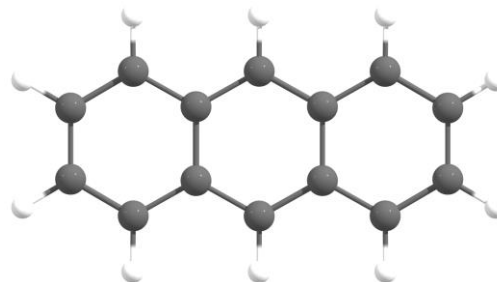
Method: (RI-)B3LYP(D3BJ)/def2-TZVPP  
Symmetry: d2h

Cartesian coordinates in Ångström:

C	-1.2181258	0.7197226	0.0000000
C	-1.2181258	-0.7197226	0.0000000
C	0.0000000	-1.3985089	0.0000000
C	1.2181258	-0.7197226	0.0000000
C	1.2181258	0.7197226	0.0000000
C	0.0000000	1.3985089	0.0000000
C	2.4691811	1.4014784	0.0000000
C	3.6447682	0.7106525	0.0000000
C	3.6447682	-0.7106525	0.0000000
C	2.4691811	-1.4014784	0.0000000
C	-2.4691811	-1.4014784	0.0000000
C	-3.6447682	-0.7106525	0.0000000
C	-3.6447682	0.7106525	0.0000000
C	-2.4691811	1.4014784	0.0000000
H	-2.4674319	2.4841934	0.0000000
H	-4.5871744	1.2418638	0.0000000
H	-4.5871744	-1.2418638	0.0000000
H	-2.4674319	-2.4841934	0.0000000
H	0.0000000	-2.4820830	0.0000000
H	0.0000000	2.4820830	0.0000000
H	2.4674319	2.4841934	0.0000000
H	4.5871744	1.2418638	0.0000000
H	4.5871744	-1.2418638	0.0000000
H	2.4674319	-2.4841934	0.0000000

SCF energy GE0OPT = -539.4353960771 H  
ZPE = 509.2 kJ/mol  
FREEH energy = 533.91 kJ/mol  
FREEH entropy = 0.38621 kJ/mol/K

# [Anthracene]<sup>2+</sup>



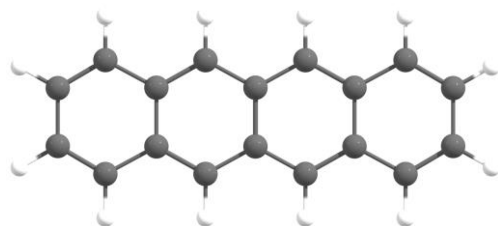
Method: (RI-)B3LYP(D3BJ)/def2-TZVPP  
Symmetry: d2h

Cartesian coordinates in Ångström:

C	-1.2293267	0.7172714	0.0000000
C	-1.2293267	-0.7172714	0.0000000
C	0.0000000	-1.4053237	0.0000000
C	1.2293267	-0.7172714	0.0000000
C	1.2293267	0.7172714	0.0000000
C	0.0000000	1.4053237	0.0000000
C	2.4491053	1.4025072	0.0000000
C	3.6667412	0.6915122	0.0000000
C	3.6667412	-0.6915122	0.0000000
C	2.4491053	-1.4025072	0.0000000
C	-2.4491053	-1.4025072	0.0000000
C	-3.6667412	-0.6915122	0.0000000
C	-3.6667412	0.6915122	0.0000000
C	-2.4491053	1.4025072	0.0000000
H	-2.4613046	2.4852481	0.0000000
H	-4.6012904	1.2362288	0.0000000
H	-4.6012904	-1.2362288	0.0000000
H	-2.4613046	-2.4852481	0.0000000
H	0.0000000	-2.4896874	0.0000000
H	0.0000000	2.4896874	0.0000000
H	2.4613046	2.4852481	0.0000000
H	4.6012904	1.2362288	0.0000000
H	4.6012904	-1.2362288	0.0000000
H	2.4613046	-2.4852481	0.0000000

SCF energy GE0OPT = -538.7516892133 H  
ZPE = 510.1 kJ/mol  
FREEH energy = 535.56 kJ/mol  
FREEH entropy = 0.39213 kJ/mol/K

Tetracene

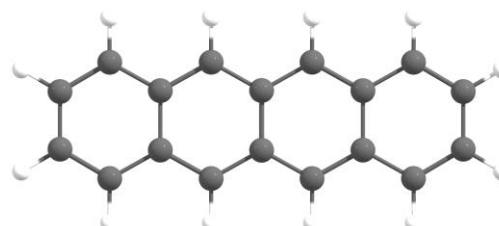


Method: (RI-)B3LYP(D3BJ)/def2-TZVPP  
Symmetry: d2h

Cartesian coordinates in Ångström:

C	0.0000000	0.7233817	0.0000000
C	0.0000000	-0.7233817	0.0000000
C	1.2300721	-1.4013027	0.0000000
C	2.4392153	-0.7231037	0.0000000
C	2.4392153	0.7231037	0.0000000
C	1.2300721	1.4013027	0.0000000
C	3.6954821	1.4037701	0.0000000
C	4.8675551	0.7130368	0.0000000
C	4.8675551	-0.7130368	0.0000000
C	3.6954821	-1.4037701	0.0000000
C	-1.2300721	-1.4013027	0.0000000
C	-2.4392153	-0.7231037	0.0000000
C	-2.4392153	0.7231037	0.0000000
C	-1.2300721	1.4013027	0.0000000
H	-1.2304291	2.4847616	0.0000000
C	-3.6954821	1.4037701	0.0000000
C	-3.6954821	-1.4037701	0.0000000
H	-1.2304291	-2.4847616	0.0000000
H	1.2304291	-2.4847616	0.0000000
H	1.2304291	2.4847616	0.0000000
H	3.6941699	2.4864666	0.0000000
H	5.8108622	1.2426158	0.0000000
H	5.8108622	-1.2426158	0.0000000
H	3.6941699	-2.4864666	0.0000000
C	-4.8675551	-0.7130368	0.0000000
C	-4.8675551	0.7130368	0.0000000
H	-3.6941699	-2.4864666	0.0000000
H	-3.6941699	2.4864666	0.0000000
H	-5.8108622	1.2426158	0.0000000
H	-5.8108622	-1.2426158	0.0000000

SCF energy GE0OPT = -693.0451534719 H  
ZPE = 631.2 kJ/mol  
FREEH energy = 662.94 kJ/mol  
FREEH entropy = 0.44084 kJ/mol/K

[Tetracene]<sup>2+</sup>

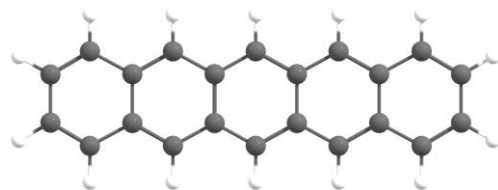
Method: (RI-)B3LYP(D3BJ)/def2-TZVPP  
Symmetry: d2h

Cartesian coordinates in Ångström:

C	0.0000000	0.7224602	0.0000000
C	0.0000000	-0.7224602	0.0000000
C	1.2198853	-1.4065981	0.0000000
C	2.4491684	-0.7190752	0.0000000
C	2.4491684	0.7190752	0.0000000
C	1.2198853	1.4065981	0.0000000
C	3.6724870	1.4045227	0.0000000
C	4.8747946	0.6968402	0.0000000
C	4.8747946	-0.6968402	0.0000000
C	3.6724870	-1.4045227	0.0000000
C	-1.2198853	-1.4065981	0.0000000
C	-2.4491684	-0.7190752	0.0000000
C	-2.4491684	0.7190752	0.0000000
C	-1.2198853	1.4065981	0.0000000
H	-1.2224260	2.4901423	0.0000000
C	-3.6724870	1.4045227	0.0000000
C	-3.6724870	-1.4045227	0.0000000
H	-1.2224260	-2.4901423	0.0000000
H	1.2224260	-2.4901423	0.0000000
H	1.2224260	2.4901423	0.0000000
H	3.6819558	2.4865112	0.0000000
H	5.8126379	1.2351034	0.0000000
H	5.8126379	-1.2351034	0.0000000
H	3.6819558	-2.4865112	0.0000000
C	-4.8747946	-0.6968402	0.0000000
C	-4.8747946	0.6968402	0.0000000
H	-3.6819558	-2.4865112	0.0000000
H	-3.6819558	2.4865112	0.0000000
H	-5.8126379	1.2351034	0.0000000
H	-5.8126379	-1.2351034	0.0000000

SCF energy GE0OPT = -692.4186262806 H  
ZPE = 634.9 kJ/mol  
FREEH energy = 667.07 kJ/mol  
FREEH entropy = 0.44423 kJ/mol/K

# Pentacene



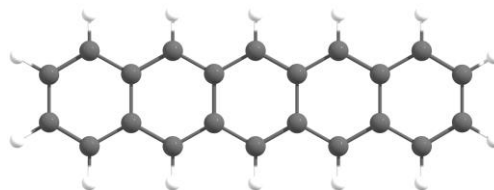
Method: (RI-)B3LYP(D3BJ)/def2-TZVPP  
Symmetry: d2h

Cartesian coordinates in Ångström:

C	-1.2208843	0.7258044	0.0000000
C	-1.2208843	-0.7258044	0.0000000
C	0.0000000	-1.4033749	0.0000000
C	1.2208843	-0.7258044	0.0000000
C	1.2208843	0.7258044	0.0000000
C	0.0000000	1.4033749	0.0000000
C	2.4569270	1.4029008	0.0000000
C	3.6617200	0.7249389	0.0000000
C	3.6617200	-0.7249389	0.0000000
C	2.4569270	-1.4029008	0.0000000
C	-2.4569270	-1.4029008	0.0000000
C	-3.6617200	-0.7249389	0.0000000
C	-3.6617200	0.7249389	0.0000000
C	-2.4569270	1.4029008	0.0000000
H	-2.4575881	2.4863326	0.0000000
C	-4.9205984	1.4050019	0.0000000
C	-4.9205984	-1.4050019	0.0000000
H	-2.4575881	-2.4863326	0.0000000
H	0.0000000	-2.4867036	0.0000000
H	0.0000000	2.4867036	0.0000000
H	2.4575881	2.4863326	0.0000000
C	4.9205984	1.4050019	0.0000000
C	4.9205984	-1.4050019	0.0000000
H	2.4575881	-2.4863326	0.0000000
C	-6.0909114	-0.7142882	0.0000000
C	-6.0909114	0.7142882	0.0000000
H	-4.9195357	-2.4876890	0.0000000
H	-4.9195357	2.4876890	0.0000000
H	-7.0346712	1.2430386	0.0000000
H	-7.0346712	-1.2430386	0.0000000
C	6.0909114	-0.7142882	0.0000000
C	6.0909114	0.7142882	0.0000000
H	4.9195357	2.4876890	0.0000000
H	7.0346712	1.2430386	0.0000000
H	7.0346712	-1.2430386	0.0000000
H	4.9195357	-2.4876890	0.0000000

SCF energy GE00PT = -846.6537237393 H  
ZPE = 752.9 kJ/mol  
FREEH energy = 791.83 kJ/mol  
FREEH entropy = 0.49553 kJ/mol/K

# [Pentacene]<sup>2+</sup>

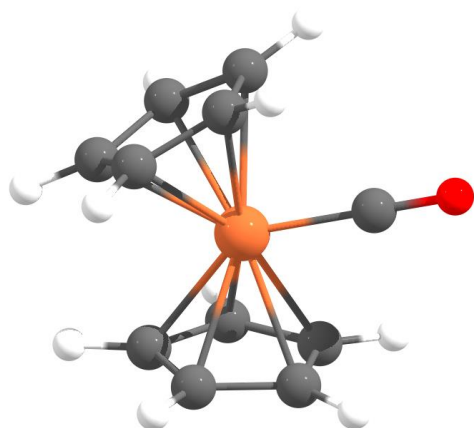
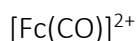


Method: (RI-)B3LYP(D3BJ)/def2-TZVPP  
Symmetry: d2h

Cartesian coordinates in Ångström:

C	-1.2226324	0.7245030	0.0000000
C	-1.2226324	-0.7245030	0.0000000
C	-0.0000000	-1.4084619	0.0000000
C	1.2226324	-0.7245030	0.0000000
C	1.2226324	0.7245030	0.0000000
C	0.0000000	1.4084619	0.0000000
C	2.4403898	1.4069182	0.0000000
C	3.6668674	0.7202753	0.0000000
C	3.6668674	-0.7202753	0.0000000
C	2.4403898	-1.4069182	0.0000000
C	-2.4403898	-1.4069182	0.0000000
C	-3.6668674	-0.7202753	0.0000000
C	-3.6668674	0.7202753	0.0000000
C	-2.4403898	1.4069182	0.0000000
H	-2.4434703	2.4899801	0.0000000
C	-4.8950440	1.4057120	0.0000000
C	-4.8950440	-1.4057120	0.0000000
H	-2.4434703	-2.4899801	0.0000000
H	0.0000000	-2.4917561	0.0000000
H	0.0000000	2.4917561	0.0000000
H	2.4434703	2.4899801	0.0000000
C	4.8950440	1.4057120	0.0000000
C	4.8950440	-1.4057120	0.0000000
H	2.4434703	-2.4899801	0.0000000
C	-6.0878111	-0.7007227	0.0000000
C	-6.0878111	0.7007227	0.0000000
H	-4.9023494	-2.4873830	0.0000000
H	-4.9023494	2.4873830	0.0000000
H	-7.0275921	1.2352079	0.0000000
H	-7.0275921	-1.2352079	0.0000000
C	6.0878111	-0.7007227	0.0000000
C	6.0878111	0.7007227	0.0000000
H	4.9023494	2.4873830	0.0000000
H	7.0275921	1.2352079	0.0000000
H	7.0275921	-1.2352079	0.0000000
H	4.9023494	-2.4873830	0.0000000

SCF energy GE00PT = -846.0687562887 H  
ZPE = 702.9 kJ/mol  
FREEH energy = 743.71 kJ/mol  
FREEH entropy = 0.51393 kJ/mol/K

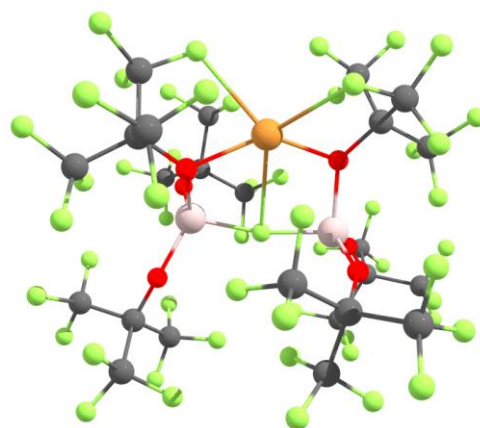


Method: (RI-)B3LYP(D3BJ)/def2-TZVPP  
Symmetry: c2v

Cartesian coordinates in Ångström:

Fe	0.0000000	0.0000000	0.2363216
C	-1.6023221	1.1633862	-0.6208676
H	-1.5068316	2.1878692	-0.9443223
C	-1.3692310	0.0000000	-1.4211044
H	-1.1399944	0.0000000	-2.4737639
C	-1.9820238	0.7321822	0.6535431
H	-2.2624790	1.3632652	1.4836290
C	-1.6023221	-1.1633862	-0.6208676
H	-1.5068316	-2.1878692	-0.9443223
C	-1.9820238	-0.7321822	0.6535431
H	-2.2624790	-1.3632652	1.4836290
C	1.9820238	0.7321822	0.6535431
H	2.2624790	1.3632652	1.4836290
C	1.6023221	1.1633862	-0.6208676
H	1.5068316	2.1878692	-0.9443223
C	1.6023221	1.1633862	-0.6208676
H	1.5068316	-2.1878692	-0.9443223
C	1.3692310	0.0000000	-1.4211044
H	1.1399944	0.0000000	-2.4737639
C	0.0000000	0.0000000	2.0701758
O	0.0000000	0.0000000	3.1953105

SCF energy GE00PT = -1763.340208584 H  
ZPE = 472.3 kJ/mol  
FREEH energy = 500.97 kJ/mol  
FREEH entropy = 0.42635 kJ/mol/K



Method: (RI-)B3LYP(D3BJ)/def2-SVP  
Symmetry: c1

Cartesian coordinates in Ångström:

Cu	-2.0849381	-1.1094746	0.3581689
Al	0.3473683	0.1812199	1.7541080
Al	-0.2101945	-0.1274327	-1.7920014
F	0.2578170	0.1059910	-0.0550121
O	-1.4303310	-0.0672026	1.9749209
C	-2.2958654	-0.0600675	3.0530932
C	-3.5894139	0.6925481	2.6035320
F	-4.2164579	-0.0393347	1.6566924
F	-4.4307130	0.8757431	3.6160059
F	-3.2841108	1.8644607	2.0688649
C	-1.6477609	0.6590692	4.2810979
F	-0.3742934	0.2451444	4.3830760
F	-1.6438335	1.9757038	4.1214779
F	-2.2813361	0.3622613	5.4113554
C	-2.6182969	-1.5475977	3.4371368
F	-1.5664413	-2.1203357	4.0083132
F	-3.6675598	-1.6461652	4.2416514
F	-2.8967643	-2.2522113	2.3124184
O	1.1596530	-1.2313907	2.2601172
C	1.8375077	-2.3631117	1.9603958
C	1.9449103	-3.2156777	3.2665159
F	0.7555522	-3.7623858	3.5539296
F	2.8374252	-4.2016806	3.1342319
F	2.3018949	-2.4484981	4.2892309
C	3.2637018	-1.9932731	1.4295024
F	3.1598055	-0.9721652	0.5722379
F	4.0534422	-1.6083376	2.4310057
F	3.8407566	-3.0187647	0.7996421
C	1.0595038	-3.1666964	0.8649554
F	1.2237891	-2.5921203	-0.3359710
F	1.4324040	-4.4361006	0.7809865
F	-0.2621887	-3.1302160	1.1352461
O	0.8982830	1.7280146	2.1837191
C	1.8265926	2.5841011	2.6824845
C	2.1697797	2.2045968	4.1638862
F	1.1678278	2.5492853	4.9813071
F	3.2810387	2.8081293	4.5877367
F	2.3412509	0.8838970	4.2648785
C	3.1271693	2.5182175	1.8123861
F	2.8117139	2.5105502	0.5190285
F	3.7943534	1.3857432	2.0740713
F	3.9392562	3.5495488	2.0472068
C	1.2194590	4.0264422	2.6324423
F	1.2064924	4.4848371	1.3747559
F	1.9252870	4.8805349	3.3789365
F	-0.0356572	4.0133457	3.0739459
O	-1.0354284	1.2882243	-2.2530493
C	-1.5285785	2.5241403	-2.0121999
C	-0.7510465	3.1932352	-0.8299170
F	-1.1514339	2.6477942	0.3364610
F	-0.9459868	4.5050502	-0.7637253



F	0.5522496	2.9505623	-0.9576827
C	-1.3567378	3.3758401	-3.3135590
F	-1.7310446	2.6693606	-4.3753963
F	-0.0747036	3.7157637	-3.4707044
F	-2.0895169	4.4940016	-3.2631137
C	-3.0447788	2.3978806	-1.6417801
F	-3.7831775	2.1487134	-2.7213709
F	-3.5136577	3.4945635	-1.0492954
F	-3.2143444	1.3617084	-0.7934071
O	1.1773467	-0.6821676	-2.5950170
C	2.2666990	-0.4346728	-3.3666802
C	3.0332918	0.8131476	-2.8141587
F	2.3423216	1.9299846	-3.0838506
F	4.2520906	0.9305007	-3.3386520
F	3.1448754	0.7262051	-1.4883657
C	3.1766808	-1.7060405	-3.3024921
F	2.4414624	-2.8030598	-3.4709739
F	3.7732468	-1.7913141	-2.1093287
F	4.1238418	-1.6792231	-4.2448857
C	1.8155214	-0.1664691	-4.8422074
F	1.3932851	-1.2978347	-5.4165490
F	2.8050585	0.3369872	-5.5816416
F	0.7968399	0.6987590	-4.8552576
O	-1.4068642	-1.4497774	-1.5099901
C	-2.1504061	-2.2913128	-2.3190208
C	-1.5716663	-2.3120215	-3.7734023
F	-0.4579630	-3.0295267	-3.8397388
F	-2.4538770	-2.8018653	-4.6392927
F	-1.2784558	-1.0510417	-4.1286334
C	-3.6280771	-1.7631277	-2.3534458
F	-4.0248550	-1.4615267	-1.0945592
F	-3.7071863	-0.6487349	-3.0716067
F	-4.4765925	-2.6587072	-2.8391136
C	-2.0984813	-3.7235677	-1.6960800
F	-2.7305319	-3.7106052	-0.5060391
F	-2.6926531	-4.6193526	-2.4787548
F	-0.8446449	-4.0996183	-1.4852341

SCF energy GE0OPT = -8975.085941769 H

ZPE = 914.8 kJ/mol

FREEH energy = 1139.45 kJ/mol

FREEH entropy = 1.92354 kJ/mol/K

- [1] S. Trofimenko, *J. Am. Chem. Soc.* **1967**, *89*, 3170.
- [2] M. Sellin, M. Seiler, M. Mayländer, K. Kloiber, V. Radke, S. Weber, S. Richert, I. Krossing, *Chem. Eur. J.* **2023**, *29*, e202300909.
- [3] A. Martens, P. Weis, M. C. Krummer, M. Kreuzer, A. Meierhöfer, S. C. Meier, J. Bohnenberger, H. Scherer, I. Riddlestone, I. Krossing, *Chem. Sci.* **2018**, *9*, 7058.
- [4] G. M. Sheldrick, *Acta Cryst. A* **2015**, *71*, 3.
- [5] G. M. Sheldrick, *Acta Cryst. C* **2015**, *71*, 3.
- [6] C. B. Hübschle, G. M. Sheldrick, B. Dittrich, *J. Appl. Cryst.* **2011**, *44*, 1281.
- [7] a) D. Kratzert, J. J. Holstein, I. Krossing, *J. Appl. Cryst.* **2015**, *48*, 933; b) D. Kratzert, I. Krossing, *J. Appl. Cryst.* **2018**, *51*, 928.
- [8] D. Kratzert, "FinalCif", can be found under <https://www.xs3.uni-freiburg.de/research/finalcif>.
- [9] C. F. Macrae, I. Sovago, S. J. Cottrell, P. T. A. Galek, P. McCabe, E. Pidcock, M. Platings, G. P. Shields, J. S. Stevens, M. Towler et al., *J. Appl. Cryst.* **2020**, *53*, 226.
- [10] C. R. Groom, I. J. Bruno, M. P. Lightfoot, S. C. Ward, *Acta Cryst. B* **2016**, *72*, 171.
- [11] S. Sajti, L. Deák, L. Bottyán, *FitSuite a general program for simultaneous fitting (and simulation) of experimental data*, **2009**.
- [12] a) M. von Arnim, R. Ahlrichs, *J. Comput. Chem.* **1998**, *19*, 1746; b) O. Treutler, R. Ahlrichs, *J. Chem. Phys.* **1995**, *102*, 346.
- [13] a) A. D. Becke, *J. Chem. Phys.* **1993**, *98*, 1372; b) Lee, Yang, Parr, *Phys. Rev. B Condens. Matter* **1988**, *37*, 785.
- [14] F. Weigend, R. Ahlrichs, *Phys. Chem. Chem. Phys.* **2005**, *7*, 3297.
- [15] a) M. Sierka, A. Hogeckamp, R. Ahlrichs, *J. Chem. Phys.* **2003**, *118*, 9136; b) F. Weigend, *Phys. Chem. Chem. Phys.* **2006**, *8*, 1057; c) R. Ahlrichs, *Phys. Chem. Chem. Phys.* **2004**, *6*, 5119.
- [16] S. Grimme, S. Ehrlich, L. Goerigk, *J. Comput. Chem.* **2011**, *32*, 1456.
- [17] P. Deglmann, F. Furche, R. Ahlrichs, *Chem. Phys. Lett.* **2002**, *362*, 511.
- [18] M. K. Kesharwani, B. Brauer, J. M. L. Martin, *J. Phys. Chem. A* **2015**, *119*, 1701.
- [19] M. K. Assefa, J. L. Devera, A. D. Brathwaite, J. D. Mosley, M. A. Duncan, *Chem. Phys. Lett.* **2015**, *640*, 175.
- [20] a) A. Klamt, *J. Phys. Chem.* **1995**, *99*, 2224; b) A. Klamt, V. Jonas, T. Bürger, J. C. W. Lohrenz, *J. Phys. Chem. A* **1998**, *102*, 5074.
- [21] a) F. Neese, *Wiley Interdiscip. Rev. Comput. Mol. Sci.* **2012**, *2*, 73; b) F. Neese, *WIREs Comput. Mol. Sci.* **2018**, *8*, e1327.
- [22] M. Römelt, S. Ye, F. Neese, *Inorg. Chem.* **2009**, *48*, 784.
- [23] V. N. Staroverov, G. E. Scuseria, J. Tao, J. P. Perdew, *J. Chem. Phys.* **2003**, *119*, 12129.
- [24] F. Neese, *Inorg. Chim. Acta* **2002**, *337*, 181.
- [25] A. Wolf, M. Reiher, B. A. Hess, *J. Chem. Phys.* **2002**, *117*, 9215.
- [26] R. Bjornsson, F. Neese, S. DeBeer, *Inorg. Chem.* **2017**, *56*, 1470.
- [27] J. Bohnenberger, M. Schmitt, W. Feuerstein, I. Krummenacher, B. Butschke, J. Czajka, P. J. Malinowski, F. Breher, I. Krossing, *Chem. Sci.* **2020**, *11*, 3592.
- [28] A. Bondi, *J. Phys. Chem.* **1964**, *68*, 441.
- [29] T. Köchner, T. A. Engesser, H. Scherer, D. A. Plattner, A. Steffani, I. Krossing, *Angew. Chem. Int. Ed.* **2012**, *51*, 6529.
- [30] a) C. C. Pye, T. Ziegler, E. van Lenthe, J. N. Louwen, *Can. J. Chem.* **2009**, *87*, 790; b) C. C. Pye, T. Ziegler, E. van Lenthe, J. N. Louwen, *Can. J. Chem.* **2009**, *87*, 790.
- [31] David R. Lide, *Handbook of Chemistry and Physics*, **2006**.
- [32] a) J. Bastide, D. Hall, E. Heilbronner, J. P. Maier, R. G. Plevy, *J. Electron Spectros. Relat. Phenomena* **1979**, *16*, 205; b) R. Bär, T. Heinis, C. Nager, M. Junger, *Chem. Phys. Lett.* **1982**, *91*, 440.

- [33] M. V. Korobov, S. V. Kuznetsov, L. N. Sidorov, V. A. Shipachev, V. N. Mit'kin, *IJMS* **1989**, 87, 13.
- [34] a) H. D. B. Jenkins, H. K. Roobottom, J. Passmore, L. Glasser, *Inorg. Chem.* **1999**, 38, 3609; b) H. D. B. Jenkins, J. F. Liebman, *Inorg. Chem.* **2005**, 44, 6359; c) H. D. B. Jenkins, L. Glasser, *J. Am. Chem. Soc.* **2004**, 126, 15809; d) L. Glasser, H. D. B. Jenkins, *Chem. Soc. Rev.* **2005**, 34, 866.